KINETICS OF BORON HYDRIDE INTERCONVERSION REACTIONS

Final Technical Report

by

R. Greatrex and N.N. Greenwood

September, 1989

United States Army

EUROPEAN RESEARCH OFFICE OF THE U.S. ARMY

London, England

CONTRACT NUMBER DAJA45-86-C-0019

Contractor: University of Leeds,
Attn. The Registrar,
Leeds LS2 9JT,
United Kingdom

SECURITY CLASSIFICATION OF THIS PAGE (When Data Entered)

REPORT DOCUMENTATION PAGE		READ INSTRUCTIONS BEFORE COMPLETING FORM
1. REPORT NUMBER	2. GOVT ACCESSION NO.	3. RECIPIENT'S CATALOG NUMBER
4. TITLE (and Subtitle) Kinetics of boron hydride interconversion reactions		5. TYPE OF REPORT & PERIOD COVERED Final May 1986 - September 1989 6. PERFORMING ORG. REPORT NUMBER
7. AUTHOR(s) R. Greatrex and N.N. Greenwood		8. CONTRACT OR GRANT NUMBER(s) DAJA45-86-C-0019
9. PERFORMING ORGANIZATION NAME AND ADDRESS University of Leeds Leeds LS2 9JT, England		10. PROGRAM ELEMENT, PROJECT, TASK AREA & WORK UNIT NUMBERS
11. CONTROLLING OFFICE NAME AND ADDRESS		12. REPORT DATE September 1989 13. NUMBER OF PAGES
14. MONITORING AGENCY NAME & ADDRESS(if different from Controlling Office)		15. SECURITY CLASS. (of this report) 15a. DECLASSIFICATION/DOWNGRADING SCHEDULE

16. DISTRIBUTION STATEMENT (of this Report)

Distribution unlimited

17. DISTRIBUTION STATEMENT (of the abstract entered in Block 20, if different from Report)

18. SUPPLEMENTARY NOTES

19. KEY WORDS (Continue on reverse side if necessary and identify by block number)

Boron hydrides, Diborane, (6) Tetraborane, (10) Pentaborane, (11) Hexaborane, (10) Tetraborane, (8) Carbonyl, Borane Interconversions, Borane Mechanisms, Borane Thermolysis, (SEE) Gas-phase kinetics, Deuterium isotope effects, Quantitative mass spectrometry, Hexaborane (12)

20. ABSTRACT (Continue on reverse side if necessary and identify by block number)

This report describes progress that has been made during the Grant period in unravelling the complex series of gas-phase reactions that occur during the thermolysis of diborane. This has involved the application of a mass spectrometric technique developed in this laboratory to monitor initial rates of reaction and product distributions, leading to rate equations, orders of reaction, and energies of activation. The work has involved detailed kinetic studies not only of the thermolysis of B_2H_6 itself (including an continued ..

DD FORM 1 JAN 73 1473 EDITION OF 1 NOV 65 IS OBSOLETE

SECURITY CLASSIFICATION OF THIS PAGE (When Data Entered)

20. Abstract *continued* ..

investigation of the effect on the rate of replacing hydrogen by deuterium), but also of the thermolysis of the arachno boranes B_4H_{10}, B_5H_{11}, and B_6H_{12}, both alone and in the presence of H_2 and other boranes. The thermolysis of B_6H_{10} in packed vessels, and in the presence of alkenes and other boranes has also been studied; the results of these latter experiments emphasise the unique properties of this borane and its pivotal role in the production of decaborane(14) and higher boranes.

Abstract

This Report describes progress that has been made during the Grant period in unravelling the complex series of gas-phase reactions that occur during the thermolysis of diborane. This has involved the application of a mass spectrometric technique developed in this laboratory to monitor initial rates of reaction and product distributions, leading to rate equations, orders of reaction, and energies of activation. The work has involved detailed kinetic studies not only of the thermolysis of B_2H_6 itself (including an investigation of the effect on the rate of replacing hydrogen by deuterium), but also of the thermolysis of the arachno boranes B_4H_{10}, B_5H_{11}, and B_6H_{12}, both alone and in the presence of H_2 and of other boranes. The thermolysis of B_6H_{10} in packed vessels, and in the presence of alkenes and other boranes has also been studied; the results of these latter experiments emphasise the unique properties of this borane and its pivotal role in the production of decaborane(14) and higher boranes.

Keywords

Boron Hydrides
Diborane(6)
Tetraborane(10)
Pentaborane(11)
Hexaborane(10)
Hexaborane(12)
Tetraborane(8) Carbonyl
Borane Interconversions
Borane Mechanisms
Borane Thermolysis
Gas-phase Kinetics
Deuterium Isotope effects
Quantitative Mass Spectrometry

Personnel

Dr M.B. Millikan was appointed as a vacation worker, for a period of six months ending on 24th October 1986, to prepare and purify B_6H_{12} for electron diffraction and gas-phase kinetic studies. Miss S.M. Lucas was appointed as a graduate student to work full-time on the Project in October 1986. She successfully defended her MSc thesis entitled " The Use of Isotopic Labels in Boron Hydride Chemistry" in 1987; a copy of the thesis was submitted with the 5th Periodic Report. Mr M.D. Attwood, a graduate student in the final year of his PhD, was supported full-time on the grant during the period October 1986 - November 1987. He successfully defended his thesis entitled "Gas-phase Thermolysis and Cothermolysis of Boron Hydrides" in 1987; a copy of the thesis was submitted together with the 5th Periodic Report. Mr M. Kirk, who graduated from the University of Leeds in June 1988, was appointed to work full-time on the Project from October 1988 as a graduate student working for a higher degree.

Other people not directly supported by the Grant but actively involved throughout the work were the Principal Investigator Professor N.N. Greenwood, the Assistant Investigator Dr R. Greatrex, and an Experimental Officer , Mr D. Singh.

Contents

a re-investigation of the deuterium kinetic isotope effect",
J. Am. Chem. Soc., 1989, in the press.

F. S.J. Cranson, P.M. Davies, R.Greatrex, D.W.H. Rankin, and H.E. Robertson,
"Electron diffraction study of tetraborane(8) carbonyl in the gas phase: structure determination of an endo/exo isomeric mixture",
J. Chem. Soc., Dalton Trans., 1989, in the press.

G. R. Greatrex, N.N. Greenwood, D.W.H. Rankin, and H.E. Robertson,
"The molecular structures of pentaborane(9) and pentaborane(11) in the gas phase as determined by electron diffraction",
Polyhedron, 1987, 6, 1849-1858.

H. R. Greatrex, N.N. Greenwood, M.B. Millikan, D.W.H. Rankin, and H.E. Robertson,
"The molecular structure of hexaborane(12) in the gas phase as determined by electron diffraction",
J. Chem. Soc., Dalton. Trans., 1988, 2335-2339.

VII. Figures

I. General Introduction

The intriguing ability of the smaller boranes such as B_2H_6, B_4H_{10}, and B_5H_{11} to interconvert in the gas phase, at room temperature or slightly above, by reaction with themselves or with each other, and their ability to aggregate further into larger and more complex borane clusters has excited attention from the earliest days of boron hydride chemistry.[1,2] The system is arguably one of the most complex in the whole of chemistry, and provides a major intellectual challenge to the experimental chemist and theoretician alike. Thermolysis of B_2H_6, in principle, provides routes to all the other boranes and in fact forms the basis of the main commercial route to $B_{10}H_{14}$ and its derivatives such as the technologically important series of carbaborane compounds. These conversions are at present somewhat inefficient, not only because of the complexity of the reactions, but also because they are generally accompanied by the formation of undesirable solid "polymers"; a more thorough understanding of the mechanisms should therefore enable the processes to be tailored to give commercially desired products in higher yield.

There has been considerable effort over the years to unravel the details of the mechanisms by which these various processes take place and, as outlined in this report, our recent work in Leeds is having a major impact in this area.[1,3-9] We have developed and refined a mass spectrometric technique which we have used to carry out systematic kinetic studies of the thermolysis of individual boranes, and of their cothermolysis with each other to test rival mechanisms. Measurement of initial rates of reaction as a function of temperature and pressure has led to rate equations and Arrhenius parameters. These kinetic data, coupled with detailed product analysis of the reacting mixtures as a function of time, have enabled us to make significant advances in our understanding of this complex interacting system.

II. Experimental Section

The method involves sampling the thermostatted gaseous reaction mixture, either continuously or periodically, by bleeding it directly into two mass spectrometers. The MS30 is used to monitor the boranes, and a smaller MS10S to analyse for dihydrogen. The intensity of each line in the spectrum is measured automatically by the DS55 data system, and the whole is then fitted by a least-squares computer programme (developed in this laboratory) using the previously measured standard mass spectra of all the component boranes (see Figure 1 for an example). With appropriate calibration procedure this gives a detailed "instantaneous" product analysis of the progress of the reaction without disturbing the bulk of the reaction mixture.

The success of the method depends heavily on reproducibility of fragmentation patterns and relative total ion currents, and this in turn relies on the achievement of "standard" operating

conditions within the mass spectrometer. Instrumental stability and sensitivity are therefore of vital importance. Accurate control of source temperature is also a factor which needs to be taken into account. Further experimental details, are described in refs. 3 and 4.

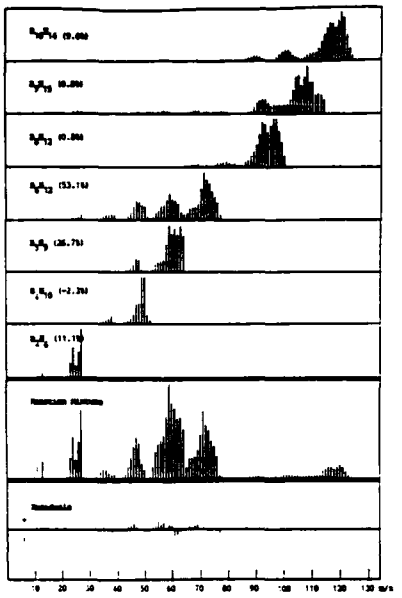

Figure 1. Typical analysis of borane mixture.

III. Results and Discussion

1. Deuterium Kinetic Isotope Effect in the Thermolysis of Diborane

The gas-phase thermolysis of diborane is known to be homogeneous in its initial stages and to follow 3/2-order kinetics (see ref. 9 for background references). This suggests that a triborane species is involved in the rate-determining step and the favoured mechanism involves the three-step process,

$$B_2H_6 \rightleftharpoons 2\{BH_3\} \qquad (1)$$

$$\{BH_3\} + B_2H_6 \rightleftharpoons \{B_3H_9\} \qquad (2)$$

$$\{B_3H_9\} \rightleftharpoons \{B_3H_7\} + H_2 \qquad (3)$$

in which the species in braces are non-isolable reactive intermediates. Cogent arguments have been advanced[10] to suggest that (3) is the rate-determining step, but a very recent high-

level computational study based on this three-step mechanism, employing many-body perturbation theory and the coupled-cluster approximation, concludes that it is the formation of $\{B_3H_9\}$ (2) rather than its decomposition (3) which is rate-determining.[11] The calculations also indicate that the $\{B_3H_9\}$ formed in step (2) carries about 80 kJ mol^{-1} of excess internal energy, suggesting that step (3) might occur so rapidly that for all practical purposes the formation of $\{B_3H_7\}$ might best be represented by the direct reaction :

$$\{BH_3\} + B_2H_6 \rightleftharpoons \{B_3H_7\} + H_2 \qquad (4)$$

This possibility, which had been considered earlier but tentatively dismissed,[12] is easier to reconcile with the qualitative observation that added H_2 not only inhibits the rate of decomposition of B_2H_6,[13] but also alters the product formation in favour of volatile boranes;[14] quantitative studies in this laboratory have shown that the initial rate of decomposition of B_2H_6 at 3.5 mmHg and 150°C is decreased by a factor of 3.4 in the presence of a 14-fold excess of H_2.[1,15] The computational study[11] also addressed the question of the relative rates of decomposition of B_2H_6 and B_2D_6 and found that, regardless of whether step (2) or (3) is rate determining, the predicted ratio of the rate constants (k_H/k_D) is ca 2 at 127 °C; the actual computed values were 1.73 and 2.4, respectively. Unfortunately the only experimental determination of this ratio (which was based on the relative rate of production of H_2 and D_2 at 88 °C),[12] gave a value of 5.0.

In an attempt to resolve these difficulties we have recently undertaken a careful reinvestigation of the relative rates of decomposition of B_2H_6 and B_2D_6.[9] We chose to monitor the rate of consumption of diborane rather than the rate of production of hydrogen since this is a more direct measure to compare with the calculated rates. The reactions were carried out at 147 °C in preconditioned spherical Pyrex bulbs (volume ca. 1 dm^3) with initial pressures of diborane about 3.5 mmHg; helium, argon, and krypton at partial pressures of 100, 1.0, and 1.0 mmHg, respectively, were also present as calibrants etc., as previously described.[3,4] Initial rates were obtained by the tangent method from plots of diborane pressure vs. time for 14 separate runs with B_2H_6 and 10 runs with with B_2D_6. Typical results are shown in Figure 2. These yielded values for the 3/2-order rate constants $k_H = (4.55 \pm 0.89) \times 10^{-4}$ and $k_D = (1.77 \pm 0.28) \times 10^{-4}$ $mol^{1/2}\ m^{1/2}\ s^{-1}$, respectively. The value for the ratio k_H/k_D is therefore 2.57 ± 0.65, which is clearly more consistent with the computed values than with the early experimental value based on the rates of production of H_2 and D_2.[12] The new experimental value is is closer to the computed value of 2.4 assuming step (3) as rate-determining than to the value of 1.73 for step (2) as rate limiting but, in view of the expected uncertainties in the theoretical values, it is probably more appropriate to suggest that both of the computed values are in adequate agreement with the new experimental value.[16] The computed overall activation energy for the decomposition of B_2H_6 is 134 kJ mol^{-1} if step (2)

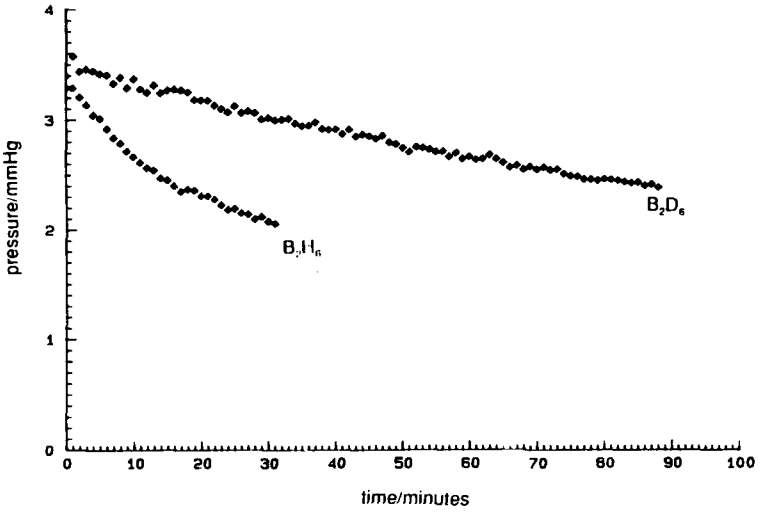

Figure 2. Concentration vs. time profiles for typical thermolyses of B_2H_6 and B_2D_6 at 147 °C.

is rate-determining, but only 92 kJ mol^{-1} if step (3) is rate-determining;[11] our own most recent experimental redetermination of this quantity (based on the rate of consumption of B_2H_6 at 11 different temperatures in the range 120-180 °C is 102.6 ± 3.3 kJ mol^{-1}. Again it would be unwise to place too great a significance on these differences, and it is probable that calculations with a larger basis set or incorporating the possibility of tunnelling would lead to a revision of the computed values for the activation energy.[11,16]

In summary, a careful re-investigation of the relative rates of decomposition of B_2H_6 and B_2D_6 has led to a value of 2.57 ± 0.65 for the rate-constant ratio k_H/k_D, which disagrees with an earlier experimental value but is close to values obtained in a recent high-level computational study. This important new result therefore removes a potential inconsistency between experiment and computation. Taken in conjunction with the experimentally observed influence of added H_2 in repressing the rate of decomposition of B_2H_6 and in altering the distribution of products, the totality of experimental and computational evidence suggests that the rate-determining step following the symmetric dissociation of diborane is neither simply the formation of $[B_3H_9]$ (2), nor its subsequent decomposition (3), but that (2) and (3) are concerted as in (4).

pressures of 3.5 mmHg and H_2 pressures of 20 mmHg, the rate is retarded by a factor of ca. 5. Of particular significance is the fact that the activation energy remains essentially unaltered (98.4 ± 1.4, compared with 99.2 ± 0.8 kJ mol^{-1}). We regard this as convincing additional evidence that B_4H_{10} decomposes via the single rate-determining step (6). If (7) occurred to any significant extent, suppression of (6) would inevitably alter the observed activation energy towards that of (7) which is most unlikely to be fortuitously identical to that of (6). It is interesting to observe in Figure 3 that the rate constants for the thermolysis of B_4H_{10} in the presence of CO[19] or of B_2H_6 also fall on the same line as those for the thermolysis of B_4H_{10} alone. The significance of these results has been discussed elsewhere.[1,5,19,20]

Typical concentration-time profiles for the thermolysis of B_4H_{10} alone and (in this case) in the presence of 50 mmHg added H_2 (Figure 4) reveal substantial differences in the product distributions:

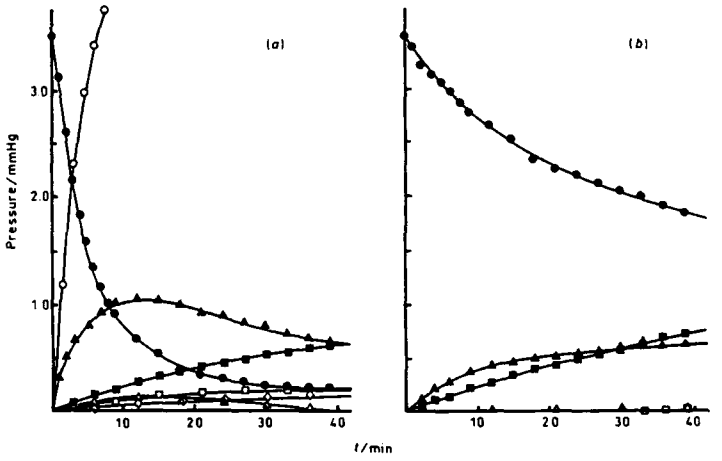

Figure 4. Concentration - time profiles for the thermolysis at ca. 90 °C of (a) B_4H_{10} alone, and (b) B_4H_{10} in the presence of H_2 (50 mmHg): O H_2, ● B_4H_{10}, ▲ B_5H_{11}, ■ B_2H_6, △ B_6H_{12}, □ $B_{10}H_{14}$, and ◇ B_5H_9. Data for H_2 not recorded in (b).

(a) the rate of decomposition is retarded by the presence of added H_2, (b) the relative initial rate of production of B_5H_{11} is unaltered, (c) there is a marked increase in the rate of production of B_2H_6, and (d) the rates of production of B_5H_9 and other higher boranes including polymer are dramatically reduced. All these observations can be interpreted on the basis of a mechanism in which step (6) is followed by step (8),

$$B_4H_{10} + [B_4H_8] \rightleftharpoons B_5H_{11} + [B_3H_7] \quad (8)$$

which in turn is followed by the reverse of reaction (4). The detailed arguments are given in refs. 1 and 7.

Unfortunately, all is not well with this mechanism, because more detailed analysis[7] reveals an inconsistency between the magnitude of the observed retardation and the experimentally observed reaction order (1st and not 2nd as predicted) for the decomposition of B_4H_{10} in the presence of excess added H_2. A possible explanation is that B_5H_{11} is formed not by step (8), but instead by the interaction of the reactive intermediate $[B_4H_8]$ with itself. We believe that it is possible to resolve this and similar problems by a carefully planned sequence of experiments in which temperature, pressure, presence of other added reagents, and isotopically enriched species are systematically varied.

One particular theme that we wish to explore in this respect involves the use of unstable adducts (e.g. B_4H_8CO) to generate the reactive borane intermediate $[B_4H_8]$ in situ in the presence of other co-reactants, and thereby to test specific steps in rival mechanisms. All of this is for the future. However, as a preliminary, we have recently determined the structure of B_4H_8CO in the gas phase by electron diffraction in collaboration with Dr D.W.H. Rankin (University of Edinburgh).[21] The sample was known from n.m.r. experiments to consist of 62% of the endo isomer and 38 % of the exo isomer and early refinements showed that the distribution in the gas phase was consistent with that found in solution. A satisfactory refinement (R_G = 0.06) was obtained with a model in which the isomers had a "butterfly" B_4 geometry with "hinge" B(1) carrying either an endo or an exo CO; the endo and exo isomers differed only in the dihedral angles between the planes of the "butterfly" structure [135(4)° and 144(2)°, respectively] and in the angles subtended by the carbon atom at the B-B "hinge" [125(2)°] and 109(2)°]. The unbridged B-B distances were 172.7(10) ("hinge") and 184.9(4) pm, and the H-bridged B-B distances were 178.0(6) pm. The B-H-B bridges were asymmetric, with the distance from the hydrogen atom to the boron atom of the "wing-tip" BH_2 group being greater by 15 pm than the distance to the "hinge" BH group. The BCO angle showed no significant deviation from 180°. This work, which was carried out predominantly by personnel not supported by Grant funds, is described in detail in the preprint included in Appendix F.

3. Gas-phase Thermolysis of the Arachno-boranes B_5H_{11} and B_6H_{12}

The gas-phase thermolyses of the arachno boranes B_5H_{11} and B_6H_{12} had, in contrast to that of B_4H_{10}, received no serious quantitative treatment prior to our own work. The results that have emerged are fascinating. We have shown that these two compounds decompose with first-order kinetics, and at comparable rates, over a wide range of temperature; i.e. they have essentially identical activation energies and pre-exponential

factors (E_a 72.6 ± 2.4 kJ mol^{-1} for B_5H_{11}[1,6,7] and 75.0 ± 5.8 kJ mol^{-1} for B_6H_{12};[8] A 1.3 x 10^{17} and 3.8 x 10^{17} s^{-1}, respectively). The two reactions also resemble one another in producing ca.0.5 mol of B_2H_6 per mol of reactant decomposed. The results strongly suggest that the rate-determining steps in the two decompositions involve very similar processes, namely elimination of a BH_3 group from the cluster, i.e. steps (9) and (10).

$$B_5H_{11} \longrightarrow \{B_4H_8\} + \{BH_3\} \quad (9)$$

$$B_6H_{12} \longrightarrow B_5H_9 + \{BH_3\} \quad (10)$$

This finds a ready interpretation in terms of the detailed molecular structures of gaseous B_5H_{11}[22] and B_6H_{12}[23] as recently determined in our electron diffraction studies with Dr D.W.H. Rankin. As shown in Figure 5, these two species bear a close

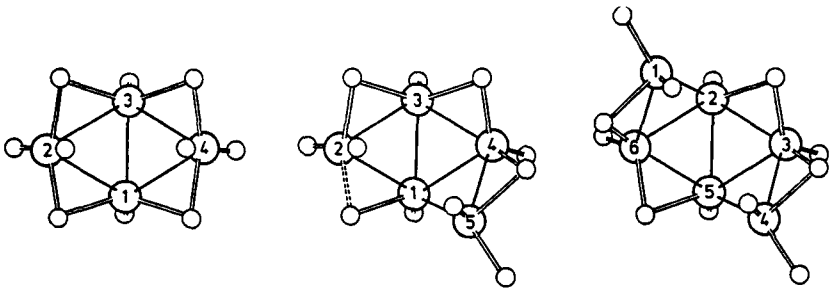

Figure 5. Structural relationship between the arachno-boranes B_4H_{10}, B_5H_{11}, and B_6H_{12}, as determined by gas-phase electron diffraction.

structural relationship to each other and to B_4H_{10}. Thus, notional replacement of H_{endo} and one H_u on, say, B(4) in B_4H_{10} by a BH_3 group yields B_5H_{11} and repetition of this process on the opposite side of the molecule, i.e. at B(2), generates the observed structure of B_6H_{12} having C_2 symmetry. In view of the similarity of the Arrhenius parameters for the decomposition of B_5H_{11} and of B_6H_{12}, it seems reasonable to identify these structurally similar BH_3 groups as the fragments involved in the initial steps (9) and (10). In B_4H_{10}, by contrast, these particular incipient groups are absent and its decomposition is characterized by quite different Arrhenius parameters (see earlier); in this case the initial step is believed to involve elimination of H_2 as discussed earlier. This type of reaction is clearly not favoured in the case of B_5H_{11} and B_6H_{12}, though small amounts of B_6H_{10} and H_2 are produced in the thermolysis of B_6H_{12}.

and further work is in progress to determine whether the B_6H_{10} and dihydrogen arise from a competing, but minor, reaction channel involving direct elimination of H_2 from B_6H_{12}. A typical concentration *vs*. time profile for the thermolysis of B_6H_{12} (which does not include an analysis for the individual hexaboranes) is shown in Figure 6 This shows clearly the 1:1:0.5 relationship, suggested by (10), between B_6H_{12} consumed, B_5H_9 produced, and B_2H_6 produced.

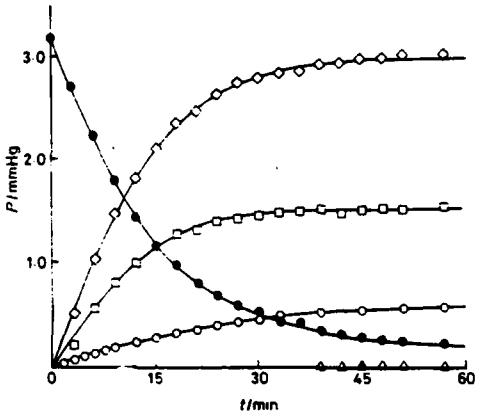

Figure 6. Concentration *vs*. time profiles for the thermolysis of B_6H_{12} at *ca*. 100 °C: ● B_6H_{12}, ◇ B_5H_9, □ B_2H_6, △ $B_{10}H_{14}$, and ○ H_2.

In the thermolysis of B_5H_{11} and of B_6H_{12} the production of B_2H_6 could involve direct dimerization of two $\{BH_3\}$ groups (a process which is known to occur with zero activation energy). Alternatively, the $\{BH_3\}$ could interact with a further mole of the starting material to abstract $\{BH_3\}$. It is not possible to distinguish between these two mechanisms on the basis of the observed stoichiometries, but detailed kinetic studies are being planned, which it is hoped will yield answers to these questions. These investigations will include cothermolysis of B_5H_{11} and of B_6H_{12}, respectively, with reagents of two types: (i) those which are capable of *generating* $\{BH_3\}$ in situ (e.g. BH_3CO, BH_3PF_3, etc.), and (ii) those which can *scavenge* $\{BH_3\}$ and other reactive intermediates (e.g. CO, PF_3, amines, etc.), and thereby prevent interactions that might otherwise have occurred between the reactive intermediate and the binary borane in question.

The values of *ca*. 10^7 s^{-1} for the pre-exponential factors for the thermolyses of B_5H_{11} and B_6H_{12} are lower by more than four orders of magnitude than the value for B_4H_{10} (6×10^{11} s^{-1}), consistent with the gross differences proposed for the initial steps in the first two decompositions as compared with that in the latter, *viz*. elimination of BH_3 and of H_2, respectively. The value for B_4H_{10} itself is at the lower end of the range of values

(ca. 10^{11} - 10^{15} s^{-1}) found for unimolecular decompositions of hydrocarbon derivatives, but is arguably acceptable for a mechanism involving release of H_2 via a loosely-bound transition state. The pre-exponential factors for both B_5H_{11} and B_6H_{12} are exceptionally low, and at first sight might appear to cast doubt on the validity of the proposed mechanisms involving (9) and (10) as unimolecular, rate-determining, initial steps. However, as discussed in detail elsewhere,[6] we believe there are cogent reasons for accepting that these unusual values do indeed correspond to these particular processes. These are among the first reliable experimental data on Arrhenius parameters to be reported for polyhedral boron hydride clusters, which are in fact a particularly unusual class of compound whose unique structural and bonding properties may well engender unexpected kinetic parameters. We hope that these important new experimental results will encourage further research and discussion in this area.

4. Influence of Added H_2 on the Thermolysis of B_5H_{11}

The observed influence of added H_2 on the gas-phase thermolysis of B_5H_{11} is also consistent with the initial steps proposed in the preceding section. From Figure 7,

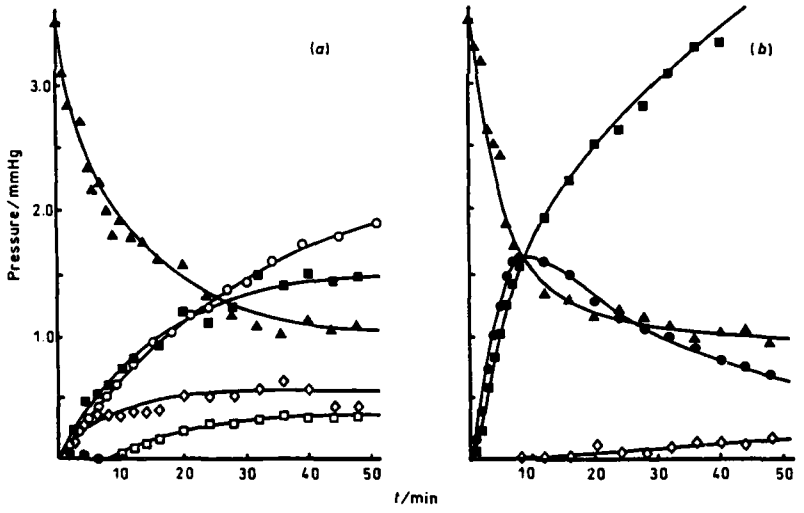

Figure 7. Concentration vs. time profiles for the thermolysis at ca. 100 °C of (a) B_5H_{11} alone, and (b) B_5H_{11} in the presence of H_2 (50 mmHg): O H_2, ■ B_2H_6, ● B_4H_{10}, ◇ B_5H_9, ▲ B_5H_{11}, and □ $B_{10}H_{14}$. Data for H_2 not recorded in (b).

which compares decompositions of 3.5 mmHg B_5H_{11} alone and in the presence of 50 mmHg added H_2, it is clear that the decomposition is greatly simplified in the latter case. B_4H_{10}, which is virtually absent in the products of the thermolysis of B_5H_{11} alone, is now the main product, its rate of formation in the initial stages being almost equal to the rate of consumption of B_5H_{11}, presumably as a result of the reaction between H_2 and the reactive intermediate $\{B_4H_8\}$ - i.e. the reverse of (6). It is notable, however, that the initial rate of consumption of B_5H_{11} remains unaltered. This point is shown more clearly in Figure 8, which reveals that the the Arrhenius plots for the decompositions of B_5H_{11} alone and in the presence of added H_2 are essentially coincident.

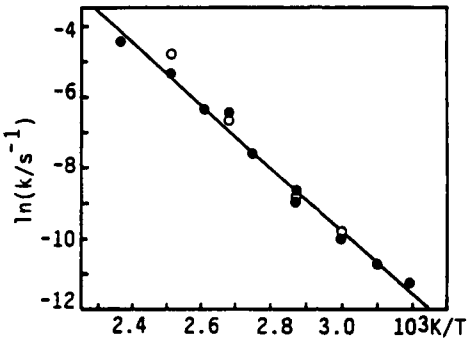

Figure 8. Arrhenius plots for the thermolysis of B_5H_{11} alone (filled circles) and in the presence of an excess of added H_2.

This clarifies a long-standing area of uncertainty; it establishes that there is no direct binary interaction between B_5H_{11} itself and H_2, and that the so-called equilibrium (11)

$$2B_5H_{11} + 2H_2 \rightleftharpoons 2B_4H_{10} + B_2H_6 \qquad (11)$$

proceeds via the rate-determining dissociation (9). B_2H_6 will then be formed as in the normal thermolysis of B_5H_{11}, and the overall product distribution is simplified because the reactive intermediate $\{B_4H_8\}$, which in the absence of added H_2 is presumably the precursor to a variety of products including solid hydride, is effectively removed from the system as B_4H_{10} via the reverse of (6).

5. Formation of Solids from Gas-phase Reactions

The solid hydride formed during these reactions is invariably deposited preferentially on the lower surfaces of the

reaction vessel, suggesting that the solids accrete from the gas phase and are not formed directly at the surface. An important general question which arises in view of this, is whether any autocatalytic or inhibitory effects occur at the surfaces of these nascent solid particles as the reactions proceed. The fact that consistent and meaningful results appear to be forthcoming from these investigations tends to suggest that such effects are negligible. The observation that excess added H_2 reduces (essentially to zero) the amount of solid hydride formed in the B_5H_{11} decomposition, without affecting the initial rate, provides rather more convincing evidence in this respect.

6. Gas phase Thermolysis of Boranes in Packed Vessels: Tests for Heterogeneity

B_2H_6 and B_4H_{10}.- Early work on the thermolysis of B_2H_6 in packed Pyrex vessels established that the decomposition occurred homogeneously in the gas phase.[13] More recently we have shown that the same is also true for the thermolysis of B_4H_{10}, no change in initial rate being observed in a clean vessel packed with Raschig rings to give a 33-fold increase in surface area.[5]

B_5H_{11} and B_6H_{12}.- The thermolyses of both B_5H_{11}[6,15] and B_6H_{12}[24] differ from those of B_2H_6 and B_4H_{10}, in that they do appear to be affected by the presence of a clean Pyrex surface. In the case of B_5H_{11} the reaction is initially an order of magnitude faster in a clean vessel packed with Raschig rings (in a similar way to the one used for the B_4H_{10} experiments), whereas the B_6H_{12} reaction is speeded up by about a factor of 6. In each case, however, the rate of the reaction in the packed vessel returns to its "normal" value (i.e. the value observed in an unpacked vessel) when the surface is conditioned by exposure to borane undergoing decomposition. The rates are therefore independent of the area of coated surface, and we conclude that under these conditions the reactions occur homogeneously in the gas phase. Further details of the effect of Pyrex surfaces on the B_5H_{11} reaction are reported elsewhere.[6,15]

B_6H_{10}.- Despite the fact that B_6H_{10} is never observable in any measurable concentration in the thermolysis of B_2H_6, it has been suggested that this borane may play an important role as an intermediate in the overall process leading to $B_{10}H_{14}$.[25,26] We therefore initiated a programme of work to look at the thermolysis of B_6H_{10} alone and also in cothermolysis with other boranes. This work was begun on a previous grant,[27] but has been continued during the present project. As referenced below, some of the work was carried out by P.M. Davies as part of his SERC-supported PhD studies.[28]

When pure, nido-B_6H_{10} is relatively stable compared with the arachno boranes discussed earlier. However, at temperatures in excess of 100 °C it decomposes by a rather unusual second-order reaction to produce H_2 and small amounts of B_5H_9 and $B_{10}H_{14}$.[3] Most of the product (ca. 90%) is a non-volatile, presumably

polymeric, solid. The effect of an increased surface area on this reaction is quite unexpected:[1,28,29] unlike the borane decompositions discussed so far, which are either unaffected or accelerated by the presence of a clean Pyrex surface, that of B_6H_{10} is retarded by an order of magnitude in a clean vessel packed as described earlier with Raschig rings. The effect is illustrated in Figure 8, which also reveals that the rate recovers slowly in successive runs in the same vessel, presumably as the surface is de-activated by the deposition of a coating of solid hydride.

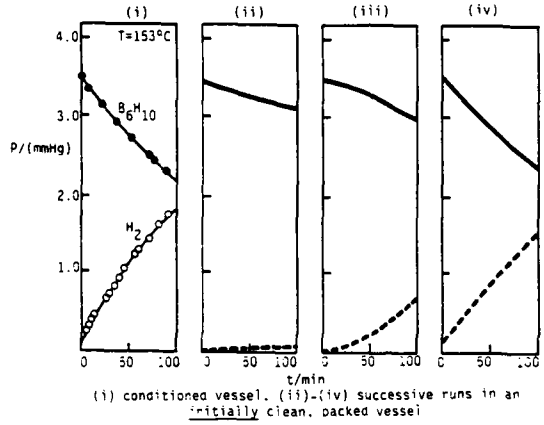

Figure 9. Effect of surface on thermolysis of B_6H_{10}.

This behaviour is typical of radical chain reactions,[30] the clean glass surface acting as a site for termination processes. Consistent with this it was found that treatment of the clean glass surfaces of a packed reaction vessel with a covering of PTFE polymer, $(CF_2)_n$, led to reaction rates comparable to those observed in a conditioned packed vessel. Moreover, the rate observed in an unpacked PTFE-coated vessel was actually faster than in an unpacked conditioned vessel, suggesting that the PTFE-coated surface was even less active in removing radicals than was the borane-conditioned surface. In the light of these results it was clear that the possibility of a radical-based mechanism for the thermolysis of B_6H_{10} required careful further study.

7. Thermolysis of B_6H_{10} in the Presence of Alkenes: New Insights into the Mechanism of Thermolysis of B_6H_{10}

Ethene and propene are well-known radical scavengers.[30] With B_6H_{10} these unsaturated hydrocarbons were found to inhibit the reaction dramatically.[1,28,29] For a pressure of 3.5 mmHg the decomposition normally has a half-life of *ca*. 100 min., whereas in the presence of 15 mole % of ethene it is stable over a period

of several days. Propene has a more pronounced effect, the addition of only 3% causing complete inhibition in the thermolysis of B_6H_{10} (3.5 mmHg) for some 20 min. even at 185 °C; larger additions increase the inhibition period proportionately. This effect is illustrated in (Figure 9). This appears to be the first well-documented example of a radical-initiated decomposition in the borane area, and further work is planned.

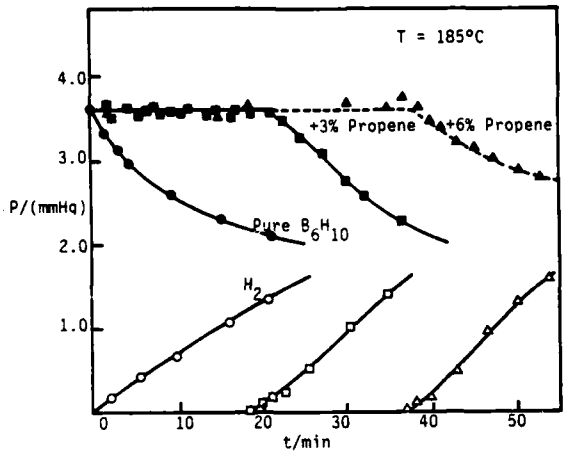

Figure 10. Inhibition of B_6H_{10} thermolysis by propene.

The initial products of these alkene reactions were shown, by very careful high-resolution accurate-mass measurements, to be trialkylboranes and the basal-alkylated hexaboranes $B_6H_{10-x}R_x$ (R = Et or Pr, x = 1-5). The very first of these alkylated hexaboranes to appear was B_6H_9R, and this was taken as strong evidence that the radical produced in the initiation step is $B_6H_9^{\cdot}$. These alkylated hexaboranes are followed by the series of alkylated monocarbaboranes $R'CB_5H_{8-x}R_x$ (x = 0-3), where R' = Me, R = Et for the ethene reaction, and R' = Et, R = Pr for the propene reaction. In one cothermolysis involving propene, which was allowed to go almost to completion, the main products were found to be $B_6H_5Pr_5$ and $EtCB_5H_{8-x}Pr_x$ (x = 0-3). It would therefore appear that the alkylboranes $B_6H_{10-x}Pr_x$ (x = 1-4) have by this stage of the reaction been converted to the corresponding monocarbaboranes, whereas the end-member of the series, in which all the basal terminal protons have been replaced, possesses enhanced stability. A typical low-resolution mass spectrum of the gaseous reaction mixture in a cothermolysis at 185 °C is shown in Figure 11.

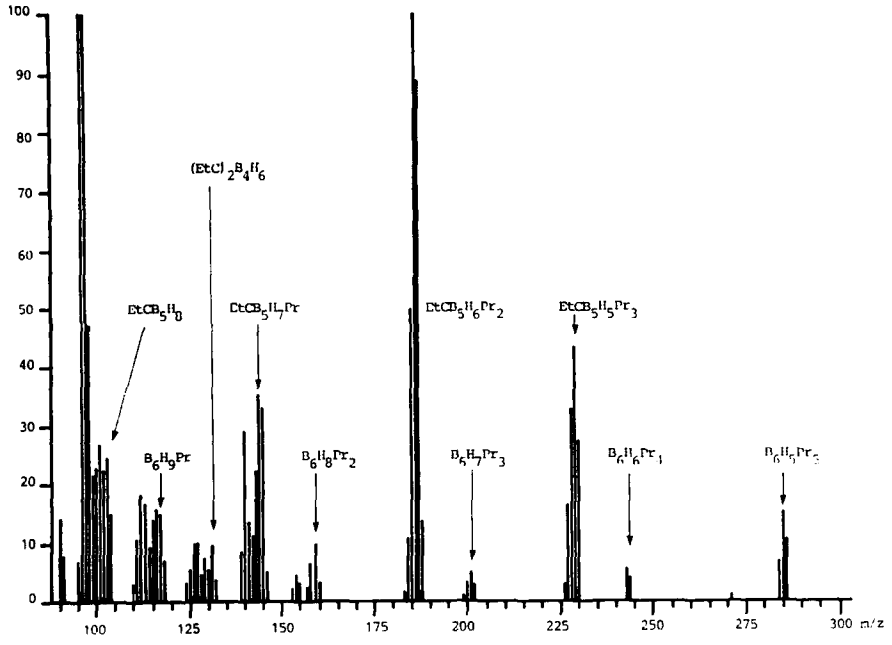

Figure 11. Mass spectrum of products in the thermolysis of B_6H_{10} and propene at 185 °C.

The results suggest that the monocarbaboranes are formed by $\{BH_3\}$ release from the base of the corresponding alkylborane, followed by incorporation of the methylene carbon and its associated protons into the ring (Figure 12).

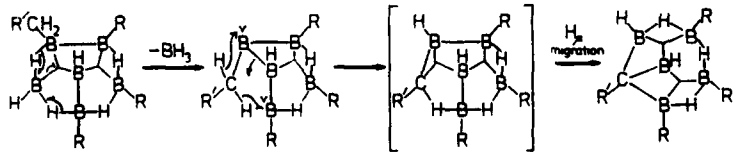

Figure 12. Possible mechanism for the formation of $R'CB_5H_{8-x}R_x$ (x = 0-3) by the elimination of $\{BH_3\}$ from $R'CH_2B_6H_{9-x}$ (x = 0-3). (R = Et or H, R' = Me; R = Pr or H, R' = Et). The superscripts on the structure of the first "reaction intermediate" indicate vacant orbitals on B.

B_6H_{10} itself is also thought to undergo $\{BH_3\}$ release as indicated in (12).

$$B_6H_{10} \longrightarrow \{B_5H_7\} + \{BH_3\} \qquad (12)$$

In the normal thermolysis of B_6H_{10} alone, this process is presumed to be a very minor side reaction leading eventually to the small production of the volatile boranes B_5H_9 and $B_{10}H_{14}$. The main chain reaction is thought to be initiated by the bimolecular reaction between two B_6H_{10} molecules to give the radical $B_6H_9^{\cdot}$ by a process of B-H bond-rupture. When this reaction is inhibited, by the presence of a radical scavenger, reaction (12) becomes relatively more important and leads to the large initial production of trialkylboranes <u>via</u> hydroboration of $\{BH_3\}$. The mechanism for the polymerisation reaction is discussed in more detail elsewhere.[1] Further work is planned, to establish whether this side reaction is (as we would now predict) a first-order reaction as distinct from the main reaction which is second-order in B_6H_{10}.

<u>8. Cothermolysis of B_6H_{10} with Other Boranes</u>

Having established the nature of the B_6H_{10} self-thermolysis, cothermolysis reactions were attempted with B_2H_6, B_4H_{10}, B_5H_9,

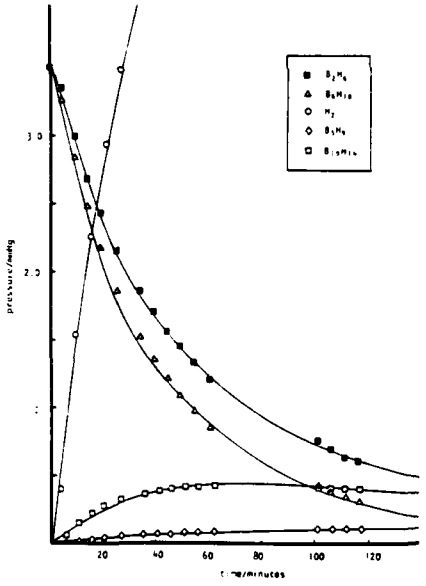

Figure 13. Concentration-time profile for a typical cothermolysis between B_6H_{10} (3.51 mmHg) and B_2H_6 (3.49 mmHg) at 425 K.

and B_5H_{11}.[1,15,31,32] It was found that in all cases except B_5H_9, the rate of consumption of B_6H_{10} was more rapid than in the self-thermolysis, clearly indicating that interactions were occurring. Typical concentration-time profiles for the B_6H_{10}/B_2H_6, B_6H_{10}/B_4H_{10}, and B_6H_{10}/B_5H_{11} cothermolyses are shown in Figures 13-15, respectively.

In the B_6H_{10}/B_2H_6 reaction (Figure 13.) the main boron-containing product is $B_{10}H_{14}$, which accounts in some cases for up to ca. 60% of the boron consumed. This compares with a value of less than ca. 5% in the thermolyses of either reactant alone. Hydrogen and B_5H_9 were also observed, together with trace amounts of B_8H_{12}, n-B_9H_{15}, and the higher boranes $B_{15}H_{23}$, and $B_{16}H_{20}$.

In the B_6H_{10}/B_4H_{10} cothermolysis (Figure 14.) the main products are seen to be H_2 and B_2H_6 together with moderate

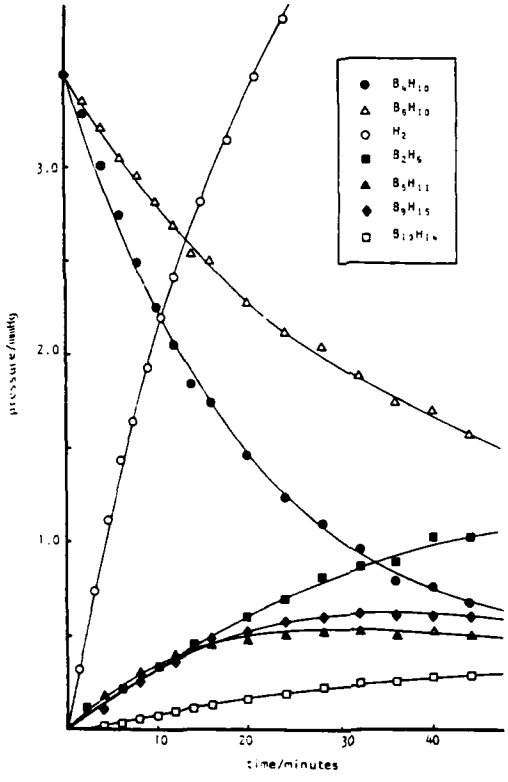

Figure 14. Concentration-time profile for a typical cothermolysis between B_6H_{10} (3.51 mmHg) and B_4H_{10} (3.51 mmHg) at 348.5 K.

amounts of pentaboranes (mainly B_5H_{11} in the early stages), B_9H_{15}, and $B_{10}H_{14}$. B_6H_{12} is also observed, but it appears somewhat later in this reaction than in the thermolysis of B_4H_{10} alone.

In the cothermolysis of B_6H_{10} and B_5H_{11} (Figure 15) the rates of consumption of the two reagents are essentially identical over the period studied (ca. 60 mins). The main products are B_2H_6 and H_2, together with smaller but significant amounts of the higher boranes B_8H_{12}, B_9H_{15}, and $B_{10}H_{14}$. Small amounts of B_4H_{10} are also observed in the early stages of the reaction. The rate of consumption of B_5H_{11} is marginally faster than that observed in the thermolysis of B_5H_{11} alone, but the rate of consumption of B_6H_{10} is increased by a massive 300/400-fold compared with its self thermolysis.

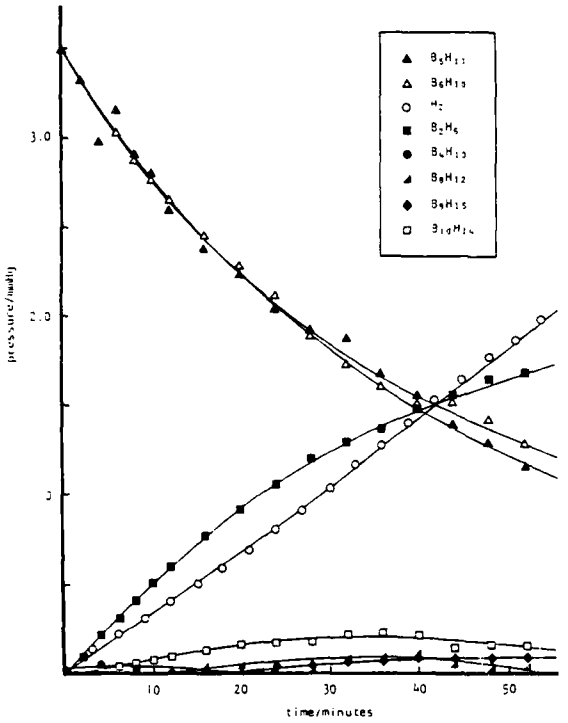

Figure 15. Cothermolysis of B_6H_{10} (3.50 mmHg) and B_5H_{11} (3.50 mmHg) at 347 K.

Detailed kinetic studies with B_2H_6[1,15,31] and B_4H_{10}[1,15,32] showed that in each case the rate was governed by the rate-

determining sequence of the co-reactant. Thus with B_2H_6 the reaction was found to be 3/2-order in B_2H_6 and zero-order in B_6H_{10}, whereas with B_4H_{10} the reaction was first-order in B_4H_{10} and zero-order in B_6H_{10}. The rate data for the disappearance of B_2H_6 and B_4H_{10}, when cothermolysed with B_6H_{10} are compatible with the Arrhenius plots for the self-reactions of these boranes (Figures 16 and 3, respectively). The activation energy for the

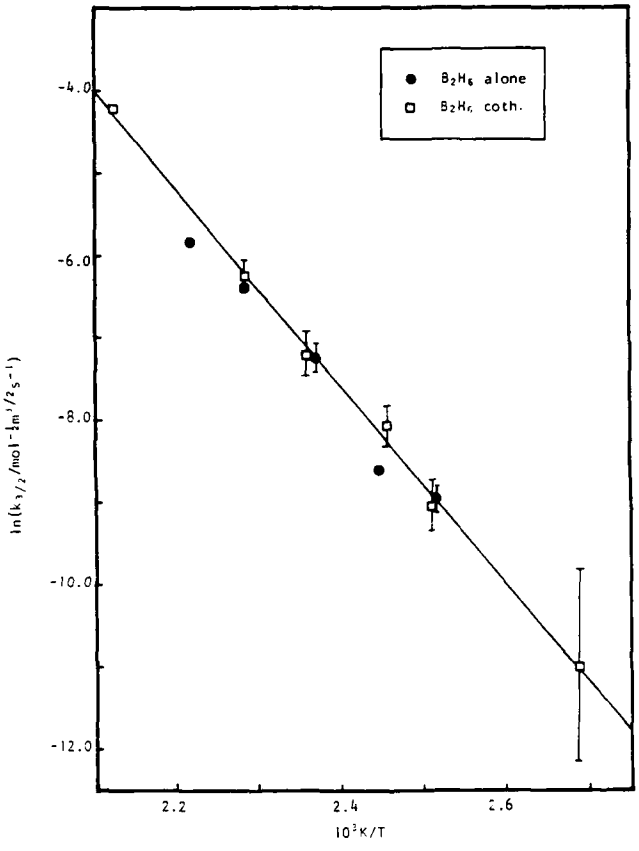

Figure 16. Comparison of Arrhenius plots for the thermal decomposition of B_2H_6 alone and in cothermolysis with B_6H_{10}.[15,31]

disappearance of B_2H_6 in the B_6H_{10}/B_2H_6 cothermolysis is 98.3 ± 3.9 kJ mol^{-1} compared with 92.3 ± 6.6 kJ mol^{-1} for the thermolysis of B_2H_6 alone.[15,31] This latter value was the result of a preliminary study involving measurements at only 5

temperatures. Our more recent definitive value of 102.6 ± 3.3 kJ mol^{-1} gives even closer agreement.[16] The activation energy for the disappearance of B_4H_{10} in the B_6H_{10}/B_4H_{10} cothermolysis is 88.6 ±6.1 kJ mol^{-1} compared with 99.2 ± 0.8 kJ mol^{-1} for B_4H_{10} alone. A considerable increase in the conversion of B_6H_{10} to $B_{10}H_{14}$ at the expense of polymeric solids was observed in both systems.

In the B_6H_{10}/B_2H_6 reaction, the observed order of 3/2 indicates that B_6H_{10} cannot react with either B_2H_6 itself or with $\{BH_3\}$; instead it must react with the $\{B_3H_7\}$ produced in step (3). This reaction, step (13), is therefore in successful competition with step (5).

$$\{B_3H_7\} + B_6H_{10} \longrightarrow B_9H_{15} + H_2 \qquad (13)$$

On this basis, if B_6H_{10} competes with 100% success for the $\{B_3H_7\}$, the absolute rate of consumption of B_2H_6 in the cothermolysis should be precisely half that in the decomposition of B_2H_6 alone. This is because step (5), i.e. the reaction between $\{B_3H_7\}$ and a second molecule of B_2H_6 to give B_4H_{10}, is now precluded. From the results in Figure 15 it would seem that, within the limits of experimental error, there is no detectable difference in the rates of the two reactions. This may be due in part to the fact that B_6H_{10} is not present in sufficient excess; however, from the observed spread in the data points at any particular temperature, it is apparent that the existing method does not yield absolute rates of sufficient accuracy to enable such small changes to be established with certainty. The answer to this important question must therefore await improvements in the basic method.

In this cothermolysis the temperature is too high for the B_9H_{15} produced in the suggested step (13) to survive, and it is presumed to decompose to $B_{10}H_{14}$. This reaction is known to occur, but isotope studies have shown that it does not take place in a single step.[33] The simplest proposed sequence of events,[25] reactions (14) - (16),

$$B_9H_{15} \longrightarrow B_8H_{12} + \{BH_3\} \qquad (14)$$

$$\{B_3H_7\} + B_8H_{12} \longrightarrow \{B_9H_{13}\} + B_2H_6 \qquad (15)$$

$$\{B_3H_7\} + \{B_9H_{13}\} \longrightarrow B_{10}H_{14} + B_2H_6 \qquad (16)$$

differs from that suggested originally[34]

In the B_6H_{10}/B_4H_{10} reaction B_9H_{15} is actually observed as a major product in the early stages of the reaction, because the temperatures required for this system are much lower than those required to achieve reaction between B_2H_6 and B_6H_{10}. A similar result has been observed in the reaction at much lower temperatures between B_4H_8CO and B_6H_{10},[34] and it seems likely that reaction (17) is responsible in each case.

$$[B_4H_8] + B_6H_{10} \longrightarrow B_9H_{15} + [BH_3] \qquad (17)$$

In the present cothermolysis, step (17) is presumed to be in competition with step (8).

The B_6H_{10}/B_5H_{11} system has not been investigated in the same detail as these two systems, but from the results mentioned earlier, it seems likely that the kinetics of this reaction are also governed by the rate-determining step in the B_5H_{11} decomposition, namely step (9). This would then be followed by step (17) to give B_9H_{15} etc. There is therefore a very strong affinity between B_6H_{10} and the reactive intermediates $[B_3H_7]$ and $[B_4H_8]$ produced in these thermolyses by the co-reactants B_2H_6 and B_4H_{10}/B_5H_{11}, respectively.

To test these competitive effects further, the effects of adding an excess of H_2 to the B_6H_{10}/B_2H_6 and B_6H_{10}/B_4H_{10} cothermolysis systems have been studied in some detail.[1,31,32] Remarkably, in a mixture containing B_2H_6 and B_6H_{10} at pressures of 1.77 and 3.5 mmHg, respectively, neither the rate of consumption of B_2H_6 nor the product distribution was found to be affected by the presence of an 8.4-fold excess of added H_2 (i.e. 15 mmHg). As discussed earlier, the rate of decomposition of B_2H_6 alone (3.5 mmHg, 423 K) is decreased by a factor of 3.4 in the presence of a 14-fold excess of added H_2. The inhibiting effect of added H_2 on the decomposition of B_4H_{10} was also reduced considerably by the presence of B_6H_{10}. For example, in a mixture containing B_4H_{10} (3.5 mmHg) and B_6H_{10} (7.0 mmHg), together with a 14-fold excess of added H_2 (50 mmHg), the rate was reduced by about a factor of 2, whereas in the absence of B_6H_{10} the rate is slowed by a factor of 5.6 in the presence of only a 5.7-fold excess of added H_2. These results confirm that B_6H_{10} competes effectively with H_2 for the reactive intermediates $[B_3H_7]$ and $[B_4H_8]$ in these systems.

9. Other Work

There are several areas of work which have been in progress in the laboratory during the Grant period that have been discussed in some detail elsewhere, and are therefore not elaborated on here. These include (i) synthesis of hexaborane(10) with a ^{10}B label in the base of the cluster (see 4th and 5th Periodic Reports),[35] (ii) study of the thermolysis of B_5H_{11}[6,15] and of B_6H_{10}[1,28] in hot/cold reactors, and (iii) preliminary work in which the changing composition of gas-phase mixtures, undergoing photolysis with an appropriate Hg vapour lamp have been monitored continuously by mass spectrometry.[1,28]

Summary

The results of this detailed study of kinetics and mechanisms of thermolysis and cothermolysis reactions of gaseous boron hydrides point to the involvement of three main processes in the initial stages of the various decompositions: elimination

of BH_3, elimination of H_2, and radical formation *via* B-H bond rupture (leading to the formation of solid hydride *via* chain polymerisation). The dissociation of B_2H_6 (step 1) and the initial steps in the thermolyses of the *arachno* boranes B_5H_{11}, B_6H_{12}, and B_9H_{15} (steps 9, 10, and 14, respectively) fall into the first of these three categories, and it is argued that, under certain conditions, *nido*-B_6H_{10} also has this mechanism available to it (step 12). By contrast, the first isolable borane B_4H_{10} and the reactive intermediate (B_3H_9) are thought to prefer the second mode of decomposition (steps 6 and 3). The only borane in the present study to fall into the third category, is B_6H_{10}.[38] There are indications in the literature that B_5H_9[37] and $B_{10}H_{14}$[38] may also decompose *via* radical intermediates at very high temperatures, but detailed evidence is lacking. When radical scavengers or electron-accepting species are present, B_6H_{10} is consumed in other ways (e.g. steps 13 and 17). B_6H_{10} is unique among the small binary boranes in its ability to behave as a strong two-electron donor, and it is thought to do this *via* the B-B bond in its basal plane. It has been suggested that this property is responsible for its failure to build up in any appreciable concentration in borane interconversion reactions,[24] and the kinetic studies add weight to this idea. BH_3 and H_2 groups are thought to be involved, not only in elimination reactions, but also in *addition* reactions leading to cluster aggregation (e.g. steps 2, 4, and 5); the exchange of BH groups (steps 8, 15, and 16) and the addition of B_3H_7 (steps 13 and 17) are also thought to be involved in these processes.

Literature Cited

1. N.N. Greenwood and R. Greatrex, "Kinetics and mechanism of the thermolysis and photolysis of binary boranes", *Pure and Appl. Chem.*, 1987, 59, 857-868; and refs. therein. This Plenary Lecture assesses much of the early work, and reviews progress in our own laboratory from 1980 through early 1987.
2. N.N. Greenwood and R. Greatrex, "Kinetics and mechanisms of borane interconversion reactions", *Chem. Revs.*, invited manuscript in preparation; and refs. therein. This is intended to be a comprehensive assessment of present knowledge in the area.
3. R. Greatrex, N.N. Greenwood, and G.A. Jump, "A kinetic study of the gas-phase thermolysis of hexaborane(10)", *J. Chem. Soc., Dalton. Trans.*, 1985, 541-548.
4. R. Greatrex, N.N Greenwood, and C.D. Potter, "A mass-spectrometric investigation of the exchange of deuterium with tetraborane(10) in the gas phase", *J. Chem. Soc., Dalton Trans.*, 1984, 2435-2437.
5. R. Greatrex, N.N. Greenwood, and C.D. Potter, "A kinetic study of the gas-phase thermolysis of tetraborane(10)", *J. Chem. Soc., Dalton Trans.*, 1986, 81-89.
6. M.D. Attwood, R. Greatrex, and N.N. Greenwood, "A kinetic study of the gas-phase thermolysis of pentaborane(11)", *J. Chem. Soc., Dalton Trans.*, 1989, 385-390.
7. M.D. Attwood, R. Greatrex, and N.N. Greenwood, "Influence of

added hydrogen on the kinetics and mechanism of thermal decomposition of tetraborane(10) and of pentaborane(11) in the gas phase",
J. Chem. Soc., Dalton Trans., 1989, 391-397.
8. R. Greatrex, N.N. Greenwood, and S.D. Waterworth, "Kinetics and mechanism of the thermal decomposition of hexaborane(12) in the gas phase",
J. Chem. Soc., Chem. Commun., 1988, 925-926.
9. R. Greatrex, N.N. Greenwood, and S.M. Lucas, "The identity of the rate-determining step in the gas-phase thermolysis of diborane: a re-investigation of the deuterium kinetic isotope effect",
J. Am. Chem. Soc., in the press.
10. T.P. Fehlner, in E.L. Muetterties (ed.)
Boron Hydride Chemistry, Academic Press, New York, 1975, 175-196.
11. J.F. Stanton, W.N. Lipscomb, and R.J. Bartlett,
J. Am. Chem. Soc., 1989, 111, 5165 - 5173.
12. R.E.Enrione and R. Schaeffer,
J. Inorg. Nuclear Chem., 1961, 18, 103-107.
13. R.P.Clarke and R.N. Pease,
J. Am. Chem. Soc., 1951, 73, 2132 - 2134.
14. L.V. McCarty, P.A. DiGorgio,
J. Am. Chem. Soc., 1951, 73, 3138 - 3143.
15. M.D. Attwood, PhD Thesis, "Gas-phase thermolysis and cothermolysis of boron hydrides", University of Leeds, 1987.
16. J.F. Stanton and W.N. Lipscomb, private communication.
17. R. Schaeffer,
J. Inorg. Nucl. Chem., 1960, 15, 190 - 193.
18. R. Schaeffer and F.N. Tebbe, "Synthesis of a boron-labelled tetraborane",
J. Am. Chem. Soc., 1962, 84, 3974.
19. G.L. Brennan and R. Schaeffer,
J. Inorg. Nuclear Chem., 1961, 20, 205 - 210.
20. J.A. Dupont and R. Schaeffer,
J. Inorg. Nuclear Chem., 1960, 15, 310 - 315.
21. S.J. Cranson, P.M. Davies, R.Greatrex, D.W.H. Rankin, and H.E. Robertson, "Electron diffraction study of tetraborane(8) carbonyl in the gas phase: structure determination of an endo/exo isomeric mixture",
J. Chem. Soc., Dalton Trans., in the press.
22. R. Greatrex, N.N. Greenwood, D.W.H. Rankin, and H.E. Robertson, "The molecular structures of pentaborane(9) and pentaborane(11) in the gas phase as determined by electron diffraction",
Polyhedron, 1987, 6, 1849-1858.
23. R. Greatrex, N.N. Greenwood, M.B. Millikan, D.W.H. Rankin, and H.E. Robertson, "The molecular structure of hexaborane(12) in the gas phase as determined by electron diffraction",
J. Chem. Soc., Dalton. Trans., 1988, 2335-2339.
24. R. Greatrex, N.N. Greenwood, and S.D. Waterworth, unpublished results.
25. L.H. Long,

J. Inorg. Nucl. Chem., 1970, 32, 1097-1113.24.
26. R. Schaeffer,
Pure Appl. Chem., 1974, 4, 1-11.
27. R. Greatrex, N.N. Greenwood, and G.A. Jump,
"Kinetics and mechanisms of thermolytic interconversions of boron hydrides",
Final Technical Report, AD-A143525/4.
28. P.M. Davies, PhD Thesis, University of Leeds, 1989.
29. P.M. Davies, R. Greatrex, N.N.Greenwood, and D. Singh,
Unpublished results.
30. K.J. Laidler, Chemical Kinetics, 3rd Edition, Harper and Row, New York, 1987.
31. M.D. Attwood, R. Greatrex, N.N. Greenwood, and C.D. Potter,
"A Kinetic study of the cothermolysis reaction of hexaborane(10) with diborane(6) in the gas phase",
Unpublished results, manuscript in preparation.
32. M.D. Attwood, R. Greatrex, and N.N. Greenwood, "Kinetic studies of the cothermolysis of hexaborane(10) with tetraborane(10) and other binary boranes",
Unpublished results, manuscript in preparation.
33. R. Maruca, J.D. Odom, and R. Schaeffer,
Inorg. Chem., 1968, 7, 412 - 418.
34. J. Rathke and R. Schaeffer,
Inorg. Chem., 1974, 13, 3008 - 3011.
35. S.M. Lucas, MSc Thesis, "The use of isotopic labels in boron hydride chemistry", University of Leeds, 1987.
36. T.J. Houser and R.C. Greenhough,
Chem. and Ind., 1967,323 - 324.
37. H.C. Beachell and J.F. Haugh,
J. Am. Chem. Soc., 1958, 80, 2939 - 2942.

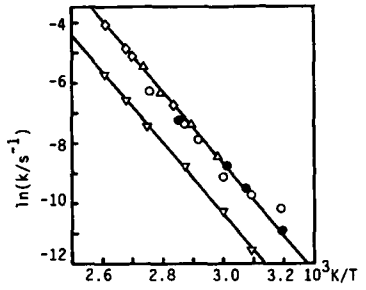

Fig.3. Arrhenius plot for thermolysis of B_4H_{10} alone ●, with CO ◇ (ref. 2e) with B_2H_6 △ (ref. 2a) and with B_6H_{10} ○. The lower set of points ▽ refers to thermolysis of B_4H_{10} in the presence of an excess of H_2

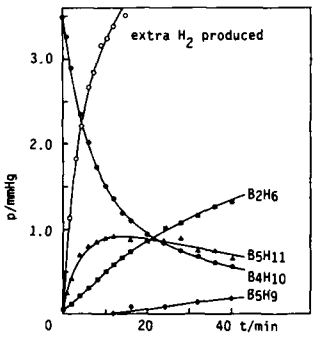

Fig. 4. Reaction profile for the cothermolysis of a mixture of B_4H_{10} (3.5 mmHg) and H_2 (20 mmHg) at 100 °C; the curve for H_2 represents the extra H_2 generated during the reaction

The detailed product analysis of this cothermolysis of (B_4H_{10} + $6H_2$) is illustrated by the typical reaction profile in Fig. 4 : the relative rates of B_5H_{11} production to B_4H_{10} consumption are unaltered from those of the thermolysis of B_4H_{10} alone, whereas there is a marked increase in the relative rate of production of B_2H_6 and almost complete inhibition of 'polymer' formation. The most striking effect is the complete absence of volatile higher boranes such as B_6H_{12} and $B_{10}H_{14}$.

All the effects of added H_2 can be interpreted on the basis of reactions already discussed. The inhibition is brought about by the increased importance of the back-reaction (-5a) which is in competition with the production of B_5H_{11} via reaction (6). The relative increase in the rate of production of B_2H_6 undoubtedly stems from the removal of the {B_3H_7}, concurrently formed in step (6), via (-3) and (-2) in conjunction with (-1). The rapid removal of {B_3H_7} likewise explains both the inhibition of polymer formation via reaction (7a) and/or (7b), and also the inhibition of B_6H_{12} formation, which probably arises in the normal thermolysis via reactions (8) and/or (9):

$$\{B_3H_7\} + B_5H_{11} \longrightarrow B_6H_{12} + B_2H_6 \qquad (8)$$

$$\{B_4H_8\} + B_5H_{11} \longrightarrow B_6H_{12} + \{B_3H_7\} \qquad (9)$$

For reasons already outlined the alternative suggested route to B_6H_{12} (namely $2\{B_3H_7\} \longrightarrow B_6H_{12} + H_2$) seems less likely though this would also be suppressed by added H_2.

THERMOLYSIS OF B_5H_{11} ALONE AND WITH ADDED H_2

Although there have been several reports in the past of qualitative studies dealing with the thermolysis of B_5H_{11} (refs. 15b, 19, 30, 31), not all of which agree about the details, there has been no attempt to establish the kinetics of this reaction. Our own work is still in progress (ref. 21) but we can report some of the main findings and their implications.

The thermolysis of pure B_5H_{11} at pressures of 1.8-10.4 mmHg and temperatures in the range 60-150 °C is found to be first-order in B_5H_{11} with an activation energy of 73.2±3.7 kJ mol^{-1} and a pre-exponential factor of 1.65×10^7 s^{-1}. The main volatile products are H_2 and B_2H_6, and these appear at rates of approximately 1 and 0.5 mole per mole of B_5H_{11} consumed. A small 'steady-state' concentration of B_4H_{10} is also present but, in agreement with the earlier work of Burg and Schlesinger (ref. 30), B_5H_9 is not detected in the initial stages. Others have claimed that B_5H_9 is formed from the outset (refs. 15b and 19) but we find that it builds up rather slowly as the reaction proceeds. $B_{10}H_{14}$ is also produced in low concentration, but as much as 50% of the boron ends up as solid 'polymer'.

The initial step in the decomposition is generally held to be the reversible dissociation (10),

$$B_5H_{11} \rightleftharpoons \{B_4H_8\} + \{BH_3\} \qquad (10)$$

and our own observations are entirely consistent with this being the rate-determining step. The initial rate of production of B_2H_6 is then readily explained by its formation from {BH3}

via reaction (-1) in ca. 100% yield. The fate of the {B_4H_8} produced in reaction (10) is less obvious. Long has conjectured (ref. 5) that it may react with itself to produce {B_3H_7} and B_5H_9, and subsequently with the {B_3H_7} to produce B_2H_6 and more B_5H_9. This would account for the B_5H_9, but would not explain its absence in the early stages. Moreover, there is as yet no direct evidence for such reactions, and in the preceding section we argued against their involvement in the B_4H_{10} thermolysis, in which {B_4H_8} features prominently. Lipscomb has calculated that the reaction of {B_4H_8} with B_5H_{11} to give B_4H_{10} is exothermic by 125.5 kJ mol^{-1}, and has suggested that this may be an important route to B_5H_9 (ref 4c). As Lipscomb has pointed out, at the temperatures required to decompose B_5H_{11}, B_4H_{10} would be decomposed to {B_4H_8} and H_2, so that {B_4H_8} is essentially a catalyst for the loss of H_2 from B_5H_{11} in this reaction. Whilst this reaction may contribute to the production of B_5H_9 and B_4H_{10} in this thermolysis, it is clear from the evidence that it is not a major sink for the {B_4H_8} produced in reaction (10). An alternative possibility is that {B_4H_8} and B_5H_{11} react to form n-B_9H_{15} via reaction (11). An advantage of this step is that it would nicely explain the

$$\{B_4H_8\} + B_5H_{11} \longrightarrow \text{n-}B_9H_{15} + 2H_2 \qquad (11)$$

observed very high initial production of H_2. The n-B_9H_{15} is presumed to be unstable under the prevailing conditions, decomposing via B_8H_{12} (see later) to produce 'polymer' and $B_{10}H_{14}$. Reaction (11) was used by Long (ref. 5) to explain the observation (ref. 32) that n-B_9H_{15} is the main product when B_5H_{11} and B_2H_6 are held together under pressure at room temperature for a few days. The B_2H_6 in this reaction was regarded as playing the dual role of increasing the {B_4H_8} concentration by syphoning off the {BH_3} molecules formed in (10), and stabilizing the n-B_9H_{15} via the reversible reaction with B_8H_{12} (ref. 5). We intend to test the possibility that reaction (11) is operative, by thermolysing B_5H_{11} under hot/cold conditions in an attempt to stabilize the n-B_9H_{15} as it is formed.

It is of interest to compare the Arrhenius parameters for B_5H_{11} with those for B_4H_{10}, and to consider the wider implications of the results. The value of 6×10^{11} s^{-1} recorded above for the pre-exponential factor for B_4H_{10} is reasonable for a unimolecular reaction (ref. 33) and is consistent with the proposed mechanism in which H_2 is ejected via a loosely bound transition state. The value for B_5H_{11} is lower by more than 4 orders of magnitude (1.6×10^{7} s^{-1}) and this inmplies considerable re-organization to a tightly bound transition state. This is consistent with the more dramatic structural changes which accompany the release of a BH_3 group from the cluster , and it will be of interest to see whether this behaviour is mirrored in the B_6H_{12} thermolysis, which we are also currently investigating. The considerably greater activation energy for B_4H_{10} compared with that for B_5H_{11} reflects a more dramatic temperature dependence of the rate constant for the former, and, from the initial rate laws, the ratio $k_{B_4H_{10}}/k_{B_5H_{11}}$ is found to vary from ~48.9 at 200 °C to ~1.67 at 40 °C. In consequence, at the lower temperatures, the rate of decomposition of the B_5H_{11} produced in the thermolysis of B_4H_{10} is only slightly less than the rate of decomposition of B_4H_{10} itself. There is therefore a need for caution in interpreting the initial-rate data in terms of possible stoichiometries for the reaction. In the light of this new information it may seem surprising that B_5H_{11} builds up to the extent that it does in the B_4H_{10} thermolysis, but it must be remembered that both {B_4H_8} and {BH_3}, the initial products of the decomposition of B_5H_{11} [see reaction (10)], themselves react further with B_4H_{10} to regenerate B_5H_{11} [reactions (6) and (-12)].

It has often been suggested (refs. 2a, 22, 30) that B_5H_{11} and B_4H_{10} are interconvertible in the presence of H_2, according to the 'equilibrium' (12). However, it was not clear whether

$$B_5H_{11} + H_2 \rightleftharpoons \tfrac{1}{2}B_2H_6 + B_4H_{10} \qquad (12)$$

the forward reaction (12) occurred as a single step (i.e. BH abstraction by H_2 from B_5H_{11} to give {BH_3}) or as a combination of reactions (10) and (-5a). We have now established unequivocally that the latter is the case, by studying the thermolysis of B_5H_{11} in the presence of added H_2 over a wide range of temperature (ref. 21). The rate of thermolysis was found to be largely unaffacted by the presence of an excess of H_2 (see Fig. 5), suggesting that the rate-determining step remains the same, i.e. reaction (10).

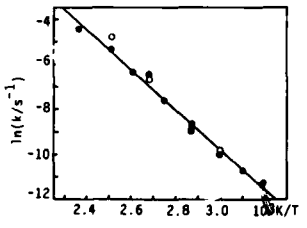

Fig. 5. Arrhenius plot for thermolysis of B_5H_{11} at a pressure of 3.5 mmHg alone ●, and with 50 mmHg added H_2 o

Pure & Appl. Chem., Vol. 59, No. 7, pp. 857–868, 1987.
Printed in Great Britain.

Kinetics and mechanism of the thermolysis and photolysis of binary boranes

Norman N. Greenwood and Robert Greatrex

School of Chemistry, The University, Leeds LS2 9JT, England

Abstract - The mechanisms by which gaseous boron hydrides so readily interconvert and build up into larger clusters has excited considerable academic and industrial interest for several decades. This paper describes recent progress that has been made in unravelling this complex series of interconversion reactions. Initial reaction rates have been studied mass spectrometrically to obtain rate equations, orders of reaction and energies of activation. Detailed and continuous product analysis for H_2 and all the volatile boranes formed, coupled with a study of cothermolysis reactions of selected pairs of boranes gives further insight into the processes occurring. Crucial aspects of the thermolysis of B_2H_6, B_4H_{10}, B_5H_{11}, and B_6H_{10} are discussed, as are the effects of added H_2 and the cothermolysis of B_6H_{10} with alkenes. The final section presents data on the UV absorption spectra and photolytic stability of eight volatile boranes and the reaction kinetics of B_6H_{10} photolysis.

INTRODUCTION

The facile interconversion of the binary boranes in the gas phase at room temperature or slightly above has excited attention from the earliest days of boron hydride chemistry (ref.1). The intriguing ability of the smaller boranes such as B_2H_6, B_4H_{10}, and B_5H_{11} to interconvert by reaction with themselves and with each other, and their ability to aggregate further into larger and more complex borane clusters has been a dominant (and particularly useful) feature of their chemistry. Indeed, the reactions occurring in gaseous mixtures of boron hydrides probably comprise one of the most complex sequences of interconnected reactions to have yet been studied in any detail in the whole of chemistry. Progress has been slow, not only because of the inherent complexity of the system, but also because of the difficulty of handling these highly reactive air-sensitive species and because of problems associated with the quantitative analysis of products formed during the course of the reactions. The elegant series of papers by Riley Schaeffer and his group (ref. 2), the penetrating and perceptive contributions by Tom Fehlner and his group (ref. 3), and the sophisticated high-level calculations of structure variants and reaction energy-profiles by Bill Lipscomb (ref. 4) are among the landmarks of the story so far, though many others have made notable contributions. As always in the uncertain world of reaction mechanisms it has proved difficult to build a firm foundation of pertinent experimental evidence on which to construct a reliable model for the system. False starts abound, and unsuspected limitations in experimental techniques have been compounded by erroneous deductions from flawed data. However, consensus has emerged concerning the earliest stages of the thermolysis of diborane to give B_4H_{10} as the first isolable intermediate, followed by B_5H_{11}. An alternative interpretation (ref. 5) has not found acceptance partly because some of the key pieces of experimental evidence on which the analysis was crucially dependent have subsequently been found to be incorrect (refs. 3,4,6,7).

The ready thermolytic interconversion and aggregation of the gaseous boranes should not be taken to imply that the bonds holding the atoms together are inherently weak. The opposite is the case: B-B and B-H bonds are amongst the strongest two-electron bonds known, and the great reactivity of the boranes is to be sought rather in the availability of alternative structures and vacant orbitals of similar energies. Some comparative data are in Table 1. The first pair of columns lists the heats of atomization of hydrogen, boron, and carbon on which the derived bond-enthalpy contributions in the rest of the Table ultimately depend. The value of $\Delta H^\circ f,298$ for H(g) is the enthalpy of dissociation of $\frac{1}{2}H_2(g)$, i.e. it is half the value of the single-bond dissociation energy E(H-H). Refinements which incorporate corrections for zero-point energy etc. can be neglected at this level of precision. The value for C(g) refers to the enthalpy of atomization of diamond and can be equated to E(C-C) for that material. The value for B(g) has been the subject of some uncertainty but there is now a consensus that it lies close to 566±15 kJ mol^{-1}.

Intercomparison of the next two columns of data in Table 1 shows that the two-electron-bond dissociation energies (or more properly the bond-enthalpy contributions, $\bar{E}$ for B-B in boranes and C-C in C_2H_6 are essentially the same (≈332 kJ mol^{-1}); likewise the value of 380 kJ mol^{-1} for BBB(3c,2e) is similar to that for $\bar{E}$(B-C) in BMe_3 (372 kJ mol^{-1}). The value of

TABLE 1. Some enthalpies of atomization ($\Delta H°_{f,298}$) and comparative bond-enthalpy contributions, $\bar{E}(X-Y)$

$\Delta H°_{f,298}$/kJ mol^{-1} (refs.8,9)		$\bar{E}(X-Y)$/kJ mol^{-1} (ref. 9)		$\bar{E}(X-Y)$/kJ mol^{-1} (refs. 8,10)	
H(g)	½x436	B-B(2c,2e)	332	C-C	331[a]
B(g)	566	BBB(3c,2e)	380	B-C	372[b]
C(g)	356	B-H(2c,2e)	381	C-H	416
		BHB(3c,2e)	441	H-H	436

[a]Value derived for C-Me in C_2H_6; this is slightly lower than the value of 356 kJ mol^{-1}for the heat of atomization of diamond.
[b]Value derived for B-Me in BMe_3; similar values are obtained from BEt_3, BBu_3, and BCy_3, but the values for B-Ph from BPh_3 and Ph_2BCl etc. are significantly higher (444, 485 kJ mol^{-1}): this has been ascribed to additional p_π-bonding (ref. 11).

381 kJ mol^{-1} for $\bar{E}$(B-H) is also similar, though slightly less than that for $\bar{E}$(C-H) (416 kJ mol^{-1}) whereas the value for BHB(3c,2e) is slightly greater than the values for $\bar{E}$(C-H) (in CH_4) and E(H-H) in H_2. It should be emphasized that the tabulated bond-enthalpy contributions for the boranes are to be regarded as approximate indications rather than as precisely determined invariant values. The reasons for this have been fully discussed, most recently in ref. 7. In particular there are insufficient experimental (or theoretically computed) data to establish the transferability of bond-enthalpy parameters from one borane to another. Indeed, the known substantial variability of B-B, B-H, and BHB interatomic distances in the boranes almost certainly implies some variability in the bond-enthalpy terms in the various borane clusters. For example, the experimentally observed range of B-B distances in binary boranes (from 160 to 200 pm) might well reflect a decrease by more than a factor of 2 (to 40%) in the corresponding B-B bond-enthalpy contributions (ref. 12). The data in Table 1 do, however, establish the robustness of the various interatomic linkages in borane clusters.

In seeking to extend our understanding of the reactions occurring during the mild thermolysis of gaseous boron hydrides we have developed a mass-spectrometric method of monitoring separately both the evolution of dihydrogen and the growth and decay of all volatile boranes in the system without disturbing the course of the reaction (refs. 13, 14). By studying the initial rates of reaction over a range of temperature and pressure it has been possible to derive rate equations, and activation energies. Moreover, the detailed and continuous product analysis as a function of time, coupled with a study of several cothermolyses of selected boranes,gives further insight into the processes occurring. In the following section, results on the thermolysis of B_2H_6 will be briefly reviewed. This will be followed by more substantial sections on the thermolysis of B_4H_{10}, B_5H_{11} and B_6H_{10} alone, and their cothermolysis with dihydrogen (or deuterium) and other boranes. The cothermolysis of B_6H_{10} with alkenes is also discussed. The paper ends with a section describing some preliminary studies on the photolytic reactions of boranes.

THERMOLYSIS OF DIBORANE

The thermal decomposition of B_2H_6 was first studied kinetically in 1951 (ref. 15) and since then there have been numerous independent studies of the system (see references cited in ref. 5, and also refs. 2j, 3e, 13, 16-19). At various times the derived order of the reaction has been thought to be ½, 1, 3/2, 2, 5/2, or variable, but there is now general acceptance that, for the homogeneous gas-phase thermolysis of B_2H_6 in the pressure range of 10-760 mmHg and the temperature range 50-200 °C, the order of the initial stages of the reaction is 3/2. This suggests that a triborane species is involved in the rate-determining step and the currently favoured mechanism envisages a three-step process:

$$B_2H_6 \rightleftharpoons 2\{BH_3\} \quad (1)$$

$$\{BH_3\} + B_2H_6 \rightleftharpoons \{B_3H_9\} \quad (2)$$

$$\{B_3H_9\} \xrightarrow{\text{slow}} \{B_3H_7\} + H_2 \quad (3)$$

The dissociation equilibrium (1) generates the reactive intermediate $\{BH_3\}$; this reacts with more B_2H_6 (step 2) to generate $\{B_3H_9\}$ which then loses dihydrogen in the rate-determining step (3). Theoretically-calculated reaction profiles have raised the possibility that the formation of $\{B_3H_9\}$ by step (2) rather than its decomposition by step (3) is the rate-determining process (ref. 4c) but this can be discounted on the cogent grounds that under the experimental conditions obtaining during the thermolysis of B_2H_6, the 'observed' rate of (2) is some 10^3-times faster than that of reaction (3) (ref. 3e). There is now also good experimental evidence for the reactive intermediates $\{BH_3\}$ and $\{B_3H_7\}$ under appropriate conditions (refs. 3, 16, 20).

We have reinvestigated this system (ref. 21) primarily to obtain a reliable set of comparative rate data for use in subsequent cothermolysis work and to check the order and activation energy of the initial reaction with our own mass-spectrometric techniques. In agreement with earlier studies, the major products of the thermolysis of diborane at temperatures between 120-150 °C were found to be H_2, B_5H_{11}, B_5H_9, and $B_{10}H_{14}$ together with smaller amounts of B_4H_{10} and traces of B_6H_{10}, B_6H_{12}, B_8H_{12}, and B_9H_{15}. There was no evidence for heptaboranes or $B_{20}H_{26}$ under these conditions. Reaction orders (determined from initial rates) both for B_2H_6 loss and H_2 production were close to 3/2. From the B_2H_6 data the activation energy E_A was 92.3±6.6 kJ mol^{-1} and the preexponential factor A was 1.58x10^8 m$^{3/2}$ mol$^{-\frac{1}{2}}$ s^{-1}. The correponding Arrhenius parameters from the initial rates of H_2 production were somewhat higher (E_A =113.0±7.3 kJ mol^{-1} and A = 3.08x10^{10} m$^{3/2}$ mol$^{-\frac{1}{2}}$ s^{-1}) possibly because the H_2 data measure not only the homogeneous gas-phase reaction but also a contribution from the heterogeneous decomposition of the solid hydride deposited on the surface of the reaction vessel.

Added H_2 is known to inhibit the decomposition of B_2H_6 (ref. 15a) and to alter the product distribution in favour of volatile boranes (ref. 15c). This inhibition is expected from the form of the rate-determining step (3) above and we have begun a quantitative evaluation of the effect. For example, the initial rate of decomposition of B_2H_6 at 3.5 mmHg and 150 °C is decreased by a factor of 3.4 in the presence of a 14-fold excess of H_2. Further quantitative work is planned in this area.

THERMOLYSIS OF B_4H_{10} AND ITS EXCHANGE WITH D_2

There is now little doubt that B_4H_{10} is the first isolable species in the thermolysis of B_2H_6 (ref. 2c). It is formed via reaction (4), though under normal thermolytic conditions

$$\{B_3H_7\} + B_2H_6 \longrightarrow B_4H_{10} + \{BH_3\} \qquad (4)$$

it is itself too unstable to be readily observed. Its thermolysis, like that of B_2H_6, has been the subject of numerous studies (refs. 2a, 2e, 5, 22-25) but there has been controversy on almost every aspect of its kinetics and mechanism of decomposition (see ref. 6 for detailed references). An early kinetic study (ref. 22) suggested that B_4H_{10} might decompose by two simultaneous unimolecular paths (5a and 5b):

$$B_4H_{10} \rightleftharpoons \{B_4H_8\} + H_2 \qquad (5a)$$

$$B_4H_{10} \rightleftharpoons \{B_3H_7\} + \{BH_3\} \qquad (5b)$$

Subsequently there was an accumulation of mass-spectrometric, kinetic, and chemical evidence (summarized in ref. 6) in favour of (5a) as the initial step in the decomposition, but this was offset by isotope-exchange studies which purported to establish the alternative route (5b). Most disconcertingly, the apparent absence of H/D exchange between B_4H_{10} and D_2 (ref. 26) led to the rejection of (5a) as an acceptable reaction step in the thermolytic decomposition of B_4H_{10} (refs. 5, 26).

An early attempt to resolve this discrepancy (ref. 27) was inconclusive, but we have subsequently been able to demonstrate (ref. 6) unequivocally that a mixture of stoichiometry B_4H_{10}:3D_2 undergoes rapid and extensive exchange at 42 °C (a temperature at which the rate of thermal decomposition of B_4H_{10} itself in the presence of hydrogen is immeasurably small). The possibility that the exchange might occur via reaction (5b) in conjunction with the reverse of reaction (3), i.e. $\{B_3H_7\} + D_2 \longrightarrow \{B_3H_7D_2\}$, can be ruled out at these temperatures since the subsequent decomposition of the postulated isotopomer of $\{B_3H_9\}$ is the rate-determining step (3) in the decomposition of B_2H_6 which does not occur appreciably below 100 °C. Reaction (5a) is therefore established as the sole (or vastly predominant) initial step in the thermolysis of B_4H_{10}. This conclusion, which is entirely consistent with Riley Schaeffer's earlier views on this system, is however at odds with another more recent study on the thermolysis of B_4H_{10} which has been interpreted in terms of a 3/2-order process predominant below 60 °C and involving reaction (5b) as the initiating step in a speculative chain mechanism (ref. 23). We therefore undertook a detailed reexamination of the thermolysis of B_4H_{10} in the pressure range 0.9-39 mmHg and at temperatures in the range 40-78 °C (ref. 25).

The main volatile products of the thermolysis of B_4H_{10} under these conditions were found to be initially H_2 and B_5H_{11}, with smaller amounts of B_2H_6, B_6H_{12}, and $B_{10}H_{14}$ each after an induction period, (see Figs. 1 and 2). There was no evidence for significant amounts of B_5H_9 or B_6H_{10}. From log-log plots of the initial rate of B_4H_{10} consumption, as well as those for the production of B_5H_{11} and H_2, it is clear that the initial reaction follows first-order kinetics. Derived activation energies for the three sets of data were $E_A(B_4H_{10})$ = 99.2±0.8, $E_A(B_5H_{11})$ = 98.8±1.8, and $E_A(H_2)$ = 107.5±1.9 kJ mol^{-1}, the value from the H_2-data again being slightly higher (as was the case for B_2H_6 in the previous section). The pre-

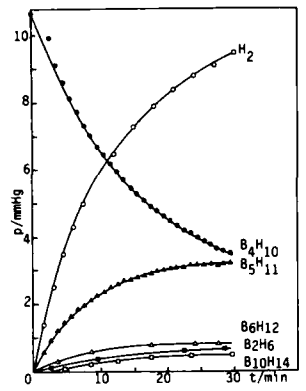

Fig. 1. Reaction profile for thermolysis of B_4H_{10} at 10.7 mmHg and 78 °C

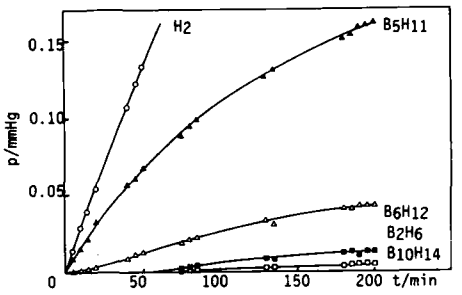

Fig.2. Reaction profile at high spectrometer gain showing build-up of the volatile boranes during the initial stages of thermolysis of B_4H_{10} at 3.9 mmHg and 40.2 °C

exponential factor for the first-order disappearance of B_4H_{10} was $A \approx 6 \times 10^{11}$ s^{-1}. These results are plotted in Fig. 3 together with earlier data from Schaeffer's group on the cothermolyses of B_4H_{10} with B_2H_6 and CO (refs. 2a,e). The fact that all the data fall on a single line (upper trace) thus confirms and extends this earlier work and leaves little doubt that the same rate-controlling step (5a) is involved in all three reactions. First-order kinetics would be preserved if this 'slow' step (5a) were followed rapidly by (6) and perhaps (7a) (ref. 25) though the alternative (7b) invoked by Sheldon Shore and his coworkers in a different context (ref. 28) may be preferable (see later).

$$\{B_4H_8\} + B_4H_{10} \longrightarrow B_5H_{11} + \{B_3H_7\} \quad (6)$$

$$\{B_3H_7\} + \{B_3H_7\} \longrightarrow \{'B_6H_{14-2m}'\}_{(polymerizes)} + mH_2 \quad (7a)$$

$$\{B_3H_7\} + \{B_3H_7\} \longrightarrow B_4H_{10} + \{'B_2H_4'\}_{(polymerizes)} \quad (7b)$$

In addition to the initial homogeneous gas-phase decomposition of B_4H_{10} to H_2 and B_5H_{11} (equations 5a and 6) and the formation of solid 'polymer', other boranes (first B_6H_{12} then B_2H_6 and $B_{10}H_{14}$) are formed after various periods of induction (Fig. 2 above). Others (refs. 5 and 29) have suggested that B_6H_{12} might result from the interaction of two $\{B_3H_7\}$ fragments but in the present system the observed induction period suggests that it is more likely to arise from a cothermolysis reaction involving B_5H_{11}. Likewise, the virtual absence of B_2H_6 in the early stages of the reaction is very significant because it suggests (ref. 25) that a number of steps that have been proposed in the past do not occur in this system. Thus, it is clear that, under these conditions, $\{B_2H_7\}$ formed in reaction (6)] does not react with B_4H_{10} to give B_5H_{11} and B_2H_6, or with $\{B_4H_8\}$ to give B_5H_9 and B_2H_6, or with itself to give $\{B_4H_8\}$ and B_2H_6, though all these reactions have previously been proposed (ref. 5). Likewise, the self-reaction of $2\{B_4H_8\}$ to form either B_6H_{10} and B_2H_6 or B_5H_9 and $\{B_3H_7\}$ are also ruled out on this basis, and their reaction to form, B_5H_{11} and $'B_3H_5$(polymer)', for which their is good evidence in a different context (ref. 28) is unlikely to be an important route in the presence of a vastly greater concentration of B_4H_{10}.

One further consequence of the recognition of reaction (5a) as the rate-determining step in the thermolysis of B_4H_{10} is the corollary that an excess of H_2 should inhibit the decomposition of B_4H_{10} and increase proportionately its conversion to B_5H_{11} and B_2H_6 [via reaction (6) and the reverse of reactions (1)-(3)] at the expense of the formation of involatile solids. Indeed, there are qualitative observations to this effect in the early literature (refs. 22, 30). We wished to put these observations on a more quantitative basis and accordingly, we thermolysed a mixture of B_4H_{10} (3.5 mmHg) and H_2 (20 mmHg) at temperatures in the range 50-110 °C. The results are included in Fig. 3 (lower line) from which it is apparent that the activation energy remains unaltered though the absolute rate of the decomposition has diminished by a factor of ~5 (ref. 21). These observations provide cogent additional evidence that B_4H_{10} decomposes via the single rate-determining initial step (5a) since, if (5b) also occurred, suppression of (5a) would inevitably alter the observed activation energy towards that of (5b) which is most unlikely to be fortuitously identical to that of (5a).

THERMOLYSIS AND COTHERMOLYSIS REACTIONS OF B_6H_{10}

A particularly intriguing aspect of the thermolysis of B_2H_6 is the virtual absence of hexaboranes and other species intermediate between the pentaboranes and $B_{10}H_{14}$. Schaeffer has suggested (ref. 2j) that B_6H_{10} may play a crucial role by virtue of its known tendency (albeit under somewhat different conditions) to react as a Lewis-base (refs. 34,35) with a Lewis-acid borane intermediates such as {BH_3}, {B_3H_7}, {B_4H_8}, B_8H_{12}, and {B_9H_{13}} to produce larger boranes such as $B_{13}H_{19}$, $B_{14}H_{22}$, and $B_{15}H_{23}$. Just how important this role is will depend on the extent to which B_6H_{10} is actually produced in the B_2H_6 decomposition, and at present this is simply not known. Under certain conditions {BH_3} can react with B_5H_9 to produce a hexaborane (ref. 3d), though this was not specifically identified as B_6H_{10}, and Long (ref. 5) has proposed several possible routes involving the reactive intermediates {B_3H_7} and {B_4H_8} e.g. {B_3H_7} + B_5H_9 ⟶ B_2H_6 + B_6H_{10}, 2{B_4H_8} ⟶ B_2H_6 + B_6H_{10}, and {B_4H_8} + B_5H_9 ⟶ {B_3H_7} + B_6H_{10}. It is also established that B_8H_{12} decomposes via the first-order reaction (13) to give B_6H_{10} and solid polymer (ref. 2g). We are at present

$$B_8H_{12} \longrightarrow B_6H_{10} + B_2H_2 \text{ (polymerizes)} \qquad (13)$$

devising ways of testing some of these steps experimentally, but in the meantime, to establish the likely behaviour of B_6H_{10} under gas-phase thermolytic conditions, we have carried out systematic studies of its thermolysis, both alone, and in the presence of other species.

The gas-phase thermolysis of B_6H_{10} for pressures in the range 1-7 mmHg and temperatures between 75 and 165 °C was found, perhaps surprisingly, to proceed by a second-order process, with an activation energy of 79.7±2.7 kJ mol^{-1} and a pre-exponential factor of 4.7×10^6 m^3 mol^{-1} s^{-1} (ref. 14). In the initial stages a typical reaction produces 1 mole of H_2 per mole of B_6H_{10} consumed, and deposits some 90% of the reacted borane from the gas phase as a yellowish non-volatile solid hydride of approximate composition $BH_{1.33}$, which then loses more H_2 to give an insoluble, intractable solid of composition BH_x (where x is ~1.0). Minor amounts of B_5H_9 and $B_{10}H_{14}$ in an approximate molar ratio of 5:1 are also produced. B_2H_6, B_8H_{12}, B_9H_{15}, as well as B_{13}, B_{14}, and B_{15} species are detected only in trace amounts at various stages of the reaction and do not accumulate in the gas phase. Added hydrogen has no observable effect on the course of the reaction

On the basis of these results it seemed likely that there were at least two reaction pathways involved in the thermolysis: a major route leading to the non-volatile solid and H_2, and a minor route producing B_5H_9 and $B_{10}H_{14}$. *In the absence of evidence to the contrary, there* seemed little justification for considering mechanisms more complex than ones involving a rate-controlling bimolecular interaction between two molecules of B_6H_{10}, and the main task was to deduce the fate of the activated complex {$B_{12}H_{20}$}‡. Such a scheme was devised (ref. 14) leading to an overall stoichiometry for this minor route of $5B_6H_{10} \longrightarrow 4B_5H_9 + B_{10}H_{14}$. Notwithstanding the good agreement between the predicted B_5H_9:$B_{10}H_{14}$ ratio and that observed experimentally, it seemed unlikely that the situation would be as simple as outlined. Accordingly, further experiments were undertaken (ref. 36) including thermolysis in the *presence of CO (to be reported elsewhere) and thermolytic experiments leading to the isolation* of a new borane $B_{24}H_{30}$, which appears to be the conjuncto dimer of the recently identified molecule $B_{12}H_{16}$ (ref. 37).

Surface studies (ref. 36)

To check for a possible heterogeneous component in the reaction rates, a thermolysis of B_6H_{10} was carried out at 3.5 mmHg and 153 °C in a clean 1 l pyrex bulb packed with Raschig rings so as to increase the surface-to-volume ratio by a factor of 33. The effect was dramatic, and unexpected: the rate of decomposition decreased by an order of magnitude relative to the rate in a conditioned unpacked vessel. In successive runs the rate slowly recovered, presumably as the surface of the vessel became deactivated with a coating of the solid product. This behaviour is typical of radical chain reactions (ref. 33), the effect of the clean glass surface being to attract the reactive species, thereby preventing further reaction. Consistent with this it was found that treatment of the clean glass surfaces of a packed reaction vessel with a covering of PTFE polymer, $(CF_2)_n$, scarcely affected the rate as observed in a packed conditioned vessel. The rate observed in an unpacked PTFE-coated vessel was actually faster than in an unpacked conditioned vessel, suggesting that the coated surface was even less active in removing radicals than was the borane-conditioned surface. Clearly the possibility of a radical-based mechanism for the thermolysis of B_6H_{10} required careful investigation.

Cothermolysis of B_6H_{10} with ethene and propene (ref. 36)

Ethene and propene are well known 'radical scavengers' (ref. 33). With B_6H_{10} these unsaturated hydrocarbons were found to inhibit the reaction dramatically. For a pressure of 3.5 mmHg the decomposition at 165 °C normally has a half-life of ca. 100 min, whereas in the presence of 15 mole % of ethene it is stable over a period of several days. Propene has a more pronounced effect, the addition of only 3% causing complete inhibition in the thermolysis of B_6H_{10} (3.5 mmHg) for some 20 min. even at 185 °C; larger additions increase the inhibition period proportionately.

The initial products of the cothermolysis, which are very slow to appear at these temperatures because of the limited extent of reaction, are trialkylboranes and the basal-alkylated hexaboranes $B_6H_{10-x}R_x$ (R = Et or Pr, x = 1-5), many of which are new compounds. These are followed by the series of alkylated monocarbaboranes $R'CB_5H_{8-x}R_x$ (x = 0-3), where R' = Me, R = Et for the ethene reaction, and R' = Et, R = Pr for the propene reaction. In one cothermolysis involving propene, which was allowed to go almost to completion, the main products were found to be $B_6H_5Pr_5$ and $EtCB_5H_{8-x}Pr_x$ (x = 0-3). It would therefore appear that the alkylboranes $B_6H_{10-x}Pr_x$ (x = 1-4) have by this stage of the reaction been converted to the corresponding monocarbaboranes, whereas the end-member of the series, in which all the basal terminal protons have been replaced, possesses enhanced stability. This suggests that the ready formation of the monocarbaborane involves $\{BH_3\}$ release from the base of the corresponding alkylborane, followed by incorporation of the methylene carbon and its associated protons into the ring (Scheme 1).

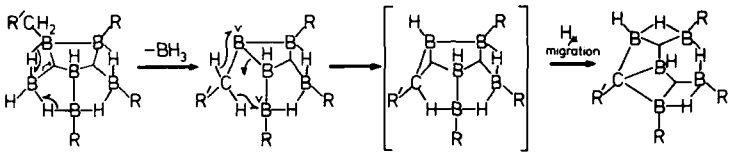

Scheme 1. Possible mechanism for the formation of $R'CB_5H_{8-x}R_x$ (x = 0-3) by elimination of $\{BH_3\}$ from $R'CH_2B_6H_{9-x}R_x$ (x = 0-3). (R = Et or H, R' = Me; R = Pr or H, R' = Et)

In the case of the penta-alkylated species, $\{BH_3\}$ release is precluded and the formation of the monocarbaborane inhibited. Its virtual absence also indicates that hydroboration of the monocarbaboranes themselves does not occur. In the presence of alkene, $\{BH_3\}$ is readily hydroborated, which accounts (in part) for the appearance of boron trialkyls.

Mechanism of B_6H_{10} thermolysis

In the light of the observed inhibitory effects of active surfaces and unsaturated hydrocarbons, there seems little doubt that the main reaction in the B_6H_{10} decomposition is a radical-type chain process. The reactive species formed in the initiation step is thought to be a genuine (odd-electron) free-radical and not simply a non-isolable reactive borane intermediate analogous to $\{BH_3\}$, $\{B_3H_7\}$, or $\{B_4H_8\}$. In the thermolyses of other boranes, as discussed earlier, such species are undoubtedly present but the reactions are not inhibited in the same dramatic way. There are indications that B_5H_9 (ref. 38) and $B_{10}H_{14}$ (ref. 39) may also decompose via radical intermediates, but detailed evidence is lacking. The initial products of the B_6H_{10}/alkene reactions provide further crucial insights into the mechanism. In particular, the fact that monoalkylated hexaboranes are the very first species to appear (along with boron trialkyls, whose significance is discussed later) provides very strong, if not conclusive, evidence that the radical intermediate formed in the initiation step is in fact $B_6H_9^{\bullet}$. In the absence of 'trapping' agents, this species will react further with B_6H_{10}, setting in train a series of events leading to the removal of some 90% of the boron from the gas phase as non-volatile oligomers. The overall mechanism, though undoubtedly complex, must resemble very closely the classic mechanism proposed for free-radical polymerization of olefins (ref. 33). This features addition of the monomer to the growing radical chain, thereby increasing its length without altering the ability of the radical to react. A possible mechanism for the thermolysis of B_6H_{10} is thus:

$$B_6H_{10} + B_6H_{10} \longrightarrow 2B_6H_9^{\bullet} + H_2 \qquad \text{Initiation}$$

$$B_6H_9^{\bullet} + B_6H_{10} \longrightarrow (B_6H_8)_2H^{\bullet} + H_2$$

$$(B_6H_8)_nH^{\bullet} + B_6H_{10} \longrightarrow (B_6H_8)_{n+1}H^{\bullet} + H_2$$

$$(B_6H_8)_nH^{\bullet} + B_6H_{10} \longrightarrow (B_6H_8)_{n+1} + H_2 + H^{\bullet} \qquad \text{Propagation}$$

$$H^{\bullet} + B_6H_{10} \longrightarrow B_6H_9^{\bullet} + H_2$$

$$(B_6H_8)_nH^{\bullet} + (B_6H_8)_mH^{\bullet} \longrightarrow (B_6H_8)_{n+m}H_2 \qquad \text{Termination}$$

When n is large the overall stoichiometry is seen to be

$$nB_6H_{10} \longrightarrow (B_6H_8)_n + nH_2$$

To account for the observed second-order kinetics (ref. 14) it is necessary to include a bimolecular initiation step involving interaction between two B_6H_{10} molecules to produce the $B_6H_9^{\bullet}$ radical. The termination steps involve any two radicals, including identical ones. The scheme provides a general description of the kinetic behaviour of the system under

thermolytic conditions, and satisfactorily explains the overall initial stoichiometry. As the reaction proceeds, further crosslinking undoubtedly occurs, with consequent evolution of additional hydrogen. The scheme as written does not account for the appearance of specific species such as $B_{13}H_{19}$, $B_{14}H_x$, $B_{15}H_{23}$ etc., but this could be dealt with by including the possibility of disproportionation in the termination steps. Such species are observed in only trace amounts in the gas phase, but are the major non-volatile products of 'hot/cold' reactions of B_6H_{10}.

The observation that the alkylhexaborane-carbaborane conversion can occur readily only when {BH_3}-release is possible, inevitably raises the question as to whether B_6H_{10} itself can release {BH_3} in this way, i.e. *via* reaction (14). In fact there is good evidence that this

$$B_6H_{10} \longrightarrow \{B_5H_7\} + \{BH_3\} \qquad (14)$$

may well be the route to the minor products of the B_6H_{10} thermolysis, rather than the bimolecular step suggested earlier. Further work will be necessary to establish whether this side-reaction is (as we would now predict) a first-order reaction, but the observed products are certainly consistent with the existence of reaction (14). Both B_5H_9 and $B_{10}H_{14}$ could arise from the reactive intermediate {B_5H_7}, the former *via* its reaction with the H_2 produced in the main reaction, and the latter *via* its self-association. The {BH_3} produced in reaction (14) would probably form B_2H_6, which in cothermolysis with B_6H_{10} would immediately give $B_{10}H_{14}$ (see later). In the cothermolysis of B_6H_{10} and alkenes, in which the main reaction to give solids is inhibited, boron trialkyls are produced in much greater concentration and at an earlier stage than the monocarbaboranes. It is therefore suggested that they arise not only from hydroboration of the {BH_3} eliminated in the conversion of the alkylated hexaboranes to the monocarbaboranes, but also from that produced in reaction (14).

Cothermolysis of B_6H_{10} with other boranes (ref. 21)

Having established the nature of the B_6H_{10} self-thermolysis, preliminary cothermolysis reactions were attempted with B_2H_6, B_4H_{10}, B_5H_9, and B_5H_{11}. In all cases except B_5H_9, the rate of consumption of B_6H_{10} was found to be more rapid than in the self-thermolysis, clearly indicating that interactions were occurring. Detailed kinetic studies with B_2H_6 and B_4H_{10} showed that in each case the rate was governed by the rate-determining sequence of the co-reactant. Thus with B_2H_6 the reaction was found to be 3/2-order in B_2H_6 and zero order in B_6H_{10}, whereas with B_4H_{10} the reaction was first-order in B_4H_{10} and zero-order in B_6H_{10}. The rate data for disappearance of B_2H_6 and B_4H_{10} (see Fig. 3) when cothermolysed with B_6H_{10} are compatible with the Arrhenius plots for the self-reactions of these boranes. Thus, the activation energy, E_A, for cothermolysis of B_6H_{10}/B_2H_6 is 98.8±3.9 kJ mol^{-1} compared with 92.3±6.6 kJ mol^{-1} for thermolysis of B_2H_6 alone, and E_A for B_6H_{10}/B_4H_{10} is 88.4±6.1 kJ mol^{-1} compared with 99.2±0.8 kJ mol^{-1} for B_4H_{10} alone.

In the B_6H_{10}/B_2H_6 cothermolysis the main volatile product apart from H_2 was found to be $B_{10}H_{14}$ in yields of up to 40%. Despite the fact that the B_2H_6 decomposition was rate-controlling, very little pentaborane was formed. In the light of these results it is clear that, under the prevailing conditions (100-198 °C), there is *no* interaction between B_6H_{10} and either B_2H_6 itself or {BH_3}. Instead it seems likely that B_6H_{10} reacts with {B_3H_7}, the product of the rate-determining step (3), to give B_9H_{15} *via* reaction (15). This step has

$$\{B_3H_7\} + B_6H_{10} \longrightarrow B_9H_{15} + H_2 \qquad (15)$$

been proposed in the past, without direct evidence (ref. 5), and it has been shown that B_6H_{10} reacts with $^{10}B_3H_7$.THF at 0 °C in the presence of BF_3 to give B_9H_{15} labelled at the 3, 4, and 9 positions (ref. 35b). If B_9H_{15} is formed, it must then decompose immediately to $B_{10}H_{14}$. This reaction is known to occur, but isotope studies have shown that it does not take place in a single step (ref. 2g). Thus, in the reaction between B_9H_{15} and $^{10}B_2H_6$, the resulting $B_{10}H_{14}$ has two labelled boron atoms, implying that the route is *via* B_8H_{12}. The simplest proposed (ref. 5) sequence of events, reactions (16)-(18), differs from that suggested originally (ref. 35b). So far, it has been assumed that B_6H_{10} reacts *via* reaction (15).

$$B_9H_{15} \longrightarrow B_8H_{12} + \{BH_3\} \qquad (16)$$

$$\{B_3H_7\} + B_8H_{12} \longrightarrow \{B_9H_{13}\} + B_2H_6 \qquad (17)$$

$$\{B_3H_7\} + \{B_9H_{13}\} \longrightarrow B_{10}H_{14} + B_2H_6 \qquad (18)$$

It is possible that the B_2H_6 decomposition proceeds as far as the production of {B_4H_8} [reactions (4) and (5a)] before the interaction with B_6H_{10} occurs to give $B_{10}H_{14}$, but results discussed later suggest that this is not the case.

In the B_6H_{10}/B_4H_{10} cothermolysis, B_9H_{15} is actually observed as a major product in the early stages of the reaction, because the temperatures required for this system are much lower than those necessary to achieve reaction between B_2H_6 and B_6H_{10}. A similar result has been

obtained in the reaction at much lower temperatures between B_4H_8CO and B_6H_{10} (ref. 35b), and it seems reasonable to invoke reaction (19) in each case. In this respect it is clear that

$$\{B_4H_8\} + B_6H_{10} \longrightarrow B_9H_{15} + \{BH_3\} \qquad (19)$$

the previously proposed (ref. 5) reaction of these two species to give $2B_5H_9$ is not significant under these conditions.

The results obtained from these two detailed cothermolysis studies demonstrate in a very striking way the strong affinity which exists between B_6H_{10} and the reaction intermediates $\{B_3H_7\}$ and $\{B_4H_8\}$. In the B_6H_{10}/B_2H_6 cothermolysis, B_6H_{10} is in competition with B_2H_6 for the $\{B_3H_7\}$ [reactions (4) and (15)], whereas in the B_6H_{10}/B_4H_{10} cothermolysis, it competes successfully with B_4H_{10} for $\{B_4H_8\}$ [reactions (6) and (19)]. To test these competitive effects further, the effect of adding an excess of H_2 to the two cothermolysis systems has been studied in some detail. The orders of the two reactions were shown to be unaffected by the presence of added H_2, confirming that the respective rate-determining sequences were unaltered, but retardation was observed only in the B_6H_{10}-B_4H_{10} case. In view of the fact that both the B_2H_6 and B_4H_{10} self-reactions are retarded by the presence of added H_2 [presumably via reactions (-3) and (-5a), respectively], the lack of inhibition in the $B_6H_{10}/B_2H_6/H_2$ system, even in the presence of a 10-fold excess of added H_2, demonstrates that B_6H_{10} is particularly effective in its competition for $\{B_3H_7\}$. Returning to an earlier point, it is now clear that B_6H_{10} does in fact react, in the B_6H_{10}/B_2H_6 cothermolysis, at the $\{B_3H_7\}$ stage.

PHOTOLYSIS OF BORANES

In comparison with the extensive studies on the thermolysis of boranes, little effort has been directed towards their photolysis, and only in the case of B_2H_6 has there previously been any kinetic treatment of the data. The situation as it existed in 1979 has been reviewed (ref.40) and there have been relatively few developments since then. Notable among these have been Irion and Kompa's UV-laser photochemical studies at 193.3 nm (ref. 41): from results on the B_2H_6/D_2 exchange reaction and from measurements of the quantum yield of BH_3 [$\phi(BH_3) = 2.0 \pm 0.25$] it was concluded that the primary photochemical step is the same as that proposed in thermolysis: $B_2H_6 + h\nu \longrightarrow 2\{BH_3\}$. As examples of the use of photolysis in borane synthesis we may note the work of Larry Sneddon's group in using mercury photosensitized reactions to make coupled boranes and carbaboranes (ref. 42) and our own work in synthesizing various geometrical isomers of conjuncto-icosaborane(26) (ref. 43). Recent work involving the cophotolysis of binary boranes such as B_5H_9 with other gas-phase species such as hexafluoroacetone suggests that there is also great synthetic potential in this area (ref. 44).

Information in the literature on the UV spectra of the binary boranes in the gas phase is surprisingly sparse: only B_2H_6, B_4H_{10}, and B_5H_9 have been studied (refs. 40a, 41a, 45, 46) and they all exhibit weak,featureless absorptions which begin at about 220-230 nm and increase down to the experimentally imposed cut-off at about 185 nm. As a necessary preliminary to a quantitative study of the photolysis of the boranes we have therefore recorded the spectra of a suite of volatile boranes (including those already mentioned and for which agreement with the published data was good). The spectra are illustrated in Fig. 6 and extinction coefficients are summarized in Table 2.

Photolysis studies were carried out in a 1l bulb containing an appropriate Hg lamp (eg. 125 watt medium-pressure, emitting mainly near 365 nm but with smaller amounts at 254, 265, 297, 303, 313, and 334 nm as well). The changing composition of the gas-phase mixture was monitored continuously by mass spectrometry. Non-volatile solids were produced in all the reactions but, with repeated cleaning of the lamp-housing, comparative rate data for the various boranes could be obtained. In kinetic runs various devices were used to calibrate the changing intensity of the transmitted light.

TABLE 2. UV parameters for binary boranes (ref. 36)

Borane	B_2H_6	B_4H_{10}	B_5H_9	B_5H_{11}	B_6H_{10}	B_6H_{12}	n-B_9H_{15}	$B_{10}H_{14}$
λ_{max}/nm	<195	<195	<195	209	247	263	260	272
$\varepsilon/m^2\ mol^{-1}$	2.0[a]	0.71[a]	88[a]	82.9	165.1	278.9	~200[b]	248.6[c]

[a]Data refer to ε at 195 nm; λ_{max} is at shorter wavelengths
[b]Approx. value: sample decomposed during measurement
[c]In hexane solution

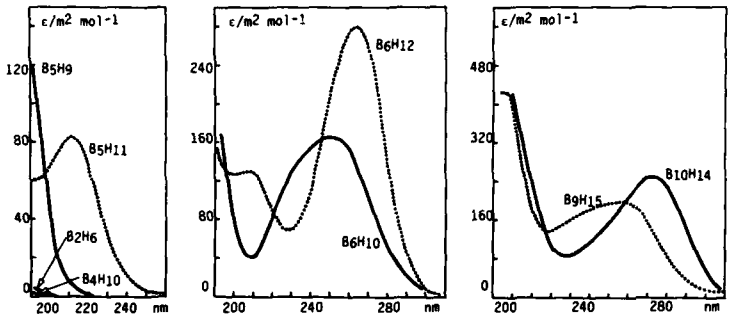

Fig. 6. UV absorption spectra of gaseous boranes ($B_{10}H_{14}$ in hexane solution)

In a series of photolyses B_2H_6, B_4H_{10}, and B_5H_9 were found to be much more stable than B_5H_{11}, B_6H_{10}, and B_6H_{12} (ref. 36). For example, the initial rates of consumption of the boranes (in arbitrary units) were ~0, 0.33, 2.5, 50, 100, and 380 respectively, and the initial rates of production of H_2 (the main volatile product) were 0.28, 0.20, 0.38, 20, 44, and 400. Qualitative correlation with the absorption spectra in Fig. 6 is clear. Inclusion of Hg vapour in the system increased the rate of B_2H_6-decomposition about 30-fold but had little effect on the rates of decomposition of the other boranes. Thus, the photolytic stability decreases in the sequence B_2H_6>B_4H_{10}~B_5H_9>>B_5H_{11}>B_6H_{10}>B_6H_{12}, in sharp contrast with the thermolytic stability of these boranes which follows the sequence B_5H_9>B_2H_6~B_6H_{10}>B_6H_{12}>B_5H_{11}>B_4H_{10}. The most notable differences are for B_4H_{10} (which is very stable to photolysis but very unstable thermally) and B_6H_{10}, for which the reverse applies. It is also noteworthy that the sequence of photolytic stability for the arachno series (B_4H_{10}>B_5H_{11}>B_6H_{12}) is precisely the opposite to that found in thermolysis.

We are at present undertaking a detailed study of the products of photolysis (and cophotolysis) as a function of time in order to establish the mechanistic pathways adopted (ref. 36). Preliminary results indicate that the initial step for B_6H_{12} might well be the elimination of $\{BH_3\}$ to give B_2H_6 and B_5H_9 as the main product boranes:

$$B_6H_{12} \longrightarrow B_5H_9 + \{BH_3\} \qquad (19)$$

Photolysis of B_5H_{11} may also involve facile elimination of $\{BH_3\}$ as the initial step.

A kinetic study of the photolysis of B_6H_{10} has revealed significant differences from the thermolysis studies described in the preceding section. It is well known that radical chain reactions can be initiated either thermally or photolytically, and that the observed kinetics will depend on the mechanism of initiation (ref. 33). The second-order kinetics observed in the thermolysis of B_6H_{10} were interpreted in terms of a bimolecular initiation. Under photolytic conditions at 0 °C, however, first-order kinetics are observed for both consumption of B_6H_{10} and production of H_2. As in thermolysis the main volatile product was H_2 and most of the boron disappeared from the gas phase. However, a significant difference from thermolysis was that B_2H_6 appeared as the sole volatile borane and B_5H_9 was virtually absent. There was also subtantially less H_2 produced proportionately in photolysis, the observed ratio of H_2 produced per mole of B_6H_{10} consumed being closer to 0.5 than the value of 1.0 observed in the initial stages of thermolysis. Further experimental results are required, however, before detailed mechanistic conclusions can be drawn.

Acknowledgements This work was supported by the UK Science and Engineering Research Council and by the US Army Research and Standardization Group (Europe). We thank Mr D. Singh for invaluable assistance with the mass spectrometers and Dr D. Baulch for helpful discussions.

REFERENCES

1. A. Stock, Hydrides of Boron and Silicon, Cornell University Press, Ithaca, 1933.
2. (a) J.A. Dupont and R. Schaeffer, J. Inorg. Nucl. Chem., 15, 310-315 (1960); (b) R. Schaeffer, ARL Tech. Rept. 60-334, 28 pp. (1960); (c) R. Schaeffer, J. Inorg. Nucl.Chem., 15, 190-193 (1960); (d) R.E. Enrione and R. Schaeffer, J. Inorg. Nucl. Chem., 18, 103-107 (1961); (e) G.L. Brennan and R. Schaeffer, J. Inorg. Nucl. Chem., 20, 205-210 (1961); (f) R. Schaeffer and F.N. Tebbe, J. Am. Chem. Soc., 84, 3974-3975 (1962); (g) R. Maruca, J.D. Odom, and R. Schaeffer, Inorg. Chem., 7, 412-418 (1968); (h) J.Dobson, R. Maruca, and R. Schaeffer, Inorg. Chem., 9, 2161-2166 (1970);(i) R.Schaeffer and L.G. Sneddon, Inorg.Chem.,11,3098-3101 (1972);R.Schaeffer,Pure Appl.Chem.,4, 1-11 (1974).

3. (a) T.P. Fehlner and W.S. Koski, J. Am. Chem. Soc., 86, 1012-1018 (1964); (b) G.W. Mappes, S.A. Fridmann, and T.P. Fehlner, J. Phys. Chem., 74, 3307-3316 (1970); (c) S.A. Fridman and T.P. Fehlner, J. Am. Chem. Soc., 93, 2824-2826 (1971); (d) S.A. Fridmann and T.P. Fehlner, Inorg. Chem., 11, 936-940 (1972); (e) T.P. Fehlner in E.L. Muetterties (Ed.), Boron Hydride Chemistry, Academic Press, New York, Chapt. 4, 175-196 (1975).
4. (a) M.L. McKee and W.N. Lipscomb, Inorg. Chem., 21, 2846-2850 (1982); (b) J.V. Ortiz and W.N. Lipscomb, Chem. Phys. Lett., 103, 59-62 (1983); (c) W.N. Lipscomb, Pure Appl. Chem., 55, 1431-1438 (1983); (d) M.L. McKee and W.N. Lipscomb, Inorg. Chem., 24, 762-764, 765-767, and 2317-2319 (1985).
5. L.H. Long, J. Inorg. Nucl. Chem., 32, 1097-1113 (1970).
6. R.Greatrex, N.N. Greenwood, and C.D. Potter, J. Chem. Soc., Dalton Trans., 2435-2437 (1984)
7. T.P Fehlner and C.E. housecroft, in J.F. Liebman and A. Greenberg (Eds.), Mol. Struct. and Energetics, 1, 149-207 (1986).
8. W.E. Dasent, Inorganic Energetics, 2nd Edn., Cambridge University Press, (1982).
9. S.R.Gunn and Le R.G. Green, J. Phys. Chem., 65, 2173-2175 (1961).
10. C.T. Mortimer, Reaction Heats and Bond Strengths, Pergamon Press, Oxford , (1962).
11. A. Finch, P.J. Gardiner, E.J. Pearn, and G.B. Watts. Trans Faraday Soc., 63, 1880-1888 (1967).
12. C.E. Housecroft and K. Wade, Inorg. Nucl. Chem. Lett., 15, 339-342 (1979).
13. T.C. Gibb, N.N. Greenwood, T.R. Spalding, and D. Taylorson, J. Chem. Soc., Dalton Trans., 1392-1397 and 1398-1400 (1979).
14. R. Greatrex, N.N. Greenwood, and G.A. Jump, J. Chem. Soc., Dalton Trans., 541-548 (1985).
15. (a) R.P. Clarke and R.N. Pease, J. Am. Chem. Soc., 13, 2132-2134 (1951); (b) J.K. Bragg, L.V. McCarty, and F.J. Norton, J. Am. Chem. Soc., 73, 2134-2140 (1951); (c) L.V. McCarty, and P.A. DiGiorgio, J. Am. Chem. Soc., 73, 3138-3143 (1951).
16. A.B. Bayliss, G.A. Pressley, E.J. Sinke, and F.E. Stafford, J. Am. Chem. Soc., 86, 5358-5359 (1964).
17. H. Fernández, J. Grotewold, and C.M. Previtali, J. Chem. Soc., Dalton Trans., 2090-2095 (1973).
18. A.J. Owen, J. Appl. Phys., 10, 483-493 (1960).
19. J.R. Morrey and G.R. Hill, U.S. Dept. Com., Office Tech. Serv. Rep. AD 154,121 (1958).
20. B.S. Askins and C. Riley, Inorg. Chem., 16, 481-484 (1977).
21. M. Attwood, R. Greatrex, and N.N. Greenwood, unpublished observations, University of Leeds (1987).
22. R.K. Pearson and L.J. Edwards, Abstracts of 132nd National Meeting of the Am. Chem.Soc., New York, p.15N, Sept. 1957.
23. A.C. Bond and H.L. Pinsky, J. Am. Chem. Soc., 92, 32-36 (1970).
24. J.P. Faust, Adv. Chem. Ser., 32, 69-77 (1961).
25. R. Greatrex, N.N. Greenwood, and C.D. Potter, J. Chem. Soc., Dalton Trans., 81-89 (1986).
26. W.S. Koski, Adv. Chem. Ser., 32, 78-87 (1961).
27. J.D. Odom, Ph.D. Thesis, Indiana Univ., Bloomington, Indiana, 1968.
28. M.A. Toft, J.B. Leach, F.L. Himpsl, and S.G. Shore, Inorg. Chem., 21, 1952-1957 (1982).
29. D.F. Gaines and R. Schaeffer, Inorg. Chem., 3, 438-440 (1964).
30. A.B. Burg and H.J. Schlesinger, J. Am. Chem. Soc., 55, 4009-4020 (1933).
31. C.A. Lutz, D.A. Phillips, and D.M. Ritter, Inorg. Chem., 3, 1191-1194 (1964).
32. J.F. Ditter, J.R. Spielman, and R.E. Williams, Inorg.Chem., 5, 118-123 (1966).
33. K.J. Laidler, Chemical Kinetics, Tata McGraw-Hill, TMH Edn. (1973).
34. A. Davison, D.D. Traficante, and S.S. Wreford, J. Am. Chem. Soc., 96, 2802-2805 (1974).
35. (a) J. Rathke and R. Schaeffer, J. Am. Chem. Soc., 95, 3402 (1973); (b) Inorg. Chem., 13, 3008-3011 (1974); (c) J. Rathke, D.C. Moody, and R. Schaeffer, Inorg. Chem., 13, 3040-3042 (1974); (d) P.J. Dolan, D.C. Moody, and R. Schaeffer, Inorg. Chem., 20, 745-748 (1981).
36. P.M. Davies, R. Greatrex, and N.N. Greenwood, unpublished observations, University of Leeds (1987).
37. C.T. Brewer, R.G. Swisher, E. Sinn, and R.N. Grimes, J. Am. Chem. Soc., 107, 3558-3564 (1985).
38. T.J. Houser and R.C. Greenough, Chem. and Ind., 323-324 (1967).
39. H.C. Beachell and J.F.Haugh, J. Am. Chem. Soc., 80, 2939-2942 (1958).
40. (a) R.F. Porter and L.J. Turbini,Top. Curr. Chem., 96, 1-41 (1981); (b) G.A. Kline and R.F. Porter, Inorg. Chem., 19, 447-451 (1980).
41. (a) M.P. Irion and K.L. Kompa, J. Chem. Phys., 76, 2338-2346 (1982); (b) J. Photochem., 32, 139-142 (1986).
42. J.S. Plotkin and L.G. Sneddon, J. Chem. Soc., Chem. Commun., 95-96 (1976); J.S. Plotkin, R.J. Astheimer, and L.G. Sneddon, J. Am. Chem. Soc., 101, 4155-4163 (1979).
43. N.N. Greenwood, J.D. Kennedy, T.R. Spalding, and D. Taylorson, J. Chem. Soc., Dalton Trans., 840-846 (1979); S.K. Boocock, N.N. Greenwood, J.D. Kennedy, W.S. McDonald, and J. Staves, J. Chem. Soc., Dalton Trans., 790-796 (1980); S.K. Boocock, Y.M. Cheek, N.N. Greenwood, and J.D. Kennedy, J. Chem. Soc., Dalton Trans., 1430-1437 (1981).
44. R.J. Astheimer and L.G. Sneddon, Inorg. Chem., 23, 3207-3212 (1984).
45. M.P. Irion, M. Seitz, and K.L. Kompa, J. Mol. Spectrosc., 118, 64-69 (1986).
46. J.R. Platt, H.B. Klevens, and G.W. Schaeffer, J. Chem. Phys., 15, 598-601 (1947).

A Kinetic Study of the Gas-phase Thermolysis of Pentaborane(11) *

Martin D. Attwood, Robert Greatrex, and Norman N. Greenwood
School of Chemistry, University of Leeds, Leeds LS2 9JT

The kinetics of thermal decomposition of pentaborane(11) have been investigated by a mass-spectrometric technique in the pressure range 1.75—10.50 mmHg and temperature range 40—150 °C. In conditioned Pyrex vessels the reaction was shown to occur by a homogeneous gas-phase process according to the first-order initial-rate law $-d[B_5H_{11}]/dt = 1.3 \times 10^7 \exp(-72\,600/RT)[B_5H_{11}]$. The main volatile products are H_2 and B_2H_6, the latter appearing at the rate of *ca.* 0.5 mol per mol of B_5H_{11} consumed. Pentaborane(9) is also produced, at less than half the rate of B_2H_6, together with even smaller amounts of hexaboranes and $B_{10}H_{14}$, and traces of B_4H_{10}; some 40—45% of the boron is converted into involatile solid hydride BH_x, where x varies from *ca.* 2.0 at 40 °C to *ca.* 1.1 at 150 °C. No obvious dependence on temperature was detected in the overall distribution of boron between volatiles and solid, but the production of B_5H_9 was favoured at higher temperatures. Mechanistic implications of these results are discussed.

arachno-Pentaborane, B_5H_{11}, is the main volatile borane to be observed in the initial stages of the gas-phase thermolysis of B_2H_6 above about 100 °C. It is thought to be formed *via* *arachno*-B_4H_{10} as a result of the series of steps (1)—(6).[1] It must

$$B_2H_6 \rightleftharpoons 2\{BH_3\} \quad (1)$$

$$\{BH_3\} + B_2H_6 \rightleftharpoons \{B_3H_9\} \quad (2)$$

$$\{B_3H_9\} \rightleftharpoons \{B_3H_7\} + H_2 \quad (3)$$

$$\{B_3H_7\} + B_2H_6 \longrightarrow B_4H_{10} + \{BH_3\} \quad (4)$$

$$B_4H_{10} \rightleftharpoons \{B_4H_8\} + H_2 \quad (5)$$

$$\{B_4H_8\} + B_2H_6 \longrightarrow B_5H_{11} + \{BH_3\} \quad (6)$$

therefore play a major role in the ensuing sequence of complex interconversion reactions leading to *nido*-$B_{10}H_{14}$, but its precise contribution is not well understood.

Previous studies of the thermal decomposition of B_5H_{11} have been essentially qualitative in nature, and have not produced a consistent picture, even of the product analysis.[2-7] There has been no detailed study of the effect of varying the initial pressure and thermolysis temperature, and no attempt to establish the kinetics of the reaction. Indeed it was not entirely clear whether the decomposition is a homogeneous gas-phase process, or whether there is a heterogeneous component under certain conditions.[4]

As part of a systematic mass-spectrometric study of the kinetics of gas-phase thermolysis and cothermolysis reactions of the boranes,[8,9] we now report a detailed initial-rate study of the thermal decomposition of B_5H_{11} at pressures in the range 1.75—10.50 mmHg and temperatures of 40—150 °C. The work includes a series of careful experiments in packed vessels to establish the importance of any activity at the Pyrex surface, and to assess the effects of surface conditioning. Experiments involving the thermolysis of B_5H_{11} under hot/cold conditions are also reported. Some preliminary aspects of this work have been referred to elsewhere.[1]

* *Non-S.I. unit employed:* mmHg ≈ 133 Pa.

Experimental

The stock of pentaborane(11) used in most of the kinetic studies was prepared from B_4H_{10} by the method of Shore and co-workers.[10] Early experiments were carried out with the same batch of material as that used in our recent electron-diffraction analysis.[11] It was purified by repeated fractionation on a low-temperature fractional distillation column, and was shown by ^{11}B n.m.r. spectroscopy to contain <0.5% B_5H_9 as the only detectable impurity; its vapour pressure at 0 °C was 52.5 mmHg, in excellent agreement with the published value.[2] The sample used in the 'packed-vessel' study (see later) was prepared from B_5H_9 by the more recent method of Wermer and Shore[12] using potassium dihydronaphthylide as the reducing agent. Standard grease-free vacuum-line techniques were used throughout.

The quantitative mass-spectrometric techniques involving continuous capillary sampling of the heated reaction mixture have been described previously together with details of the methods of data analysis.[8,9] All thermolyses were carried out in spherical Pyrex bulbs in the presence of a large background of an inert-gas mixture (partial pressure 100 mmHg) comprising helium, argon, and krypton in the relative proportions 98.0:1.0:1.0, made up to our specifications by BOC Ltd. As indicated in the Results section, the bulbs were either unpacked (volume *ca.* 1.1 dm^3), or packed with Pyrex Raschig rings to give a 33-fold increase in surface-to-volume ratio (volume *ca.* 0.79 dm^3). The bulbs (and any packing) were first washed with water, acetone, and light petroleum, and then baked out under vacuum at *ca.* 150 °C; except where otherwise indicated, they were conditioned prior to use as already discussed.[9]

Hot/cold thermolyses were carried out in a concentric-tube reactor with an annular volume of 1.2 dm^3, similar to that described by Klein *et al.*[13] The outer surface was cooled to 0 °C whilst the inner surface was heated to temperatures in the range 110—205 °C by means of a coil immersed in silicone fluid (Dow Corning 550). Typical initial pressures of B_5H_{11} were 21 and 40 mmHg.

Results

General Features.—Typical reaction profiles for the thermolysis of B_5H_{11} at 110.4 and 150.7 °C are shown in Figures 1 and 2, respectively, for an initial pressure of *ca.* 3.5 mmHg; a complete set of reaction profiles for the thermolyses discussed in this work can be found elsewhere.[14] From these results it is clear

Table 1. Initial-rate data for thermolysis of B_5H_{11}

T K	$p_0(B_5H_{11})$/mmHg	$10[B_5H_{11}]_0$/mol m^{-3}	$-10^6(d[B_5H_{11}]/dt)_0$	$10^6(d[H_2]/dt)_0$	$10^6(d[B_2H_6]/dt)_0$
			mol m^{-3} s^{-1}		
313.4	3.53	1.81	2.4	0.6	1.1
322.7	3.49	1.73	3.6	1.5	1.5
333.6	3.50	1.68	7.3	3.7	6.5
349.1	1.75	0.80	13.9	6.4	10.4
348.5	3.02	1.39	17.9	12.4	14.8
347.9	3.47	1.60	30.2	11.5	*
348.2	5.29	2.44	43.5	27.1	25.1
347.5	6.88	3.17	56.4	30.4	41.8
347.8	10.36	4.78	79.4	34.8	59.2
363.9	3.53	1.56	76.3	32.8	*
373.0	3.52	1.51	198	55.2	57.3
383.5	3.47	1.45	264	184	170
398.4	3.52	1.42	667	418	626
423.8	3.50	1.32	1 548	1 194	1 135

* Unreliable data because of incorrect level settings.

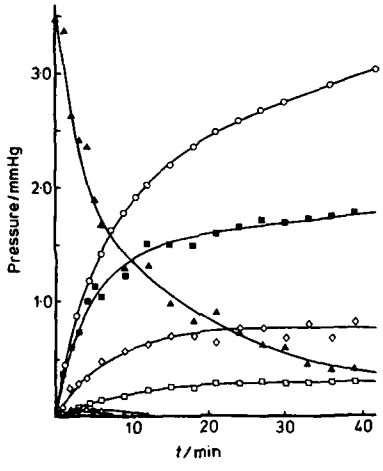

Figure 1. Reaction profile for the thermolysis of B_5H_{11} (p_0 = 3.47 mmHg) at 110.4 °C: (○) H_2, (▲) B_5H_{11}, (■) B_2H_6, (◇) B_5H_9, (□) $B_{10}H_{14}$, (●) B_4H_{10}, and (△) B_6H_{12}

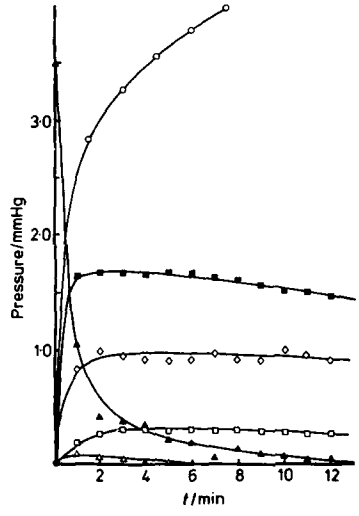

Figure 2. Reaction profile for the thermolysis of B_5H_{11} (p_0 = 3.50 mmHg) at 150.7 °C: symbols as in Figure 1

that the thermolysis is an exceedingly complex reaction; several volatile products appear from the moment the gaseous mixture enters the heated reaction vessel, and (see later) there is a concurrent deposition, predominantly on the lower surfaces of the reaction vessel, of a pale yellow involatile solid hydride.

The main volatile products, in decreasing order of amount on a molar basis, are hydrogen, B_2H_6, B_5H_9, and $B_{10}H_{14}$; smaller amounts of B_4H_{10} and B_6H_{12}, and traces of B_8H_{12} and B_9H_{15} are also observed. There is, however, some temperature dependence in the product distribution: B_5H_9 is produced in slightly greater quantities in runs carried out at the higher temperatures, whereas B_4H_{10} is more abundant at lower temperatures (below 100 °C). There is also some indication that formation of B_2H_6 is favoured by lower temperatures and $B_{10}H_{14}$ by higher temperatures, but the differences are small compared with the associated errors and may not be significant. The rate of formation of H_2 relative to the rate of consumption of B_5H_{11} appears to increase as the temperature is raised. These results are presented in a more quantitative form in later sections.

The reaction at 150.7 °C (Figure 2) is very rapid indeed, being virtually complete within about 3—4 min. Thereafter, the concentrations of the main volatile borane products (B_2H_6 and B_5H_9) remain essentially constant, indicating that there is little reaction between them, despite the relatively high temperature. In this respect it is interesting that $B_{10}H_{14}$ is formed only during the early part of the thermolysis, and no longer continues to build up after the B_5H_{11} has been consumed.

Kinetic Studies.—In common with other borane thermolyses, the decomposition of B_5H_{11} rapidly produces a complex mixture, and for this reason we have studied the kinetics by the initial-rate method to minimize the effects of interference from products.

Reaction order. Initial rates of consumption of B_5H_{11} and production of H_2 and B_2H_6 were measured at 75.1 ± 0.5 °C for six pressures in the range 1.75—10.36 mmHg. The initial rates were obtained by the tangent method from reaction profiles of

Table 2. First-order rate constants for thermolysis of B_5H_{11}[a]

T K (±0.5)	$10^6 k_{1,B_5H_{11}}$	$10^6 k_{1,H_2}$	$10^6 k_{1,B_2H_6}$
	s^{-1}		
313.4	13.1	3.4	5.9
322.7	20.7	8.4	8.5
333.6	43.4	22.2	38.3
348.2	168 ± 19[b]	86.8 ± 13.8[b]	118 ± 12[b]
363.9	491	211	
373.0[c]	1 310	365	379
383.5	1 820	1 260	1 170
398.4	4 710	2 950	4 420
423.8	11 700	9 010	8 570

[a] The data listed are evaluated from the expressions $k_{1,B_5H_{11}} = -(d[B_5H_{11}]\,dt)_0/[B_5H_{11}]_0$, $k_{1,H_2} = (d[H_2]/dt)_0/[B_5H_{11}]_0$, and $k_{1,B_2H_6} = (d[B_2H_6]\,dt)_0/[B_5H_{11}]_0$. Errors are estimated to be *ca.* 5—10%. [b] Mean values taken from six runs at this temperature (see Table 1); errors quoted are standard deviations. [c] From Figure 4 it is apparent that the ln k_1 values for both consumption of B_5H_{11} and production of H_2 fall off the lines of least-squares best fit; moreover, the deviations occur in opposite senses, thereby maximizing any errors in the value of the ratio $k_{1,H_2}/k_{1,B_5H_{11}}$ (see text), and in the results of mass-balance calculations based on these data (see Table 3, footnote *a*).

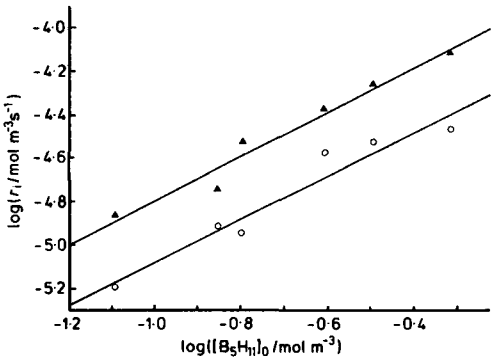

Figure 3. Logarithm of the initial rate (r_i) *versus* the log of the initial concentration of B_5H_{11} for thermolyses at 75.1 °C. Filled triangles refer to B_5H_{11} consumption and open circles to hydrogen production. The slopes of the lines of least-squares best fit to the two sets of data (*i.e.* the reaction orders with respect to [B_5H_{11}]) are, respectively, 1.04 ± 0.11 and 1.02 ± 0.13. A similar plot for the production of B_2H_6 yields a slope of 1.01 ± 0.09. Correlation coefficients lie between 0.97 and 0.99

the type shown in Figures 1 and 2. The results are included in Table 1 and recorded in the form of log–log plots in Figure 3. The slopes of the lines of least-squares best fit to the data are very close to unity in all cases (see caption to Figure 3), indicating that the reaction is accurately first order.

Activation energy. The activation energy of the thermal decomposition of B_5H_{11} was determined by recording the first-order rate constants at nine temperatures in the range 40—150 °C. Initial rates are given in Table 1, together with the data already discussed, and the rate constants are recorded in Table 2. Arrhenius plots of the data are shown in Figure 4 for the consumption of B_5H_{11} and production of hydrogen. Excellent linear plots were obtained not only for these but also for the production of B_2H_6 (not shown, see ref. 14). The values of the activation energies obtained from the slopes of these plots are

Table 3. Stoicheiometry of the involatile solid as a function of temperature[a]

T K	t[b] min	Stoicheiometry, x in BH_x
313.4	84	2.0
322.7	44	1.9
333.6	28	1.6
348.2	15	1.6
383.5	6	1.2
398.4	2	1.2
423.8	2	1.1

[a] A value of x = 1.9 determined at 373.0 K is probably erroneous and is omitted from the Table (see Table 2, footnote *c*). [b] Reaction time at which calculation was carried out.

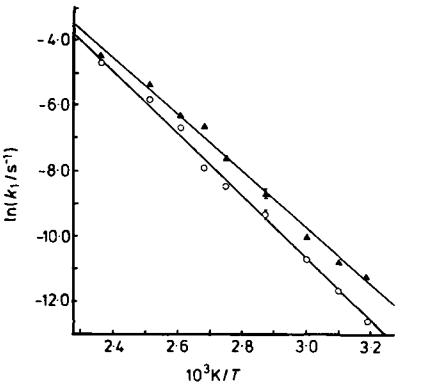

Figure 4. Arrhenius plots based on initial-rate constants for the consumption of B_5H_{11} (▲) and appearance of H_2 (○) in the thermal decomposition of B_5H_{11}. The data points at 75 °C are mean values from six separate runs; standard deviations are indicated by error bars

$E_{a,B_5H_{11}} = 72.6 \pm 2.4$, E_a (from H_2 production) = 80.1 ± 2.0, and E_a (from B_2H_6 production) = 76.3 ± 3.5 kJ mol^{-1}; the corresponding pre-exponential factors obtained from the intercepts are $A_{B_5H_{11}} = e^{16.4\pm0.8}$ (*ca.* 1.3 × 10^7), A (from H_2 production) = $e^{18.2\pm0.7}$ (*ca.* 7.8 × 10^7), and A (from B_2H_6 production) = $e^{17.1\pm1.2}$ (*ca.* 2.7 × 10^7) s^{-1}.

Reaction Stoicheiometry, and Composition of the Involatile Solid.—As discussed earlier, the thermolysis of B_5H_{11} is a complex reaction in which several products are formed simultaneously from the moment the mixture is heated. Hydrogen and B_2H_6 are formed in relatively large amounts, and their initial rates of appearance can therefore be measured with reasonable precision and accuracy; the same is true of the initial rate of consumption of the B_5H_{11} itself (see Table 1). It is generally a much more difficult problem to obtain reliable and reproducible initial-rate data for the minor products, and for this reason we have not attempted to specify an overall *initial* stoicheiometry for the reaction. The initial-rate data in Table 2 indicate that, on average, 1 mol of B_5H_{11} *initially* generates 0.6 ± 0.2 mol of B_2H_6 and 0.5 ± 0.2 mol of H_2, though it is important to note that this latter average value conceals a marked temperature dependence. The relative rates of production of H_2 and B_2H_6 are, in fact, *time*-dependent as is clear from Figures 1 and 2. The implications of these observations become apparent when mass-balance calculations are carried out to

Table 4. Initial-rate data (mol m^{-3} s^{-1}) for the thermolysis of B_5H_{11} (p_0 = 3.50 mmHg[a]) in a packed vessel at 74 °C[b]

Run no.[c]	$-10^6(d[B_5H_{11}]/dt)_0$	$10^6(d[H_2]/dt)_0$	$10^6(d[B_2H_6]/dt)_0$	$10^6(d[B_5H_9]/dt)_0$
1	218	16	118	29
2	64	8	27	10
3	34	9	15	
4	31	10	18	8
5	30	10	16	9
6	30	12	14	10

[a] 0.162 mol m^{-3}. [b] Average temperature over six runs 347.0 ± 0.4 K. [c] Runs 1—6 correspond to consecutive thermolyses in an initially clean vessel, packed with Raschig rings to give a 33-fold increase in the ratio surface area/volume.

determine the approximate amount and composition of the involatile solid hydride formed in these thermolyses. In fact, some 40—45 atom% of the boron content of the reacted B_5H_{11} appears as an involatile solid and this proportion is essentially independent of temperature. In contrast (see Table 3), the hydrogen content of the solid is markedly dependent on temperature, its composition varying from $BH_{2.0}$ at 40 °C to $BH_{1.1}$ at 150 °C.

Surface Studies.—To check for possible surface activity, six consecutive thermolyses were carried out at 74 °C in an initially clean Pyrex vessel packed with Raschig rings as described in the Experimental section. The initial pressure of B_5H_{11} in each case was 3.5 mmHg. From the results in Table 4 it can be seen that the initial rate of decomposition of B_5H_{11} in the first run is almost an order of magnitude greater than that observed (see Table 1) for the run at the same temperature and initial pressure in an unpacked, conditioned vessel (2.18×10^{-4} compared with 0.3×10^{-4} mol m^{-3} s^{-1}). However, in successive runs the initial rate slows down and eventually stabilizes at the same value as that observed for the thermolysis in an unpacked (conditioned) vessel. The initial rates of production of H_2, B_2H_6, and B_5H_9 in the *conditioned*, packed vessel are also similar to those in the unpacked vessel. The mechanistic significance of this important result is discussed later.

It is also clear from Table 4 that the initial rate of production of B_2H_6 (r_{i,B_2H_6}) relative to the initial rate of consumption of B_5H_{11} ($r_{i,B_5H_{11}}$) is about the same in all the packed-vessel runs, regardless of the extent of conditioning. For the six experiments the average value observed for the ratio $r_{i,B_2H_6}/r_{i,B_5H_{11}}$ is 0.51 ± 0.06, which is in excellent agreement with the value of 0.52 derived from the least-squares best fits to the data recorded at this temperature (74 °C) for the thermolysis in an unpacked vessel and with the average value of 0.6 ± 0.2 for all measurements referred to earlier. In contrast, there is a dramatic increase in the relative product of H_2 as the packed vessel becomes conditioned. Thus, in successive runs the ratio $r_{i,H_2}/r_{i,B_5H_{11}}$ increases steadily from 0.07 to 0.40, the final value being again in good agreement with the value of 0.44 taken from the data in Figure 4 for runs in a conditioned, unpacked vessel. There may be a similar trend in the initial rate of production of B_5H_9 but in view of the large errors involved in determining the initial rate of formation of this minor product, these values should be treated with caution. The average value of 0.24 ± 0.08 for the ratio $r_{i,B_5H_9}/r_{i,B_5H_{11}}$ is probably a more meaningful quantity, and this implies that the B_5H_9 is produced at slightly less than half the rate of B_2H_6 at this temperature.

Discussion

The thermal decomposition of B_5H_{11} *has been studied* qualitatively by several groups in the past, with differing results, but no detailed kinetic work on the system has been published. Burg and Schlesinger,[2] Bragg *et al.*,[3] and Morrey and Hill[4] have *all identified* H_2 *and* B_2H_6 *as the major volatile products*, but have given no specific indication of their rates of formation relative to the rate of consumption of B_5H_{11}. The compound B_5H_9 has been detected as a stable product in all of these studies, but opinions have differed as to whether it is formed from the very beginning of the thermolysis[3,4,7] or at a later stage when many other species are present.[2] Similar doubts have existed concerning the time at which the involatile solids appear, and B_4H_{10}, B_8H_{12}, and $B_{10}H_{14}$ have been detected in some studies but not in others. The present study has shown that these species are indeed all formed, together with minor amounts of B_6H_{12} and traces of B_9H_{15}. It is also clear that B_5H_9 and involatile solids are produced from the beginning of the reaction. In the case of B_5H_9 we were ourselves mistaken on this point in the early stages of our work, after analysing several runs at the lower end of the temperature range, where there are difficulties in detecting B_5H_9 because of its relatively slow rate of formation.[1]

The initial step in the thermolysis of B_5H_{11} is now generally thought to be the dissociation (7), and the important

$$B_5H_{11} \longrightarrow \{B_4H_8\} + \{BH_3\} \quad (7)$$

observation from molecular-beam studies[6] that $\{B_4H_8\}$ and $\{BH_3\}$ are present in the thermolysis of B_5H_{11} in a flow reactor adds weight to this. Moreover, the present work, in establishing that the reaction follows first-order kinetics, and that B_2H_6 is produced at the rate of *ca.* 0.5 mol per mol of B_5H_{11} consumed, leaves little room for doubt that (7) is indeed the rate-determining step. The observed rate of production of B_2H_6 is then readily explained by its formation from the rapid combination of two $\{BH_3\}$ units *via* the reverse of equation (1) with *ca.* 100% efficiency. In agreement with previous speculation,[15,16] the direct unimolecular liberation of H_2 from B_5H_{11} to give B_5H_9 can therefore be eliminated as an important initial step in this reaction. To account for the formation of B_5H_9, Schaeffer[16] has proposed the unlikely sequence of events in which two hydrogen atoms are transferred from B_5H_{11} to B_4H_{10}, which then splits up to give two molecules of B_2H_6. This reaction seems never to have been put to the test, either in a separate cothermolysis reaction or in an isotopic labelling experiment, but for reasons which have been put forward by Long[15] it must be considered very doubtful. A most unsatisfactory feature of this proposed reaction is that it relies on the prior production of B_4H_{10}, *via* the (assumed) rate-controlling interaction of B_5H_{11} with H_2 formed from minor secondary reactions or by hydrolysis resulting from the presence of traces of water on the walls. On the basis of the present results this hypothetical sequence is no longer tenable.

Another possibility is that the B_5H_9 *results from the* interaction of B_5H_{11} with the $\{B_4H_8\}$ production in equation (7). Lipscomb[17] has calculated that this reaction (8), which also

$$\{B_4H_8\} + B_5H_{11} \longrightarrow B_4H_{10} + B_5H_9 \quad (8)$$

produces B_4H_{10}, is exothermic by 125.5 kJ mol^{-1}. As Lipscomb has pointed out, at the temperatures required to decompose B_5H_{11}, B_4H_{10} would be appreciably dissociated to $\{B_4H_8\}$ and H_2, so that $\{B_4H_8\}$ would be essentially a catalyst for the loss of H_2 from B_5H_{11} in this reaction. Although this step cannot be entirely ruled out on the basis of the present results, it is clear from the relatively slow rate of production of B_5H_9 that it is certainly not the main route by which the $\{B_4H_8\}$ is consumed. An alternative possibility is that $\{B_4H_8\}$ reacts with B_5H_{11} to produce hydrogen and B_9H_{15}, followed rapidly by the decomposition of the latter to give 'polymer' and $B_{10}H_{14}$.[15] However, in the present work, thermolysis of B_5H_{11} under hot/cold conditions, produced negligible amounts of B_9H_{15}, and $B_{10}H_{14}$ (which is a likely stable product from *n*-B_9H_{15} under thermolytic conditions) did not build up in quantity, either in the hot/cold experiments or in the normal thermolysis reactions.

It has been suggested that $\{B_4H_8\}$ can react with *itself* to produce $\{B_3H_7\}$ and B_5H_9, and subsequently with the $\{B_3H_7\}$ to produce B_2H_6 and more B_5H_9 [reactions (9) and (10)

$$\{B_4H_8\} + \{B_4H_8\} \longrightarrow B_5H_9 + \{B_3H_7\} \quad (9)$$

$$\{B_3H_7\} + \{B_4H_8\} \longrightarrow B_5H_9 + B_2H_6 \quad (10)$$

respectively].[15] these reactions may well be operative, but it is clear that other processes are also occurring, because insufficient B_5H_9 is produced initially, and a significant proportion of the $\{B_4H_8\}$ appears to be converted into non-volatile BH_x solid. Even if all the $\{B_3H_7\}$ produced in (9) were diverted to give 'polymer,' it would still be necessary to invoke other reaction channels involving the production of 'polymer' from $\{B_4H_8\}$. Possibilities could include reactions (11) and (12).

$$\{B_4H_8\} + \{B_4H_8\} \longrightarrow \text{solid 'polymer'} + mH_2 \quad (11)$$

$$\{B_4H_8\} + \{B_4H_8\} \longrightarrow B_5H_{11} + \text{solid 'polymer'} + nH_2 \quad (12)$$

The latter was invoked by Shore and co-workers[10] to explain the high-yield synthesis of B_5H_{11} in the low-temperature reactions involving hydride-ion abstraction from $[B_9H_9]^-$. In view of the observed temperature dependence in the yield of B_5H_9 in the thermolysis of B_5H_{11}, it is possible that reactions such as (9) and (12) are in a temperature-dependent competition, with the former being favoured at higher temperatures. Details of the amount of H_2 produced in these thermolyses and its temperature dependence can also be understood in terms of steps such as these.

Of the other boranes formed in this system, B_4H_{10} has only a fleeting existence because of its thermal instability at the temperatures employed.[9] It is undoubtedly formed from the reaction between $\{B_4H_8\}$ and H_2 generated in the reaction. Hexaboranes appear in the form of B_6H_{12}, but the concentrations are very small and the mechanism of formation is uncertain. The compound $B_{10}H_{14}$ *does* become an important final product, and it is interesting that it no longer continues to build up rapidly when the B_5H_{11} has been consumed. This is illustrated in Figure 2, which shows the reaction profile at 150 °C. The observation that the concentrations of B_2H_6, B_5H_9, and $B_{10}H_{14}$ become more or less constant could be taken to indicate that the latter is not formed in this system from the cothermolysis of the two smaller boranes. However, this is probably an erroneous conclusion, and it is likely that the lack of reaction in the later stages of the thermolysis can be attributed to the inhibiting effect of the substantial amount of H_2 that has accumulated. The route to $B_{10}H_{14}$ in the B_2H_6/B_5H_9 cothermolysis system is thought to proceed *via* the interaction of $\{B_3H_7\}$ [formed in steps (1)—(3)] with B_5H_9.[15] In the later stages of the B_5H_{11} thermolysis there will be a competition between H_2 and B_5H_9 for the $\{B_3H_7\}$, and it seems likely that H_2 is successful in reversing the sequence (1)—(3), thereby reducing the amount of $\{B_3H_7\}$ available for reaction with B_5H_9.

The results of the packed-vessel study are of crucial importance in establishing that the thermolysis of B_5H_{11} in 'conditioned' vessels is a homogeneous gas-phase reaction. In consequence, the activation parameters, which have been determined for the first time in this work, can be meaningfully compared with those recorded for gas-phase decompositions of other boranes. Thus, the activation energy of B_5H_{11} (72.6 ± 2.4 kJ mol^{-1}) is considerably less than that for B_4H_{10} (99.4 ± 3.4 kJ mol^{-1}), reflecting a more dramatic temperature dependence of the rate constant for the latter. More specifically, the ratio of the first-order rate constants ($k_{1,B_4H_{10}}/k_{1,B_5H_{11}}$) is found to vary from 49 at 200 °C to 1.7 at 40 °C, implying that the two boranes should have similar stabilities at the lower temperatures. At first sight it may therefore seem surprising that, in the thermolysis of B_4H_{10},[9] B_5H_{11} builds up to the extent that it does. It must be remembered, however, that both $\{B_4H_8\}$ and $\{BH_3\}$ (which are the initial products of the decomposition of B_5H_{11}) may themselves react further with B_4H_{10} to regenerate B_5H_{11}. Nevertheless, these considerations highlight the need for caution in interpreting the initial-rate data in terms of possible stoicheiometries in such complex interconversion systems.

The value of 1.6×10^7 s^{-1} for the pre-exponential factor for the thermolysis of B_5H_{11} is lower by four orders of magnitude than the value for B_4H_{10} (6×10^{11} s^{-1}), consistent with the gross differences proposed for the initial steps in the two decompositions, *viz.* elimination of BH_3 and of H_2, respectively. The value for B_4H_{10} itself is at the lower end of the range of values (*ca.* 10^{11}—10^{15} s^{-1}) found for unimolecular decompositions of hydrocarbon derivatives,[18,19] and is acceptable for a mechanism involving release of H_2 *via* a loosely bound transition state. The pre-exponential factor for the decomposition of B_5H_{11} as determined both from the rate of consumption of the reactant and from the appearance of the products (*e.g.* H_2 or B_2H_6) is exceptionally low, and at first sight might appear to cast doubt on the validity of the proposed mechanism involving (7) as the initial, unimolecular, rate-determining step. However, we believe that there are cogent reasons for accepting this unusual value. First, a very similar A value (and E_a value) has recently been observed in the gas-phase decomposition of B_6H_{12},[20] whose structure[21] is closely related to that of B_5H_{11}. Secondly, it is important to appreciate that these are among the first reliable experimental data on Arrhenius parameters to be reported for the boron hydrides, which are in fact a particularly unusual class of compounds whose unique structural and bonding properties could well engender unexpected kinetic parameters. The much lower A factor for B_5H_{11} compared with B_4H_{10} may reflect considerable reorganization in a tightly bound transition state, consistent with the more extensive changes that would accompany the release of a BH_3 group from the cluster. An additional point is that the slow initial step (7) is expected to dominate the overall Arrhenius parameters for the reaction and, though subsequent rapid steps such as (8) and (12) which consume or regenerate B_5H_{11} will of course contribute, it is most unlikely that these would lead to a reduction of several orders of magnitude in the observed pre-exponential factors.

The dramatic increase in the rate of decomposition of B_5H_{11} in a clean, packed vessel is reproducible and implies that the reaction is catalysed by the clean Pyrex surface. Evidence that this is the case, and that a spurious reaction with adsorbed

moisture or other species is not occurring, comes from the observation that the rate of production of B_2H_6 relative to the rate of consumption of B_5H_{11} remains the same, regardless of the extent or condition of the surface. The rate-controlling initial step is therefore the same [*i.e.* reaction (7)] as in the homogeneous gas-phase reaction, but is accelerated. The data are not sufficiently accurate to reveal any major changes in product distribution, apart from the dramatic reduction in the relative production of H_2 in the clean, packed vessel. It seems most unlikely that this is caused by adsorption of H_2 on the surface, and implies that the formation of a hydrogen-rich solid is favoured under these conditions. It should perhaps be noted that Morrey and Hill[4] have suggested that B_5H_{11} may be converted catalytically into B_5H_9 by the presence of a brass surface, but this does not occur at the Pyrex surface in our experiments.

Conclusions

In the temperature range 40—150 °C and pressure range 1.75—10.5 mmHg the homogeneous gas-phase decomposition of B_5H_{11} has been shown to proceed with first-order kinetics and an activation energy of 72.6 ± 2.4 kJ mol^{-1}. The initial step [equation (7)] involves the release of a BH_3 group from B_5H_{11} *via* a tightly bound transition state, and this is followed by the rapid dimerization of $\{BH_3\}$ to give B_2H_6 with *ca.* 100% efficiency. The precise fate of the fugitive $\{B_4H_8\}$ intermediate is more complex in this reaction system and the relative importance of various possible routes has not been established in detail; it may react with itself *via* several channels [*e.g.* reactions (9), (11), and (12)] in temperature-dependent competition, or with B_5H_{11} [reaction (8)], to give the final products which are mainly B_5H_9 and involatile solids, though $B_{10}H_{14}$ also accumulates.

The effect of added hydrogen on the thermolysis of B_5H_{11} has been studied in detail in an attempt to resolve these and related mechanistic questions. The results of these further studies and those of added hydrogen on B_4H_{10} are the subject of a subsequent paper.

Acknowledgements

We thank Mr. D. Singh for invaluable experimental assistance and Dr. D. L. Baulch for helpful discussions. This work was supported by the S.E.R.C. and by the U.S. Army Research and Standardization Group (Europe).

References

1 N. N. Greenwood and R. Greatrex, *Pure Appl. Chem.*, 1987, **59**, 857.
2 A. B. Burg and H. I. Schlesinger, *J. Am. Chem. Soc.*, 1933, **55**, 4009.
3 J. K. Bragg, L. V. McCarty, and F. J. Norton, *J. Am. Chem. Soc.*, 1951, **73**, 2134.
4 J. R. Morrey and G. R. Hill, U.S. Dept. Com., Office Tech. Serv. Report No., AD154, 121, 1958.
5 C. R. Phillips, Ph.D. Thesis, Indiana University, 1967; *Diss. Abstr. Int. B*, 1968, **28**, 3630.
6 R. E. Hollins and F. E. Stafford, *Inorg. Chem.*, 1970, **9**, 877.
7 T. C. Gibb, N. N. Greenwood, T. R. Spalding, and D. Taylorson, *J. Chem. Soc., Dalton Trans.*, 1979, 1392.
8 R. Greatrex, N. N. Greenwood, and G. A. Jump, *J. Chem. Soc., Dalton Trans.*, 1985, 541.
9 R. Greatrex, N. N. Greenwood, and C. D. Potter, *J. Chem. Soc., Dalton Trans.*, 1986, 81.
10 M. A. Toft, J. B. Leach, F. L. Himpsl, and S. G. Shore, *Inorg. Chem.*, 1982, **21**, 1952.
11 R. Greatrex, N. N. Greenwood, D. W. H. Rankin, and H. E. Robertson, *Polyhedron*, 1987, **6**, 1849.
12 J. R. Wermer and S. G. Shore, *Inorg. Chem.*, 1987, **26**, 1644.
13 M. J. Klein, B. Harrison, and I. Soloman, *J. Am. Chem. Soc.*, 1958, **80**, 4149.
14 M. D. Attwood, Ph.D. Thesis, University of Leeds, 1987.
15 L. H. Long, *J. Inorg. Nucl. Chem.*, 1970, **32**, 1097.
16 R. Schaeffer, *J. Chem. Phys.*, 1957, **26**, 1349.
17 W. N. Lipscomb, *Pure Appl. Chem.*, 1983, **55**, 1431.
18 P. J. Robinson and K. A. Holbrook, 'Unimolecular Reactions,' *Wiley-Interscience, London*, 1972.
19 K. J. Laidler, 'Chemical Kinetics,' Tata McGraw-Hill, New York, 1973.
20 R. Greatrex, N. N. Greenwood, and S. D. Waterworth, *J. Chem. Soc., Chem. Commun.*, 1988, 925.
21 R. Greatrex, N. N. Greenwood, M. B. Millikan, D. W. H. Rankin, and H. E. Robertson, *J. Chem. Soc., Dalton Trans.*, 1988, 2335.

Received 25*th January* 1988; *Paper* 8/00263K

Influence of Added Hydrogen on the Kinetics and Mechanism of Thermal Decomposition of Tetraborane(10) and of Pentaborane(11) in the Gas Phase *

Martin D. Attwood, Robert Greatrex, and Norman N. Greenwood
School of Chemistry, University of Leeds, Leeds LS2 9JT

The effects of added hydrogen on the kinetics of the first-order thermal decomposition of the two *arachno* species tetraborane(10) and pentaborane(11) have been studied in detail by a mass-spectrometric method. In the case of B_4H_{10}, the order and activation energy were unaltered, but the reaction rate was retarded and there was a marked change in product distribution: the percentage yield of B_5H_{11} remained the same, but B_2H_6 was formed in preference to B_5H_9, B_6H_{12}, $B_{10}H_{14}$, and involatile solids. These results provide cogent new evidence that B_4H_{10} decomposes *via* the single rate-determining step (i), but raise doubts about the validity of subsequent steps in the

$$B_4H_{10} \rightleftharpoons \{B_4H_8\} + H_2 \quad \text{(i)}$$

previously proposed mechanism. In the thermolysis of B_5H_{11} there was a dramatic change in product distribution, but the order, activation energy, *and* initial rate of disappearance of B_5H_{11} were all unaffected by the presence of the added H_2. These results establish for the first time that the so-called 'equilibrium' (ii) proceeds in the forward direction *via* the rate-determining

$$B_5H_{11} + H_2 \rightleftharpoons B_4H_{10} + \tfrac{1}{2}B_2H_6 \quad \text{(ii)}$$

dissociation (iii), followed by the rapid reactions (−i) and (iv). They also imply that in the thermolysis

$$B_5H_{11} \longrightarrow \{B_4H_8\} + \{BH_3\} \quad \text{(iii)}$$

$$2\{BH_3\} \longrightarrow B_2H_6 \quad \text{(iv)}$$

of B_5H_{11} in the absence of added H_2 the reactive intermediate $\{B_4H_8\}$ reacts subsequently with itself and is not consumed by reaction with B_5H_{11}.

arachno-Tetraborane, B_4H_{10}, is a highly reactive gas which readily interconverts to other boranes above about 40 °C. There has been uncertainty in the literature about almost all aspects of its thermolysis, but we have recently resolved many of these problems by means of a detailed mass-spectrometric study.[1] At the centre of these discussions has been the question of the precise nature of the initial step. Our earlier reports have reviewed the background to this subject, and have outlined our reasons for believing that the reaction proceeds *via* the (reversible) unimolecular elimination of H_2 from B_4H_{10} [reaction (1)], rather than the elimination of $\{BH_3\}$ or, as was

$$B_4H_{10} \rightleftharpoons \{B_4H_8\} + H_2 \quad (1)$$

originally suggested,[2] by a combination of both routes. The reactive intermediate $\{B_4H_8\}$ is then thought to react rapidly with B_4H_{10} to give B_5H_{11} as the main volatile borane product [equation (2)]. On this basis an excess of added H_2 should

$$\{B_4H_8\} + B_4H_{10} \longrightarrow B_5H_{11} + \{B_3H_7\} \quad (2)$$

inhibit the decomposition of B_4H_{10} and alter the product distribution. There are in fact qualitative indications to this effect in the literature,[2,3] but we wished to put these observations on a more quantitative basis. In particular we wished to determine the Arrhenius parameters for the thermolysis of B_4H_{10} in the presence of added H_2, to establish whether the suppression of reaction (1) would alter the observed activation energy, and thereby reveal the presence of any competing rate-determining step.

We have recently completed a detailed kinetic study of the thermolysis of B_5H_{11} in the absence of added H_2 which, by contrast, strongly suggests that the initial step for this borane involves the rate-determining release of $\{BH_3\}$, followed by rapid dimerization of the latter to give B_2H_6 with approximately 100% efficiency [equations (3) and (4)].[4] The precise fate

$$B_5H_{11} \longrightarrow \{B_4H_8\} + \{BH_3\} \quad (3)$$

$$2\{BH_3\} \rightleftharpoons B_2H_6 \quad (4)$$

of the reactive intermediate $\{B_4H_8\}$ was not established in detail, and it was hoped, again, that experiments with added H_2 would give further insights into the processes occurring. It has often been suggested[2,3,5] that B_5H_{11} and B_4H_{10} are interconvertible in the presence of H_2, according to the 'equilibrium' (5). However, it was not clear whether the forward reaction

$$B_5H_{11} + H_2 \rightleftharpoons B_4H_{10} + \tfrac{1}{2}B_2H_6 \quad (5)$$

occurred as a single step (*i.e.* BH abstraction by H_2 from B_5H_{11}) or as a combination of reactions (3), (4), and (−1).

To resolve these various problems we have carried out detailed studies of the effects of added H_2 on the kinetics of thermal decomposition of both B_4H_{10} and B_5H_{11} over a range

* *Non-S.I. unit employed:* mmHg ≈ 133 Pa.

Table 1. Initial-rate data for thermolysis of B_4H_{10} in the presence of added H_2[a]

T K (±0.5)	$p_0(B_4H_{10})$ mmHg	$10[B_4H_{10}]_0$ mol m^{-3}	$p_0(H_2)$ mmHg	$10[H_2]_0$ mol m^{-3}	$-10^6 \times (d[B_4H_{10}]/dt)_0$	$10^6 \times (d[H_2]/dt)_0$[b]	$10^6 \times (d[B_2H_6]/dt)_0$	$10^6 \times (d[B_5H_{11}]/dt)_0$
					mol m^{-3} s^{-1}			
323.3	3.51	1.74	20.0	9.9	1.7		0.3	0.5
332.9	3.48	1.68	19.9	9.6	5.6		0.7	1.4
348.2	3.49	1.61	19.9	9.2	24.1		3.8	17.9
362.1	1.78	0.79	50.0	22.1	47.6		12.9	12.7
362.8	3.51	1.55	0.0	0.0	344		17.5	169
361.8	3.51	1.55	50.1	22.2	60.8		20.2	39.4
361.8	5.30	2.35	50.0	22.2	88.6		24.6	51.1
361.7	7.05	3.13	50.0	22.2	128		37.0	59.5
362.1	13.5	5.98	49.9	22.1	274		91.4	151
363.5	3.50	1.54	20.1	8.9	91.9	123	14.1	49.6
373.1	3.49	1.50	20.1	8.6	212	462	31.8	125
383.7	3.49	1.46	20.1	8.4	476	794	89.3	288

[a] Systematic errors in pressure measurements *ca.* ±1%, and in initial rates *ca.* 5%. [b] Data for H_2 not recorded for most runs because of large background from added H_2.

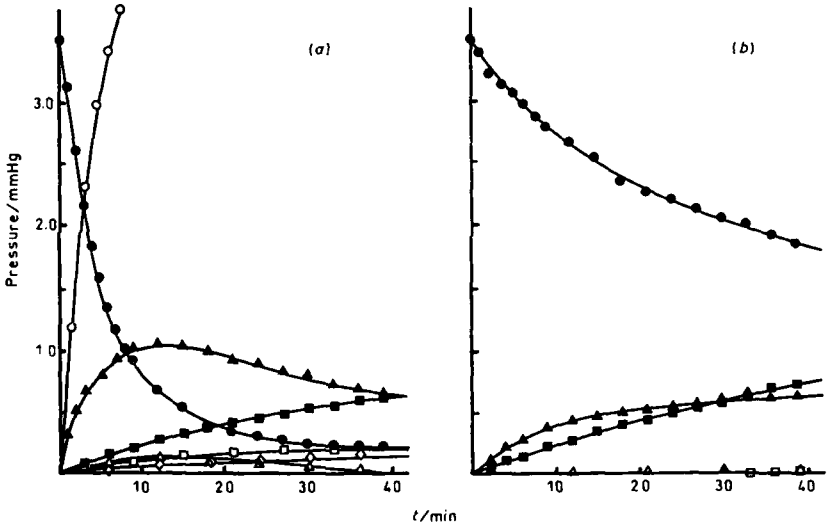

Figure 1. Reaction profiles for the thermolysis of (*a*) B_4H_{10} (p_0 = 3.51 mmHg) at 89.7 °C and (*b*) B_4H_{10} (p_0 = 3.51 mmHg) and H_2 (p_0 = 50.1 mmHg) at 89.7 °C, showing the influence of added hydrogen: (○) H_2, (●) B_4H_{10}, (▲) B_5H_{11}, (■) B_2H_6, (△) B_6H_{12}, (□) $B_{10}H_{14}$, and (◇) B_5H_9. Data for H_2 were not recorded in (*b*) because of the large initial background from added H_2

of temperature and pressure. Some preliminary findings have been referred to elsewhere,[6] but we now report a full account of the work.

Experimental

The quantitative mass-spectrometric techniques used in this work have been described in detail elsewhere.[1,7] All thermolyses were carried out in 'conditioned,' spherical Pyrex bulbs in the presence of a large background of an inert-gas mixture (partial pressure 100 mmHg) comprising helium, argon, and krypton in the relative proportions 98.0:1.0:1.0.[4] From the results of our previous work with B_4H_{10}[1] and B_5H_{11}[4] it seems reasonable to conclude that, under the present experimental conditions, we are dealing with homogeneous gas-phase reactions: both of the decompositions were shown to be unaffected by 'conditioned' Pyrex surfaces, and it is most unlikely that the presence of added H_2 would induce any heterogeneous component.

The boranes were prepared by the methods of Shore and co-workers,[8,9] and handled throughout using standard grease-free vacuum-line techniques. Purification was achieved by trap-to-trap fractionation, followed where necessary by fractionation on a low-temperature column.[4]

Results

Reaction Profiles and Initial-rate Data.—Typical reaction profiles for the thermolysis of B_4H_{10} alone and in the presence of *ca.* 50 mmHg added H_2 are compared in Figure 1, and similar results for B_5H_{11} are shown in Figure 2. These particular

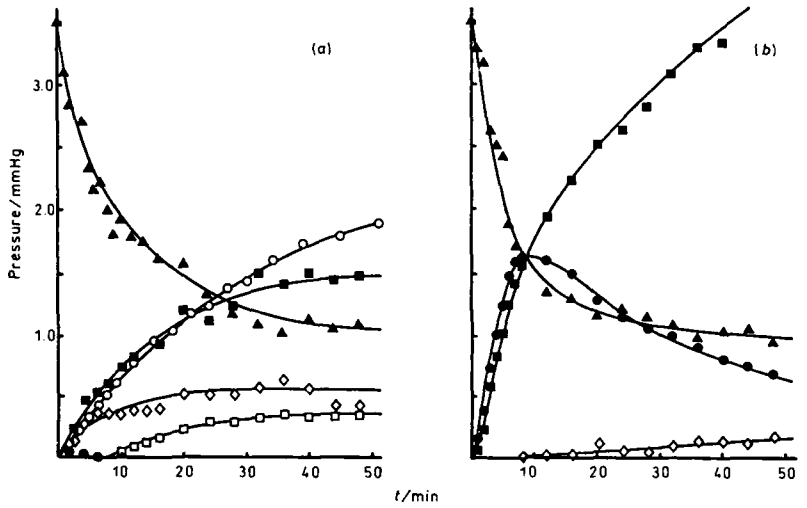

Figure 2. Reaction profiles for the thermolysis of (*a*) B_5H_{11} (p_0 = 3.52 mmHg) at 99.9 °C (data from ref. 4) and (*b*) B_5H_{11} (p_0 = 3.53 mmHg) and H_2 (49.9 mmHg) at 100.1 °C, showing the influence of added hydrogen on the thermolysis of B_5H_{11}; symbols as in Figure 1

Table 2. First-order rate constants for the thermolysis of B_4H_{10} alone and in the presence of added H_2[a]

Added H_2 p/mmHg	T/K (±0.5)	10^6k_1/s^{-1} From B_4H_{10} consumption	From B_2H_6 production	From B_5H_{11} production
0.0	362.8	2 217	113	1 090
20.0	323.3	9.8	1.7	2.9
19.9	332.9	33.3	4.2	8.3
19.9	348.2	150	23.6	109
20.1	363.5	597	91.6	322
20.1	373.1	1 415	212	835
20.1	383.7	3 260	617	1 969
50.0	361.8	448 ± 82[b]	134 ± 22[b]	215 ± 36[b]

[a] Evaluated from the expressions k_1(from B_4H_{10} consumption) = $-(d[B_4H_{10}]/dt)_0/[B_4H_{10}]_0$, k_1(from B_2H_6 production) = $(d[B_2H_6]/dt)_0/[B_4H_{10}]_0$ and k_1(from B_5H_{11} production) = $(d[B_5H_{11}]/dt)_0/[B_4H_{10}]_0$. [b] Mean values from five runs at this temperature (see Table 1); errors quoted are standard deviations.

B_4H_{10} runs were performed at *ca.* 90 °C and the B_5H_{11} runs at *ca.* 100 °C, but the initial pressures of the boranes were the same (*ca.* 3.5 mmHg) in each case. A complete set of reaction profiles for the numerous thermolyses performed in this work can be found elsewhere.[10] Initial rates, determined by the tangent method, are listed in Tables 1—3 together with the derived first-order rate constants.

From Figure 1 it is clear that the thermal decomposition of B_4H_{10} is substantially inhibited by the presence of added H_2, and that there is a dramatic change in product distribution. After 6 min in the thermolysis of B_4H_{10} alone [Figure 1(*a*)] the distribution of boron amongst the various products is 49% as B_5H_{11}, 8% as $B_{10}H_{14}$, 6% as B_6H_{12}, 4% as B_2H_6, 2% as B_5H_9, and 31% as involatile solids (from mass-balance calculations). In contrast, in the presence of added H_2 [Figure 1(*b*)] the distribution of boron is 59% as B_5H_{11}, 34% as B_2H_6, 1% as B_5H_9, and <6% as solids. However, from the results in Table 1, it is particularly interesting that on a molar basis the relative rates of production of B_5H_{11} ($r_{i,B_5H_{11}}$) to consumption of B_4H_{10} ($r_{i,B_4H_{10}}$) in the presence of H_2 are unaltered from those of the thermolysis of B_4H_{10} alone. For the six runs carried out with 20 mmHg added H_2 the average value of the ratio $r_{i,B_5H_{11}}/r_{i,B_4H_{10}}$ is 0.50 ± 0.18, and for the five runs with 50 mmHg added H_2 the average is 0.50 ± 0.13. These values are in excellent agreement with the value of 0.49 obtained in this study, and the values in the range 0.4—0.5 reported in our earlier, more detailed, study of B_4H_{10} alone.[1] On the other hand, the ratio $r_{i,B_2H_6}/r_{i,B_4H_{10}}$ is found to increase systematically from 0.05 in the B_4H_{10}-alone thermolysis, through 0.16 ± 0.02 in the runs with 20 mmHg added H_2, to 0.30 ± 0.03 in the presence of 50 mmHg added H_2.

Turning now to the thermolysis of B_5H_{11}, it can be seen from the typical reaction profile in Figure 2 that in this case also there is a marked change in product formation when excess of H_2 is added to the system. The compound B_4H_{10}, which is virtually absent in the thermolysis of B_5H_{11} alone, is now the main product, its rate of formation in the initial stages being almost equal to the rate of consumption of B_5H_{11}. However, its concentration reaches a maximum, after about 10 min in this particular thermolysis (100 °C), and then drops steadily as the reaction proceeds. The only other volatile borane produced in the early stages, B_2H_6, appears at a somewhat faster rate than it does when H_2 is not added initially, and from mass-balance calculations it is apparent that, after 3 min, some 30% of the boron from the B_5H_{11} consumed is present as B_2H_6. Thereafter, its concentration continues to rise steadily throughout the thermolysis. Hydrogen is the only other volatile species produced initially, but its concentration has not been recorded in these experiments because of difficulties of obtaining accurate data when a large added background is present initially. Formation of all other boranes, including B_5H_9, B_6H_{12}, $B_{10}H_{14}$, and involatile solid, is almost entirely suppressed by the presence of an excess of added H_2, at least in the early stages of the reaction. Despite these major effects on the product

Table 3. Initial-rate data and first-order rate constants for thermolysis of B_5H_{11} in the presence of added H_2.[a]

T K (±0.5)	$p_0(B_5H_{11})$ mmHg	$10[B_5H_{11}]_0$ mol m^{-3}	$p_0(H_2)$ mmHg	$10[H_2]_0$ mol m^{-3}	$-10^6 \times (d[B_5H_{11}]\,dt)_0$ mol m^{-3} s^{-1}	$10^3 k_{1,B_5H_{11}}$[b] s^{-1}
333.5	3.52	1.69	49.9	24.0	9.4	0.055
348.2	3.51	1.62	50.1	23.1	23.0	0.142
373.2	3.53	1.52	49.9	21.5	198	1.30
398.3	3.53	1.42	49.9	20.1	748	5.26

[a] See footnotes to Table 1. [b] Evaluated from the expression $k_{1,B_5H_{11}} = -(d[B_5H_{11}]\,dt)_0/[B_5H_{11}]_0$.

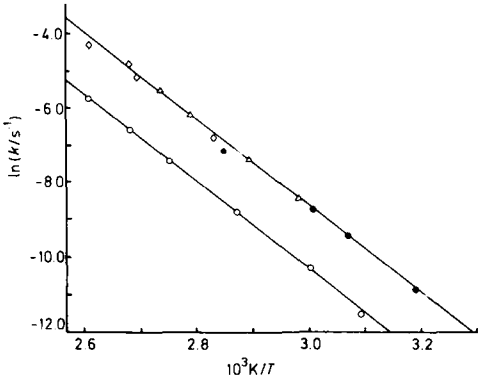

Figure 3. Arrhenius plots for the thermolysis of B_4H_{10} alone (●),[1] in cothermolysis with B_2H_6 (△)[5a] and CO (▽),[11] and in the presence of 20 mmHg added H_2 (○, this work)

distribution it is remarkable that the initial rate of consumption of B_5H_{11} is virtually unaltered by the presence of a 14-fold excess of added H_2. This specific point is considered in more detail in the following section, and is later shown to have important mechanistic implications.

Reaction Order and Arrhenius Parameters.—The initial-rate data from Table 1 for the B_4H_{10}/H_2 cothermolysis at *ca.* 90 °C when plotted in the form of log(initial rate) *versus* log(initial concentration) give slopes that in each case are very close to unity, indicating that the consumption of B_4H_{10} and the production of both B_2H_6 and B_5H_{11} are all first order with respect to the initial concentration of B_4H_{10}. The actual slopes of the lines of best fit are 0.88 ± 0.05 for consumption of B_4H_{10}, 0.95 ± 0.14 for the production of B_2H_6, and 1.10 ± 0.11 for the production of B_5H_{11}. Order plots of this type have not been obtained for the B_5H_{11}/H_2 cothermolysis, but as will become apparent this reaction is also first order with respect to the initial concentration of B_5H_{11} but zero order with respect to the concentration of hydrogen.

The first-order rate constants given in Tables 2 and 3 for the consumption of B_4H_{10} and B_5H_{11} in their respective cothermolyses with H_2 are recorded in the form of Arrhenius plots in Figures 3 and 4. Figure 3 also includes, for comparison (upper line), data for the thermolysis of B_4H_{10} alone,[1] and in cothermolysis with B_2H_6[5a] and CO.[11] It is at once apparent that the presence of 20 mmHg added H_2 leads to a consistent diminution (by a factor of *ca.* 5) in the rate of decomposition of B_4H_{10}, but leaves the activation energy unaltered. Essentially similar values for the activation energy were obtained from plots based on the rate constants for the production of B_2H_6

Table 4. Arrhenius parameters for the thermolysis of B_4H_{10} and B_5H_{11} alone and in the presence of added H_2

System	Activation energy, E_a kJ mol^{-1}	Pre-exponential factor, A/s^{-1}	Ref.
B_4H_{10}	99.2 ± 0.8	$e^{27.3\pm0.3}$(*ca.* 6.0 × 10^{11})	1
$B_4H_{10} + H_2$[a]	98.4 ± 1.4	$e^{25.1\pm0.5}$(*ca.* 8.0 × 10^{10})	This work
B_5H_{11}	72.6 ± 2.4	$e^{16.4\pm0.8}$(*ca.* 1.3 × 10^{7})	4
$B_5H_{11} + H_2$[b]	80.1 ± 5.4	$e^{19.0\pm1.9}$(*ca.* 1.8 × 10^{8})	This work

[a] $p_0(H_2)$ = 20 mmHg, ratio $H_2:B_4H_{10}$ = 5.73. [b] $p_0(H_2)$ = 50 mmHg, ratio $H_2:B_5H_{11}$ = 14.2.

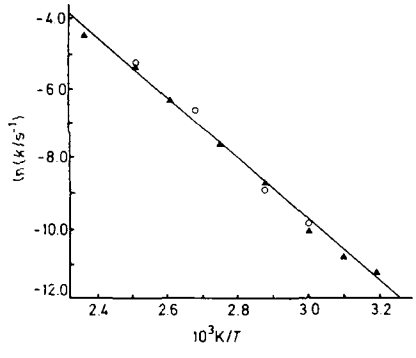

Figure 4. Arrhenius plots for the thermolysis of B_5H_{11} alone (▲)[4] and in the presence of 50 mmHg added H_2 (○, this work). The line drawn through the data is the least-squares best fit to the data for the thermolysis of B_5H_{11} alone; the least-squares best fit to the data for the B_5H_{11}/H_2 cothermolysis yields a slightly greater activation energy, but the difference is not thought to be significant (see text)

and B_5H_{11} (Table 2). The Arrhenius data for B_5H_{11} in Figure 4 demonstrate the point made earlier that the intial rates are unaltered by the presence of a 14-fold excess of added H_2. The activation energies are therefore essentially the same as in the thermolysis of B_5H_{11} alone, despite the fact that the observed product distributions are quite different. The numerical values of the activation energies and pre-exponential factors determined, respectively, from the slopes and intercepts of these plots are gathered together in Table 4 with values obtained in our earlier work for the thermolyses of B_4H_{10}[1] and B_5H_{11}[4] in the absence of added H_2. The apparent difference in the activation energies for the thermolysis of B_5H_{11} alone and in the presence of 50 mmHg added H_2 is within the error limits defined by the standard deviations, and is therefore not thought to be significant. This view was confirmed by the results of an additional series of experiments carried out with smaller initial pressures of B_5H_{11} (1 mmHg) and H_2 (10 mmHg), so that initial

rates of production of H_2 could be monitored without causing saturation problems (see Table 1, footnote *b*). These measurements are not discussed in detail here because the initial rates are in general less precisely defined, owing to the smaller amounts of material involved. However, despite somewhat greater scatter in the data, the rate constants for both consumption of B_5H_{11} and production of H_2 were generally in good agreement with the Arrhenius data for the thermolysis of B_5H_{11} alone.

Discussion

Cothermolysis of Tetraborane(10) *and Hydrogen.*—As mentioned in the Introduction, our recent results on the thermolysis of B_4H_{10} alone have been interpreted in terms of a mechanism involving the initial rate-determining elimination of H_2 to produce the short-lived reactive intermediate $\{B_4H_8\}$ [reaction (1)], followed by the rapid reaction of this species with B_4H_{10} to give B_5H_{11} and $\{B_3H_7\}$ [reaction (2)].[1] The changes in product distribution observed in the present study, when H_2 is added initially to the thermolysis of B_4H_{10}, are entirely consistent with this mechanism. Thus, inhibition is accounted for by the increased importance of the back reaction (−1), which is in competition with reaction (2), but the percentage yield of B_5H_{11} is expected to be unaltered, as observed experimentally. Moreover, the relative increase in the rate of formation of B_2H_6 can be explained by the increased importance of reactions (6), (7), and (4).

$$\{B_3H_7\} + H_2 \rightleftharpoons \{B_3H_9\} \quad (6)$$

$$\{B_3H_9\} \rightleftharpoons B_2H_6 + \{BH_3\} \quad (7)$$

These three steps are the reverse of the accepted sequence by which B_2H_6 is thought to decompose,[12] and are seen to channel the reactive species $\{B_3H_7\}$ into the formation of this volatile borane at the expense of involatile 'polymer' which may otherwise be formed *via* reactions such as (8)[1] and/or (9).[8] The virtual absence of B_6H_{12} can also be understood in terms of the competitive removal by added H_2 of the reactive intermediates $\{B_3H_7\}$ and $\{B_4H_8\}$ *via* reactions (6) and (−1) rather than their participation in reactions (10)—(12) which could otherwise arise in the normal thermolysis of B_4H_{10} (though there are reasons[1] why the last of these is less likely).

$$2\{B_3H_7\} \longrightarrow \{'B_6H_{14-2m}'\}(\text{polymerizes}) + mH_2 \quad (8)$$

$$2\{B_3H_7\} \longrightarrow B_4H_{10} + \{'B_2H_4'\}(\text{polymerizes}) \quad (9)$$

$$\{B_3H_7\} + B_5H_{11} \longrightarrow B_6H_{12} + B_2H_6 \quad (10)$$

$$\{B_4H_8\} + B_5H_{11} \longrightarrow B_6H_{12} + \{B_3H_7\} \quad (11)$$

$$2\{B_3H_7\} \longrightarrow B_6H_{12} + H_2 \quad (12)$$

However, all is not well with this mechanism since there appears to be an inconsistency between the magnitude of the observed retardation and the experimentally observed reaction order for the decomposition of B_4H_{10} in the presence of excess of added H_2. Thus, by application of 'steady-state' arguments, it can be shown that the expected rate of consumption of B_4H_{10} is given by equation (13), and the expected order by equation (14). From the form of equation (14) it follows that the order would be 2, if $k_{-1}[H_2]_0 \gg k_2[B_4H_{10}]_0$. However if the rates of reactions (−1) and (2) approach one another (*i.e.* $k_{-1}[H_2]_0 = k_2[B_4H_{10}]_0$) the expected order drops to 3/2, and as the relative rate of (2) increases further the order approaches unity. This is illustrated in Figure 5, which shows the calculated dependence of the reaction order on the ratio $k_2[B_4H_{10}]_0/k_{-1}[H_2]_0$ for the three-step mechanism (1), (−1), and (2). Equations (13) and (14) both assume of course that subsequent to the rate-determining step there are no other significant reactions involving B_4H_{10} and $\{B_4H_8\}$ in the 'initial' stages of the reaction. Now, on the basis of equation (13), the *ca.* 5-fold reduction observed in the inital rate in the presence of 20 mmHg added H_2 implies a value of *ca.* 0.7 for the rate-constant ratio k_{-1}/k_2, and from equation (14) this leads to a predicted order (in the presence of 50 mmHg added H_2) of *ca.* 1.9, which disagrees with the values of *ca.* 1 observed experimentally. It therefore appears that the mechanism referred to above is either oversimplified or incorrect.

$$\frac{-d[B_4H_{10}]}{dt} = \frac{2k_1k_2[B_4H_{10}]^2}{k_{-1}[H_2] + k_2[B_4H_{10}]} \quad (13)$$

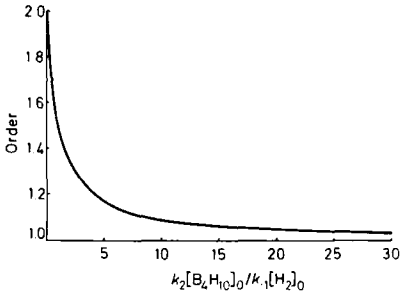

Figure 5. Theoretical dependence of reaction order* on the ratio $k_2[B_4H_{10}]_0/k_{-1}[H_2]_0$ for the proposed three-step mechanism in the thermolysis of B_4H_{10} in the presence of added H_2. This plot is based on equation (13), and assumes that steps (1), (−1), and (2) are the only important reactions involving B_4H_{10} and $\{B_4H_8\}$ in the initial stages (*This refers to the order for the consumption of B_4H_{10} with respect to the concentration of B_4H_{10}.)

$$\text{Order} = \frac{d\log(d[B_4H_{10}]/dt)_0}{d\log[B_4H_{10}]_0} = 2 - \frac{k_2[B_4H_{10}]_0}{k_{-1}[H_2]_0 + k_2[B_4H_{10}]_0} \quad (14)$$

In seeking an alternative explanation, it seems most unlikely that the proposed initial step [reaction (1)] is incorrect. The evidence in favour of the elimination of H_2 in the absence of added H_2 is now overwhelming,[1] and the results in Figure 3, from which it is apparent that the activation energy remains unaltered though the absolute rate of decomposition has diminished by a factor of *ca.* 5, provide cogent additional evidence that this is also the case when excess of added H_2 is present. If a concurrent rate-determining step such as release of BH_3 also occurred, suppression of (1) would favour this presumed concurrent step and this could explain the persistence of first-order kinetics in the presence of added H_2. However, it is not obvious that such a mechanism would leave the percentage yield of B_5H_{11} unchanged and, in any case, suppression of (1) would inevitably alter the observed activation energy towards that of the alternative route; it is most unlikely that this would fortuitously be identical to that of (1). It is also worth noting that there is no evidence in this work, kinetic or otherwise, for the existence of the hypothetical transient species $\{B_4H_{12}\}$,[13] whose formation *via* the direct interaction of B_4H_{10} and H_2 might have been expected to be favoured under the present experimental conditions.

It is possible that the second step involves the mutual interaction of the short-lived intermediate species $\{B_4H_8\}$ to give B_5H_{11} and the reactive intermediate $\{B_3H_5\}$ [reaction (15)].

$$2\{B_4H_8\} \longrightarrow B_5H_{11} + \{^{\prime}B_3H_5^{\prime}\}\ (polymerizes) \quad (15)$$

Such a reaction has been invoked by Shore and co-workers[8] in a different context to account for the high-yield synthesis of B_5H_{11} in solution at low temperature. In the absence of H_2 the $\{^{\prime}B_3H_5^{\prime}\}$ could polymerize, as indicated, but in the presence of added H_2 it could be converted *via* $\{B_3H_7\}$ into $\{B_3H_9\}$ and subsequently *via* reactions (7) and (4) to B_2H_6. This alternative mechanism is more difficult to analyse on the basis of 'steady-state' considerations of the type discussed earlier. It can be shown that under conditions where the rate of the back reaction (−1) is very much faster than that of the second step [reaction (15)], then the expected order is again 2. However, it is not obvious whether this situation prevails in the present experiments, because the form of the expression for the rate of consumption of B_4H_{10} does not readily yield a value for the rate-constant ratio $k_{-1}.k_2$ from the observed retardation. Further work is clearly required in this area.

Cothermolysis of Pentaborane(11) *and Hydrogen.*—The observation that the initial rate of decomposition of B_5H_{11} remains unaltered in the presence of a 14-fold excess of added H_2 (see Figures 2 and 4) has major mechanistic implications. Taken together with the dramatically altered product distribution, this new result enables important conclusions to be drawn about the detailed sequence of events involved in the thermolysis of B_5H_{11}, both in the presence of added H_2 and alone. As a result, several long-standing areas of uncertainty can be resolved.

Thus, it is at once clear that the forward reaction (5) does not occur in a single step by the direct abstraction of a BH group from B_5H_{11} by H_2. If this were the case, the reaction rate and activation energy would undoubtedly be different from the values obtained in the absence of added H_2. The alternative mechanism involving prior dissociation of the B_5H_{11} *via* reaction (3) is therefore preferred. Further evidence in favour of this route is manifest in the product analysis. In the *initial* stages of the reaction, the rate of production of B_4H_{10} is seen to match very closely the rate of consumption of B_5H_{11} [*e.g.* Figure 2(*b*)], which is precisely as one would expect if reaction (−1) were *ca.* 100% effective. Likewise the rapid formation of B_2H_6 is readily explained by the recombination *via* (4) of the $\{BH_3\}$ fragments produced in (3). On the basis of this simple three-step mechanism [(3), (4), and (−1)], B_2H_6 is expected to be formed at half the rate of B_4H_{10}. Close inspection of Figure 2(*b*) reveals that in the first minute or two this is probably the case. However, after this initial period the two species appear at approximately the same rate, presumably because the B_4H_{10} is itself decomposing along the lines already outlined, yielding further B_2H_6 as a major product.

As suggested at the beginning of this section, the new results provided by this first systematic quantitative study of the effect of added H_2 on the kinetics of the thermal decomposition of B_5H_{11} have important implications with regard to the thermolysis of B_5H_{11} on its own. In the absence of added H_2, reaction (−1) is no longer important and the reactive intermediate $\{B_4H_8\}$ must therefore be consumed *via* an alternative route. In our recent study of this system,[4] several options were considered but it was not possible, on the basis of the evidence available at that time, to decide between them. However, in the light of the new evidence that the rate of consumption of B_5H_{11} is unaltered when excess of H_2 is present, it is possible to rule out several potential steps involving interaction of $\{B_4H_8\}$ with B_5H_{11} itself. The possibility of straight exchange of BH_3 between B_5H_{11} and $\{B_4H_8\}$ according to equation (16) cannot

$$\{B_4H_8\} + B_5H_{11} \longrightarrow B_5H_{11} + \{B_4H_8\} \quad (16)$$

of course be ruled out on the basis of these experiments since it does not alter the concentration of the two polyborane species. However, all other types of reaction can be discounted because, if any such reaction were to occur, the initial rate of consumption of B_5H_{11} would be at least doubled in the absence of H_2 because an extra mol of B_5H_{11} would be rapidly removed by the $\{B_4H_8\}$ produced in the initial slow step (3). Thus the conclusion from the hot/cold study[4] that the preferred route is *not* primarily *via* n-B_9H_{15} is reinforced by these detailed new kinetic results, and reaction (17) can therefore be eliminated

$$\{B_4H_8\} + B_5H_{11} \not\rightleftharpoons n\text{-}B_9H_{15} + 2H_2 \quad (17)$$

as an important step under the present conditions. Likewise, reaction (18) which Lipscomb[14] has suggested as an energetically favourable route to B_5H_9 in these interconversion

$$\{B_4H_8\} + B_5H_{11} \not\rightleftharpoons B_5H_9 + B_4H_{10} \quad (18)$$

reactions is also ruled out on this basis. As Lipscomb has remarked, if this reaction were to occur, the B_4H_{10} would be dissociated to $\{B_4H_8\}$ under the conditions of the experiment and the latter would behave as a catalyst for the production of H_2 from B_5H_{11}. In this case the addition of excess of H_2 to the reaction would be expected to have a dramatic effect on the initial rate of consumption of B_5H_{11}, which it manifestly does not.

One is therefore forced to conclude that the $\{B_4H_8\}$ produced in the initial step in the thermal decomposition of B_5H_{11} is consumed (in the absence of added H_2) not by reaction with a further mol of B_5H_{11} but with itself, just as the $\{BH_3\}$ which accompanies its production is presumed to react with itself to give B_2H_6. Long[15] has suggested that such an interaction might yield B_5H_9 plus the reactive intermediate $\{B_3H_7\}$, and in this way the formation of B_5H_9 in the thermolysis of B_5H_{11} alone is naturally accounted for, *i.e.* reaction (19). He also suggests that

$$2\{B_4H_8\} \longrightarrow B_5H_9 + \{B_3H_7\} \quad (19)$$

$$\{B_3H_7\} + \{B_4H_8\} \longrightarrow B_5H_9 + B_2H_6 \quad (20)$$

subsequent interaction between the two reactive intermediates might yield a further mol of B_5H_9 together with B_2H_6, as in reaction (20). However, from the overall initial stoicheiometry observed in our earlier study of B_5H_{11} alone it is clear that the interaction between two $\{B_4H_8\}$ molecules can, and must, proceed simultaneously through one or more other routes. The simplified picture discussed so far predicts a more rapid production of B_2H_6 and, in particular, B_5H_9 than is actually observed in the thermolysis of B_5H_{11} alone; moreover, the substantial production of polymer and H_2 in that reaction is not accounted for. It seems likely, therefore, that reactions such as those proposed by Shore and co-workers[8] in a different context, to account for the high-yield syntheses of B_4H_{10} and B_5H_{11} in solution at low temperature, may well be operative in these gas-phase systems also, *i.e.* reactions (9) and (15). Routes leading exclusively to polymer *via* reactive hexa- and octa-borane intermediates are also possible, *e.g.* reactions (8) and (21).[1] Such

$$2\{B_4H_8\} \longrightarrow \{^{\prime}B_8H_{16-2n}^{\prime}\}(polymerizes) + nH_2 \quad (21)$$

reactions involving the mutual interaction of, for example, two $\{B_4H_8\}$ molecules *via* different channels, *e.g.* reactions (19), (15), and (21), would undoubtedly be characterized by different Arrhenius parameters; *i.e.* their relative importance would depend on temperature. The fact that B_5H_{11} is produced

essentially pure in the low-temperature synthesis, *via* the proposed[8] reaction (15), suggests that the latter has a very low activation energy (though it may also have a low frequency factor) compared with reaction (19), which apparently gains in importance somewhat at the higher temperatures employed in the gas-phase thermolysis of B_5H_{11}.[4]

Conclusions

In establishing that the activation energy (E_a = 99.2 ± 0.8 kJ mol^{-1}) for the first-order thermal decomposition of B_4H_{10} remains unaltered in the presence of an excess of added H_2 (E_a = 98.4 ± 1.4 kJ mol^{-1}), this work has provided compelling new evidence that the reversible unimolecular reaction (1) is the *sole* rate-determining step. The observed inhibition is then naturally explained in terms of the reverse reaction (−1), but the results raise doubts about the validity of subsequent steps in the previously proposed mechanism, and the need for further work is apparent.

In the case of B_5H_{11}, there is again a marked change in product distribution when an excess of H_2 is added to the system, but the initial rate remains unaltered by this addition over a wide range of temperature, and the activation energy is, therefore, unaltered also. The decomposition is thought to proceed *via* the rate-determining elimination of $\{BH_3\}$ [reaction (3)] followed by the rapid, and essentially 100% efficient, dimerization of the latter to give B_2H_6 [reaction (4)]. The $\{B_4H_8\}$ is scavenged by H_2 in the initial stages to give B_4H_{10} in high yield [reaction (−1)], but competitive reactions soon set in and the later stages of the B_5H_{11}/H_2 cothermolysis reflect many of the features displayed by the B_4H_{10}/H_2 system, most notably an increase in the production of B_2H_6 and a decrease in the formation of higher volatile boranes and involatile solids. A particularly interesting conclusion is that, in the absence of added H_2, $\{B_4H_8\}$ appears to react *not* with B_5H_{11} to give various products but with itself, *via* several alternative routes in temperature-dependent competition. Very low temperatures favour the regeneration of B_5H_{11} perhaps *via* reaction (15), whereas higher temperatures lead to B_5H_9 and involatile solids possibly *via* reactions such as (19) and (21).

Acknowledgements

We thank Mr. D. Singh for invaluable experimental assistance and Dr. D. L. Baulch for helpful discussions. The work was supported by the S.E.R.C. and by the US Army Research and Standardization Group (Europe).

References

1 R. Greatrex, N. N. Greenwood, and C. D. Potter, *J. Chem. Soc., Dalton Trans.*, 1984, 2435; 1986, 81.
2 R. K. Pearson and L. J. Edwards, Abstracts of 132nd National Meeting of the Am. Chem. Soc., New York, September 1957, p. 15N.
3 A. B. Burg and H. J. Schlesinger, *J. Am. Chem. Soc.*, 1933, **55**, 4009.
4 M. D. Attwood, R. Greatrex, and N. N. Greenwood, *J. Chem. Soc., Dalton Trans.*, preceding paper.
5 (*a*) J. A. Dupont and R. Schaeffer, *J. Inorg. Nucl. Chem.*, 1960, **15**, 310; (*b*) R. G. Adler and R. D. Stewart, *J. Phys. Chem.*, 1961, **65**, 172.
6 N. N. Greenwood and R. Greatrex, *Pure Appl. Chem.*, 1987, **59**, 857.
7 R. Greatrex, N. N. Greenwood, and G. A. Jump, *J. Chem. Soc., Dalton Trans.*, 1985, 541.
8 M. A. Toft, J. B. Leach, F. L. Himpsl, and S. G. Shore, *Inorg. Chem.*, 1982, **21**, 1952.
9 J. R. Wermer and S. G. Shore, *Inorg. Chem.*, 1987, **26**, 1644.
10 M. D. Attwood, Ph.D. Thesis, University of Leeds, 1987.
11 G. L. Brennan and R. Schaeffer, *J. Inorg. Nucl. Chem.*, 1961, **20**, 205.
12 T. P. Fehlner, Boron Hydride Chemistry, ed. E. L. Muetterties, Academic Press, New York, 1975, ch. 4, pp. 175–196.
13 (*a*) M. L. McKee and W. N. Lipscomb, *Inorg. Chem.*, 1982, **21**, 2846; 1985, **24**, 2317; (*b*) I. M. Pepperberg, T. A. Halgren, and W. N. Lipscomb, *ibid.*, 1977, **16**, 363.
14 W. N. Lipscomb, *Pure Appl. Chem.*, 1983, **55**, 1431.
15 L. H. Long, *J. Inorg. Nucl. Chem.*, 1970, **32**, 1097.

Received 26*th February* 1988; *Paper* 8 00888D

Kinetics and Mechanism of the Thermal Decomposition of Hexaborane(12) in the Gas Phase

Robert Greatrex, Norman N. Greenwood, and Simon D. Waterworth
School of Chemistry, University of Leeds, Leeds LS2 9JT, U.K.

The gas-phase thermolysis of *arachno*-B_6H_{12} produces predominantly B_5H_9 and B_2H_6 in a molar ratio of 2 : 1 *via* a first-order reaction having Arrhenius parameters which are essentially identical to those reported for the decomposition of the structurally related B_5H_{11}; these results imply a mechanism involving elimination of BH_3 as the rate-determining initial step in both reactions.

Reprinted from the Journal of The Chemical Society
Chemical Communications 1988

Kinetics and Mechanism of the Thermal Decomposition of Hexaborane(12) in the Gas Phase

Robert Greatrex, Norman N. Greenwood, and Simon D. Waterworth
School of Chemistry, University of Leeds, Leeds LS2 9JT, U.K.

The gas-phase thermolysis of *arachno*-B_6H_{12} produces predominantly B_5H_9 and B_2H_6 in a molar ratio of 2 : 1 *via* a first-order reaction having Arrhenius parameters which are essentially identical to those reported for the decomposition of the structurally related B_5H_{11}; these results imply a mechanism involving elimination of BH_3 as the rate-determining initial step in both reactions.

Progress has been slow in elucidating a coherent mechanistic description of the facile thermal interconversions of the simple binary boranes, not only because of the inherent complexity of the reactions but also because of difficulties in acquiring reliable kinetic data for these highly reactive, air-sensitive species.[1] We have developed a quantitative mass spectrometric technique for monitoring these reactions in detail, and have thereby gained new insights into the thermal decompositions and interconversion reactions of *nido*-B_6H_{10}[2] and the two *arachno* species B_4H_{10}[3,4a] and B_5H_{11}.[4] We now report preliminary results of the first quantitative kinetic study on B_6H_{12}. The results are important because they provide the first opportunity to correlate kinetic, mechanistic, and structural patterns of behaviour in a unique series of closely related *arachno* binary boranes.

A typical reaction profile for the thermolysis of B_6H_{12} at *ca.* 100 °C is shown in Figure 1 for an initial pressure of 3.14 mmHg. From this and similar profiles recorded over the pressure and temperature ranges 1.8—10.0 mmHg and 75—150 °C, it emerges that this thermolysis is the most straightforward of all borane decompositions studied so far. The overall stoicheiometry is very well defined, with at least 80% of the B_6H_{12} decomposing to B_5H_9 plus $\frac{1}{2}B_2H_6$. From a detailed analysis of initial rates, the consumption of B_6H_{12} and the production of B_5H_9 and of B_2H_6 were all found to be accurately first-order with respect to the concentration of B_6H_{12}. In addition, a small amount of H_2 is produced, and even less B_6H_{10}; the latter builds up rather slowly but persists in the later stages of the reaction when all the B_6H_{12} has decomposed. Only traces of higher boranes such as $B_{10}H_{14}$ are observed, and involatile solid hydrides account for as little as 10% of the boron consumed, compared with typical values of 40—50% in the thermolysis of B_4H_{10}[3] and B_5H_{11}.[4b]

These results can readily be explained by a simple two-step mechanism involving the first order rate-determining elimination of $\{BH_3\}$ which then rapidly dimerizes to B_2H_6 [reactions (1) and (2)]. Previous qualitative studies of the decomposition of B_6H_{12} in the gas phase[5] have yielded no mechanistic information and have sometimes suggested more complex behaviour than observed in the present work.

$$B_6H_{12} \xrightarrow{\text{slow}} B_5H_9 + \{BH_3\} \quad (1)$$

$$2\{BH_3\} \rightleftharpoons B_2H_6 \quad (2)$$

$$B_5H_{11} \rightarrow \{B_4H_8\} + \{BH_3\} \quad (3)$$

Our recent kinetic study of B_5H_{11}[4] has shown that this borane also decomposes *via* the initial rate-determining elimination of $\{BH_3\}$ from the cluster [reaction (3)], and it is therefore particularly significant that the activation energy and pre-exponential factor now found for the B_6H_{12} thermolysis (E_a 75.0 ± 5.8 kJ mol^{-1}; A 3.8 × 10^7 s^{-1}) are essentially identical to the values obtained for B_5H_{11} (E_a 72.6 ± 2.4 kJ mol^{-1}; A 1.3 × 10^7 s^{-1}). This is persuasive additional evidence that the rate-determining steps in the two decompositions do indeed involve very similar processes and this finds a ready interpretation in terms of the detailed molecular structures of gaseous B_5H_{11}[6] and B_6H_{12},[7] as recently determined by electron diffraction. As shown in Figure 2, [7] these two species bear a close structural relationship to each other and to B_4H_{10}.[8] Thus, notional replacement of H_{endo} and one H_μ on, say, B(4) in B_4H_{10} by a BH_3 group yields B_5H_{11} and

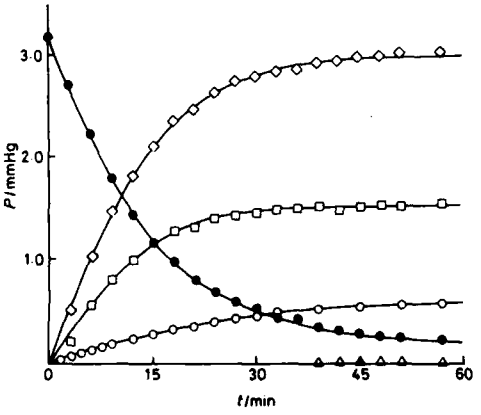

Figure 1. Reaction profile for the thermolysis of B_6H_{12} (P_i 3.14 mmHg) at 99.4 °C. ● B_6H_{12}, ◇ B_5H_9, □ B_2H_6, △ $B_{10}H_{14}$, and ○ H_2.

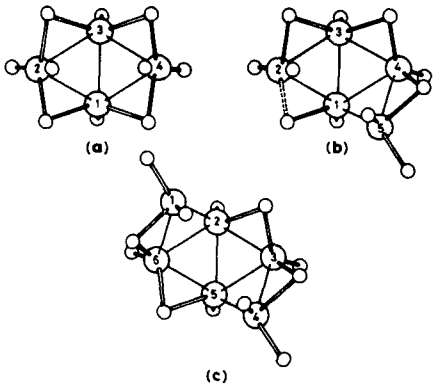

Figure 2. Structural relationship between the *arachno*-boranes (a) B_4H_{10},[8] (b) B_5H_{11},[6] and (c) B_6H_{12},[7] as determined by gas-phase electron diffraction.

repetition of this process on the opposite side of the molecule, *i.e.* at B(2), generates the observed structure of B_6H_{12} having C_2 symmetry. In view of the similarity of the Arrhenius parameters for the decomposition of B_6H_{12} and B_5H_{11}, it seems reasonable to identify these structurally similar BH_3 groups as the fragments involved in the initial steps (1) and (3). In B_4H_{10}, by contrast, these particular incipient BH_3 groups are absent and its decomposition is characterized by quite different Arrhenius parameters (E_a 99.2 ± 0.8 kJ mol^{-1}; A 6.0 × 10^{11} s^{-1}).[3] In this case the initial step is believed to involve elimination of H_2 to give $\{B_4H_8\}$. This type of reaction is clearly not favoured in the case of B_5H_{11} and B_6H_{12}, though small amounts of B_6H_{10} are produced in the thermolysis of B_6H_{12}, and further work is necessary to determine whether this species and dihydrogen arise from a competing, but minor, reaction channel involving direct elimination of H_2 from B_6H_{12}.

We thank Mr. D. Singh for experimental assistance and the S.E.R.C. for a maintenance grant (to S. D. W.).

Received, 22nd March 1988; Com. 8/01156G

References

1 N. N. Greenwood and R. Greatrex, *Pure Appl. Chem.*, 1987, **59**, 857, and references therein.
2 R. Greatrex, N. N. Greenwood, and G. A. Jump, *J. Chem. Soc., Dalton Trans.*, 1985, 541.
3 R. Greatrex, N. N. Greenwood, and C. D. Potter, *J. Chem. Soc., Dalton Trans.*, 1986, 81.
4 (a) M. D. Attwood, R. Greatrex, and N. N. Greenwood, *J. Chem. Soc., Dalton Trans.*, submitted for publication; (b) *ibid.*, submitted for publication.
5 D. F. Gaines and R. Schaeffer, *Inorg. Chem.*, 1964, **3**, 438; A. L. Collins and R. Schaeffer, *ibid.*, p. 2153; C. A. Lutz, D. A. Phillips, and D. M. Ritter, *ibid.*, p. 1191; S. J. Steck, G. A. Pressley, F. E. Stafford, J. Dobson, and R. Schaeffer, *ibid.*, p. 2452; T. C. Gibb, N. N. Greenwood, T. R. Spalding, and D. Taylorson, *J. Chem. Soc., Dalton Trans.*, 1979, 1392.
6 R. Greatrex, N. N. Greenwood, D. W. H. Rankin, and H. E. Robertson, *Polyhedron.*, 1987, **6**, 1849.
7 R. Greatrex, N. N. Greenwood, M. B. Millikan, D. W. H. Rankin, and H. E. Robertson, *J. Chem. Soc., Dalton Trans.*, in the press.
8 C. J. Dain, A. J. Downs, G. S. Laurenson, and D. W. H. Rankin, *J. Chem. Soc., Dalton Trans.*, 1981, 472.

The Identity of the Rate-Determining Step in the Gas-Phase Thermolysis of Diborane: A Reinvestigation of the Deuterium Kinetic Isotope Effect

Robert Greatrex, Norman N. Greenwood, and Susan M. Lucas
School of Chemistry, University of Leeds, Leeds LS2 9JT, England

---

The gas-phase thermolysis of diborane is known to be homogeneous in its initial stages and to follow 3/2-order kinetics over a wide range of temperature and pressure.[1-3] This suggests that a triborane species is involved in the rate-determining step and the currently favoured mechanism involves a three-step process:[3-5]

$$B_2H_6 \rightleftharpoons 2\{BH_3\} \quad (1)$$

$$\{BH_3\} + B_2H_6 \rightleftharpoons \{B_3H_9\} \quad (2)$$

$$\{B_3H_9\} \longrightarrow \{B_3H_7\} + H_2 \quad (3)$$

A triborane species has been generated by reaction of $\{BH_3\}$ with B_2H_6 in a fast-flow system and detected mass-spectrometrically but it was not possible to determine the number of hydrogen atoms in the species.[6]

Cogent arguments have been advanced to suggest that (3) is the rate-determining step[3,4] but a very recent high-level computational study employing many-body perturbation theory and the coupled-cluster approximation implies that it is the formation of $\{B_3H_9\}$ (2) rather than its decomposition (3) which is rate-determining.[7] The calculations also indicate that the $\{B_3H_9\}$ formed in step (2) carries about 80 kJ mol^{-1} of excess internal energy, suggesting that step (3) might occur so rapidly that for all practical purposes the formation of $\{B_3H_7\}$ might best be represented by the direct reaction:

$$\{BH_3\} + B_2H_6 \longrightarrow \{B_3H_7\} + H_2 \quad (4)$$

This possibility, which had been considered earlier but tentatively dismissed,[3] is easier to reconcile with the qualitative observation that added H_2 not only inhibits the rate of decomposition of B_2H_6,[1] but also alters the product

distribution in favour of volatile boranes;[8] our own quantitative studies with Dr M.D. Attwood[5,9] show that the initial rate of decomposition of B_2H_6 at 3.5 mmHg and 150 °C is decreased by a factor of 3.4 in the presence of a 14-fold excess of H_2. The computations[7] also addressed the question of the relative rates of decomposition of B_2H_6 and B_2D_6 and found that, at 127 °C, the ratio of the rate constants ($\underline{k}_H/\underline{k}_D$) was 1.73 if step (2) were rate-determining and 2.4 if it were step (3); unfortunately the only experimental determination of this ratio (which was based on the relative rate of production of H_2 and D_2 at 88 °C),[3] gave a value of 5.0 which is compatible with neither of the computed values.

In an attempt to resolve these difficulties we decided to undertake a careful experimental reinvestigation of the relative rates of decomposition of B_2H_6 and B_2D_6 using a mass-spectrometric technique to monitor the initial stages of the reaction. We chose to monitor the rate of consumption of diborane rather than the rate of production of hydrogen since this was a more direct measure to compare with the calculated rates. The reactions were carried out at 147 °C in preconditioned spherical Pyrex bulbs (volume *ca.* 1 dm^3) with initial pressures of diborane about 3.5 mmHg; helium, argon, and krypton at partial pressures of 100, 1.0, and 1.0 mmHg respectively were also present as calibrants etc., as previously described.[10,11] Initial rates were obtained by the tangent method from plots of diborane pressure *vs.* time for 14 separate runs with B_2H_6 and 10 runs for B_2D_6: these yielded values for the 3/2-order rate constants $\underline{k}_H = (4.55 \pm 0.89) \times 10^{-4}$ and $\underline{k}_D = (1.77 \pm 0.28) \times 10^{-4}$ $mol^{-\frac{1}{2}}\ m^{3/2}\ s^{-1}$, respectively. The value of the ratio $\underline{k}_H/\underline{k}_D$ is therefore 2.57 ± 0.65, which is clearly more consistent with the computed values[7] than with the early experimental value based on the rates of production of H_2 and D_2.[3] The new experimental value is closer to the computed value of 2.4 assuming

step (3) as rate-determining than to the value of 1.73 for step (2) as rate limiting but, in view of the expected uncertainties in the theoretical values, it is probably more appropriate to suggest that both of the computed values are in adequate agreement with the new experimental value.[12] We note parenthetically that the computed overall activation energy for the decomposition of diborane is 134 kJ mol^{-1} if step (2) is rate-determining but only 92 kJ mol^{-1} if step (3) is rate-determining;[7] our own most recent experimental redetermination of this quantity (based on the rate of consumption of B_2H_6 at eleven temperatures in the range 120-180 °C) is 102.6 ± 1.7 kJ mol^{-1}. Again it would be unwise to place too great a significance on these differences, and it is probable that calculations with a larger basis set or incorporating the possibility of tunnelling would lead to a revision of the computed values for the activation energy.[7,12]

In summary; a careful re-investigation of the relative initial rates of decomposition of B_2H_6 and B_2D_6 has led to a value of 2.57±0.65 for the rate-constant ratio $\underline{k}_H/\underline{k}_D$, which disagrees with an earlier experimental value but is close to values obtained in a recent high-level computational study. This important new result therefore removes a potential inconsistency between experiment and computation. Taken in conjunction with the experimentally observed influence of added H_2 in repressing the rate of decomposition of B_2H_6 and in altering the distribution of products, the totality of experimental and computational evidence suggests that the rate-determining step following the symmetric dissociation of diborane is neither simply the formation of $\{B_3H_9\}$ from $\{BH_3\}$ and B_2H_6, nor the subsequent decomposition of $\{B_3H_9\}$ to give $\{B_3H_7\}$ and H_2, but the <u>concerted</u> formation and decomposition of $\{B_3H_9\}$ as represented by step (4).

Acknowledgement. We thank Professors J.F. Stanton and W.N. Lipscomb for sending us a preprint of their paper, D. Singh for assistance with the mass spectrometers, the S.E.R.C. for a maintenance grant (to S.M.L.) and the U.S. Army Research and Standardization Group (Europe) for financial support.

References

(1) Clarke, R.P.; Pease, R.N. J.Am.Chem.Soc. 1951, 73, 2132-2134.

(2) Bragg, J.K.; McCarty, L.V.; Norton, F.J. J.Am.Chem.Soc. 1951, 73, 2134-2140.

(3) Enrione, R.E.; Schaeffer, R. J.Inorg.Nucl.Chem. 1961, 18, 103-107.

(4) Fehlner, T.P. in Muetterties, E.L. (ed.) Boron Hydride Chemistry, Academic Press, New York, 1975, 175-196.

(5) Greenwood, N.N.; Greatrex, R. Pure Appl. Chem. 1987, 59, 857-868, and references therein.

(6) Fridmann, S.A.; Fehlner, T.P., J.Am.Chem.Soc. 1971, 93, 2824-2826; Inorg.Chem. 1972, 11, 936-940.

(7) Stanton, J.F.; Lipscomb, W.N.; Bartlett, R.J. J.Am.Chem.Soc. 1989, 111, 5165-5173.

(8) McCarty, L.V.; DiGiorgio, P.A. J.Am.Chem.Soc. 1951, 73, 3138-3143.

(9) Attwood, M.D. PhD Thesis, University of Leeds, 1987. Attwood, M.D.; Greatrex, R.; Greenwood, N.N.; Potter, C.D. J.Chem.Soc., Dalton Trans. to be submitted.

(10) Greatrex, R.; Greenwood, N.N.; Jump, G.A. J.Chem.Soc., Dalton Trans. 1985, 541-548.

(11) Greatrex, R.; Greenwood, N.N.; Potter, C.D. J.Chem.Soc., Dalton Trans. 1986, 81-89.

(12) Stanton, J.F.; Lipscomb, W.N., private communication, 1989.

The Identity of the Rate-Determining Step in the Gas-Phase Thermolysis of Diborane: A Revinvestigation of the Deuterium Kinetic Isotope Effect

Robert Greatrex, Norman N. Greenwood, and Susan M. Lucas,
School of Chemistry, University of Leeds, Leeds LS2 9JT, England

Abstract:

The rate constants, $\underline{k}$, for the initial 3/2-order gas-phase thermal decomposition of B_2H_6 and B_2D_6 have been redetermined at 420 K and lead to a value of 2.57 ± 0.65 for the ratio $\underline{k}_H/\underline{k}_D$, which is closer to values obtained in a recent high-level computational study than to earlier experimental values. The activation energy for the decomposition and the influence of added H_2 on the rate have also been studied. Taken as a whole the experimental and computational evidence suggest that the rate-determining step following the symmetric dissociation of diborane is neither simply the formation of $\{B_3H_9\}$ from $\{BH_3\}$ and B_2H_6, nor the subsequent decomposition of $\{B_3H_9\}$ to give $\{B_3H_7\}$ and H_2, but the concerted formation and decomposition of $\{B_3H_9\}$.

Proofs to : Dr R Greatrex, School of Chemistry, University of Leeds, LS2 9JT.

Electron Diffraction Study of Tetraborane(8) Carbonyl in the Gas Phase : Structure Determination of an *endo/exo* Isomeric Mixture

Simon J. Cranson, Paul M. Davies, and Robert Greatrex*
School of Chemistry, University of Leeds, Leeds LS2 9JT.

David W.H. Rankin* and Heather E. Robertson
Department of Chemistry, University of Edinburgh, West Mains Road, Edinburgh EH9 3JJ

The molecular structures of the individual isomers present in a gaseous mixture of arachno-B_4H_8CO have been determined by electron diffraction. The sample was known from n.m.r. experiments to consist of 62% of the *endo* isomer and 38% of the *exo* isomer and early refinements showed that the distribution in the gas phase was consistent with that found in solution. A satisfactory refinement (R_G = 0.06) was obtained with a model in which the isomers had a "butterfly" B_4 geometry with "hinge" B(1) carrying either an *endo* or *exo* CO. The *endo* and *exo* isomers were allowed to differ only in the dihedral angles between the planes of the "butterfly" structure [135(4) and 144(2)°, respectively] and in the angles subtended by the carbon atom at the B-B "hinge" [125(2)] and 109(2)°]. The unbridged B-B distances were 172.7(10) ("hinge") and 184.9(4) pm, and the two H-bridged B-B distances were 178.0(6) pm. The BCO angle showed no significant deviation from 180°.

Tetraborane(8) carbonyl, B_4H_8CO, was the first known compound in which the reactive intermediate (B_4H_8) was stabilized. It was reported by Burg and Spielman in 1959,[1] and has been the subject of several n.m.r. studies. The early measurements[2,3] were consistent with a structure similar to that found by X-ray diffraction analysis of $B_4H_8.PF_2N(CH_3)_2$,[4] in which the B_4H_8 framework is structurally similar to that of B_4H_{10} but lacking two bridging hydrogens. The more recent work was interpreted in terms of the presence of two geometrical isomers in an approximate ratio of 60:40.[5,6] This raised interesting questions about the mode of formation of these isomers and about factors responsible for their relative amounts. In the context of our work on the thermal interconversions of the boranes[7] we wished to obtain definitive answers to some of these questions and have embarked upon a detailed n.m.r. study, the results of which will be reported elsewhere.[8] In the meantime to gain information about the nature of B_4H_8CO in the gas phase, and in particular to determine accurate molecular dimensions and bond angles, we have undertaken a study of its structure by means of electron diffraction.

Experimental

Tetraborane(8) carbonyl was made from B_4H_{10} by the method of Spielman and Burg.[2] It was purified by low-temperature fractional distillation with continuous monitoring of the distillate by mass spectrometry. The vapour pressure at 0°C was found to be 70.5 ± 0.5 mmHg, in excellent agreement with the reported value.[1,2] In solution (CD_2Cl_2) the sample was known from detailed n.m.r. work[8] to consist of 62% of the *endo* isomer and 38% of the *exo* isomer. This same ratio was observed for several different samples and did not change with temperature. Attempts to separate the isomers on the low-temperature column have so far proved unsuccessful. The boranes were handled in conventional high-vacuum systems equipped with greaseless O-ring taps and spherical joints [J. Young (Scientific Glassware) Ltd.].

Electron diffraction data were recorded on Kodak Electron Image plates using the Edinburgh gas diffraction apparatus,[9] operating at *ca.* 45 kV. Samples were maintained at 250 K and the nozzle at room temperature during the exposures, three at a nozzle-to-plate distance of 128 mm and three at 285 mm. Data were obtained in digital form using a Joyce-Loebl MDM6 microdensitometer.[10] The program used to control this instrument, and those used for data reduction and least squares refinements have been described previously.[10,11] Scattering factors used were taken from ref. 12.

Calibration plates of benzene were also taken, to give the precise camera distances and electron wavelengths listed in Table 1, together with weighting functions used to set up the off-diagonal least-squares weight matrices.[11]

Molecular Model

The model used in the least-squares refinements allowed for the presence of both isomeric forms, and early refinements showed that the distribution in the gas-phase was consistent with that found in solution (see Experimental section). As the isomers could not be separated by low-temperature fractionation, the 62:38 ratio was subsequently assumed to apply to the diffraction data.

The isomers were allowed to differ only in respect of the angles between the planes B(1)B(2)B(3) and B(1)B(3)B(4), and the angles B(3)B(1)C. (The atom numbering is shown in Figure 1). Otherwise the only assumptions imposed by the model were C_s symmetry for each isomer, the equality of the bondlengths B(1)-H(1) and B(3)-H(3) and of B(2)-H(2)$_{endo}$ and B(2)-H(2)$_{exo}$, and a constraint of these last two bonds to lie in the plane bisecting the angle B(1)B(2)B(3). The heavy-atom skeleton of each isomer was then defined by eight parameters, and a further nine parameters were needed to give coordinates of hydrogen atoms. These parameters and their definitions are given in Table 2.

Structure Refinement

Attempts to refine the structure of B_4H_8CO led initially to two distinct false minima. They were recognised as such by physically unreasonable parameters, notably very wide dihedral angles between the two BBB planes, small B(3)B(1)C angles and marked deviation from linearity in the BCO fragment. However, after taking great care in the choice of starting parameters, making particular use of data for crystalline $B_4H_8.PF_2NMe_2$[4], a structure was found which had reasonable geometrical and vibrational parameters, while giving an R factor substantially lower than those obtained earlier.

The B-B bond lengths all refined without difficulty, although B(1)-B(2) was shorter than B(2)-B(3) in the false minima, whereas it was longer in the final structure. The amplitudes of vibration for the B-B bonds were refined as a single parameter, with an e.s.d. of 0.8 pm, but were fixed in the final stages of the work. The B-C and C-O distances and B-C amplitude of vibration all refined satisfactorily, but the C-O amplitude dropped to the rather small value of 3.2(3) pm when freed, and so was reset to the more reasonable 3.7 pm.

While the bond lengths were assumed to be identical for the two isomers, the angles describing the heavy-atom structures were allowed to differ. Starting values for the dihedral angles between the planes B(1)B(2)B(3) and B(1)B(3)B(4) and the angles B(3)B(1)C were those found in the analogous compound $B_4H_8.PF_2NMe_2$,[4] 137 and 135° respectively. This phosphine complex exists entirely in the *endo* form, so these values are a more reliable guide to likely angles in the *endo* isomer of B_4H_8CO than to those in the *exo* isomer. Three of the four parameters refined without any difficulty giving 135(4) and 125(2)° for the dihedral and BBC angles in the *endo* form, and 144(2)° for the *exo* dihedral angle. The BBC angle in the *exo* isomer wandered in the range 108-114° as refinements progressed, ultimately settling at 109(2)°. The quoted error in this case should clearly be regarded as an underestimate. Finallly, the BCO angle was allowed to vary, and values in the range 173-185° were obtained, with e.s.d.'s of *ca.* 4°. There was thus no significant deviation from linearity, and

so this was assumed in the remaining refinements, for both isomers.

Parameters relating to hydrogen atom positions are not well determined, and in the final refinement only the mean terminal and mean bridge distances were included, with amplitudes of vibration for bonded B-H atom pairs, and for a group of two-bond B···H pairs, where the inter-atomic distance was between 250 and 270 pm. Several other hydrogen atom parameters were varied stepwise, with negligible effects on R factor or other parameters. The values chosen for these parameters are mainly derived from those observed for B_4H_{10}.[13]

Geometrical parameters, interatomic distances and amplitudes of vibration obtained in the final refinement, for which R_G was 0.06, are listed in Tables 2 and 3, and Table 4 contains the most significant elements of the least-squares correlation matrix. Molecular scattering intensities are shown in Figure 2, the radial distribution curve in Figure 3, and perspective views of the molecules in Figure 1.

Discussion

The structural analysis of gaseous B_4H_8CO confirms the earlier conclusions from n.m.r. data that the cluster framework geometry (see Figure 1) is closely related to that of crystalline $B_4H_8.PF_2N(CH_3)_2$.[4] It is also apparent that there is very close agreement between all the main interatomic distances in the phosphine derivative and the corresponding ones in the carbonyl species, and that the dihedral ("butterfly") angles at B(1)B(3) in the two *endo* molecules are essentially identical. This latter observation in particular gives confidence in the details of the present analysis.

It is perhaps surprising that the dihedral angle for *exo*-B_4H_8CO is ~~significantly~~ larger than that for the *endo* isomer [144(2)° compared with 135(4)°]. On steric grounds one might at first sight have expected the opposite to be the case. Whilst it is possible that interaction between C and H(2) might increase this angle in the *exo* form, it seems more likely that the explanation

lies in the details of the bonding. In this respect it is interesting that La Prade and Nordman have suggested that the gross differences in the geometry of the B_4H_8 group in $B_4H_8.PF_2N(CH_3)_2$ and B_4H_{10} indicated in Table 5, namely those involving the dihedral angle at B(1)B(3) and the H-bridged interatomic distances B(2)-B(3) and B(3)-B(4), might be accounted for in terms of the non-bonded repulsion of the fluorine atom on the concave side of the molecule. However, in view of the fact that these differences persist when the bulky phosphine ligand is replaced by CO, it now seems unlikely that this can be the case, and one is forced to conclude that factors other than purely steric ones are involved in this aspect also.

Acknowledgements

We thank Professor N. N. Greenwood for initiating this work and for helpful discussions. We are grateful to the SERC for financial support, including maintenance grants (to SJC and PMD), and for the provision of the microdensitometer service at the Daresbury Laboratory.

References

1. A.B. Burg and J.R.Spielman, *J. Am. Chem. Soc.*, 1959, **81**, 3479.
2. J.R. Spielman and A.B. Burg, *Inorg. Chem.* 1963, **2**, 1139.
3. A.D. Norman and R. Schaeffer, *J. Am. Chem. Soc.*, 1966, **88**, 1143.
4. M.D. La Prade and C.E. Nordman, *Inorg. Chem.*, 1969, **8**, 1669.
5. E.J. Stampf, A.R. Garber, J.D. Odom, and P.D. Ellis, *Inorg. Chem.*, 1975, **14**, 2446.
6. J.D. Odom, F.T. Moore, W.H. Dawson, A.R. Garber, and E.J. Stampf, *Inorg. Chem.*, 1979, **18**, 2179.
7. N.N. Greenwood and R. Greatrex, *Pure Appl. Chem.*, 1987, **59**, 857.
8. S.J. Cranson, X.L.R. Fontaine, R. Greatrex, and N.N. Greenwood, unpublished observations.
9. C.M. Huntley, G.S. Laurenson, and D.W.H. Rankin, *J. Chem. Soc., Dalton Trans.*, 1980, 954.
10. S. Cradock, J. Koprowski, and D.W.H. Rankin, *J. Mol. Struct.*, 1981, **77**, 113.
11. A.S.F. Boyd, G.S. Laurenson and D.W.H. Rankin, *J. Mol. Struct.*, 1981, **71**, 217.
12. L. Schäfer, A.C. Yates, and R.A. Bonham, *J. Chem. Phys.*, 1971, **55**, 3055.
13. C.J. Dain, A.J. Downs, G.S. Laurenson, and D.W.H. Rankin, *J. Chem. Soc., Dalton Trans.*, 1981, 472.

Table 1. Camera distances, weighting functions and other experimental data

Camera distance mm	Δs	s_{min}	sw_1	sw_2	s_{max}	Correlation parameter	Scale factor	Wavelength pm
		nm^{-1}						
285.43	2	20	40	122	144	0.310	0.596(6)	5.687
128.33	4	60	80	280	356	0.302	0.637(10)	5.686

Table 2. Geometrical parameters (distances/pm, angles/degrees)

P_1	r B-B (mean)	179.7(2)
P_2	Δr B(1)-B(3) minus mean of others	- 8.8(11)
P_3	Δr B(2)-B(3) minus B(1)-B(2)	- 6.9(9)
P_4	r B-C	151.7(4)
P_5	r C-O	113.7(4)
P_6	< B(1)B(2)B(3)/B(1)B(3)B(4)[a]	134.9(38)
P_7	< B(3)B(1)C[a]	124.6(23)
P_8	< B(1)B(2)B(3)/B(1)B(3)B(4)[b]	144.0(23)
P_9	< B(3)B(1)C[b]	108.5(21)
P_{10}	< BCO	180.0 (fixed[c])
P_{11}	r B-H (terminal) (mean)	119.7(5)
P_{12}	Δr B-H (terminal)[d]	2.0 (fixed)
P_{13}	r B-H (bridge) (mean)	131.9(18)
P_{14}	Δr B(2)-H(2,3) minus B(3)-H(2,3)	15.0 (fixed)
P_{15}	< $H(2)_{exo}$ B(2)$H(2)_{endo}$	114.0 (fixed)
P_{16}	< BH_2 wag[e]	2.0 (fixed)
P_{17}	< B(1)B(3)H(3)	120.0 (fixed)
P_{18}	< CB(1)H(1)	120.0 (fixed)
P_{19}	< B(2)H(2,3)B(3)/B(1)B(2)B(3)	0.0 (fixed[c])

Errors (in parentheses) are estimated standard deviations obtained in the least squares analysis, and include an allowance for systematic errors.

a *Endo* isomer, 62%

b *Exo* isomer, 38%

c Refined earlier : see text

d [B(1)-H(1) + B(3)-H(3) - B(2)-$H(2)_{exo}$ - B(2) - $H(2)_{endo}$]/2

e Angle between bisectors of angles $H(2)_{exo}$B(2)$H(2)_{endo}$ and B(1)B(2)B(3) : positive angle moves H atoms away from B(4).

Table 3. Interatomic distances and amplitudes of vibration/pm

			Distance	Amplitude
r_1	B(1)-B(3)		172.7(10)	6.6 (fixed[a])
r_2	B(1)-B(2)		184.9(4)	7.0 (fixed[a])
r_3	B(2)-B(3)		178.0(6)	6.8 (fixed[a])
r_4	B(2)-H(2)		119.1(5)	
r_5	B(1)-H(1)		121.1(5)	8.2(14)
r_6	B(3)-H(2,3)		124.4(18)	
r_7	B(2)-H(2,3)		139.4(18)	
r_8	B-C		151.7(4)	6.0(7)
r_9	C-O		113.7(4)	3.7 (fixed[a])
r_{10}	B(2)···B(4)	*endo*	294.5(33)	7.5 (fixed)
		exo	303.3(17)	
r_{11}	B(2)···C	*endo*	240.9(11)	8.1(11)
		exo	283.5(11)	8.4(19)
r_{12}	B(3)···C	*endo*	287.4(21)	
		exo	263.6(22)	8.1 (tied to u_{11} endo)
r_{13}	B(1)···O		265.4(5)	7.4(13)
r_{14}	B(3)···O	*endo*	390.3(26)	13.4(9)
		exo	359.7(30)	
r_{15}	B(2)···O	*endo*	325.7(16)	19.1 (tied to u_{14})
		exo	381.1(15)	13.4 (tied to u_{14})
r_{16}	B···H (two bond)		251-269	8.6(12)

Other non-bonded B···H, C···H, O···H and H···H distances were included in the refinements, but are not listed here.

a Refined earlier : see text.

Table 4. Least Squares correlation matrix x 100[a]

P_2	P_3	P_6	P_7	P_9	P_{13}	u_4	u_{12}	u_{13}	u_{14}	
57	-52			-60						P_1
	-74						61			P_2
							-59			P_3
					-54	87				P_5
			-62			53	-65	-51		P_6
		-70	73							P_8
			57							P_9
					-52					P_{11}
		-61				-78				P_{13}
									55	u_{11}
							68		-55	u_{13}

a only elements with absolute values > 50 are included.

Table 5. A comparison of some molecular parameters for *endo*- and *exo*-B_4H_8CO with those for B_4H_{10} and $B_4H_8.PF_2N(CH_3)_2$

Parameter	*endo*-B_4H_8CO	*exo*-B_4H_8CO	B_4H_{10}	*endo*-$B_4H_8.PF_2N(CH_3)_2$
Dihedral angle at B(1)B(3)/°	135(4)	144(2)	117	137
B(1)-B(2)/pm	184.9(4)	184.9(4)	185.6(0.4)	184.4(11)
B(1)-B(4)/pm	"	"	"	182.6(11)
B(1)-B(3)/pm	172.7(10)	172.7(10)	170.5(1.2)	168.7(12)
B(2)-B(3)/pm	178.0(6)	178.0(6)	185.6(0.4)	175.9(13)
B(3)-B(4)/pm	"	"	"	175.3(14)

Legends to Figures

Figure 1 Perspective view of the structures of B_4H_8CO isomers.

Figure 2 Observed and final weighted difference molecular scattering intensities for B_4H_8CO at camera distances of (a) 285 and (b) 128 mm.

Figure 3 Observed and final weighted difference radial distribution curves, P(r)/r, for B_4H_8CO. Before Fourier inversion the data were multiplied by $s.\exp(-0.00002\ s^2)/(Z_B-f_B)(Z_C-f_C)$.

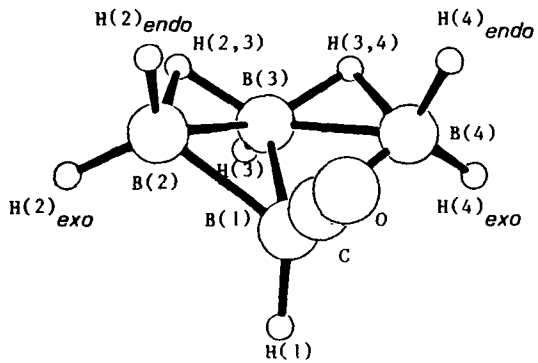

endo

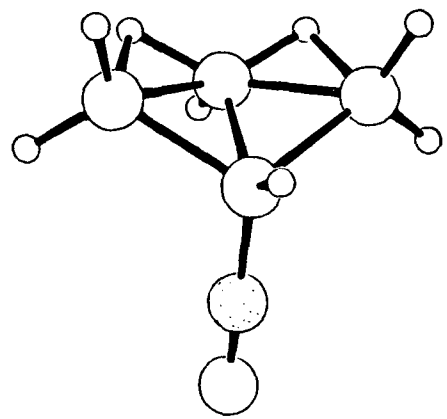

exo

Ed. Some form of light shading of the C and O atoms, as indicated, might help to distinguish them from the B atoms.

Figure 1

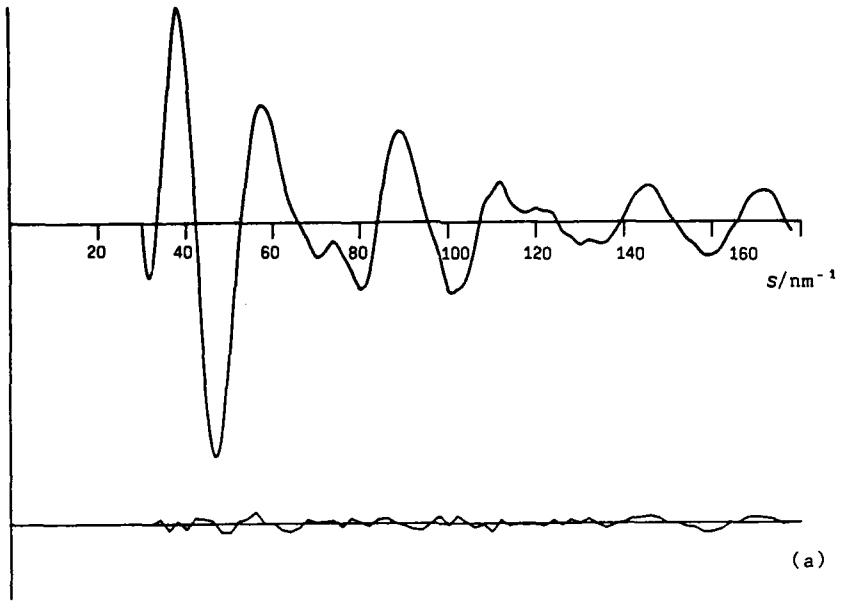
20
40
60
80
100
120
140
160
s/nm⁻¹
(a)

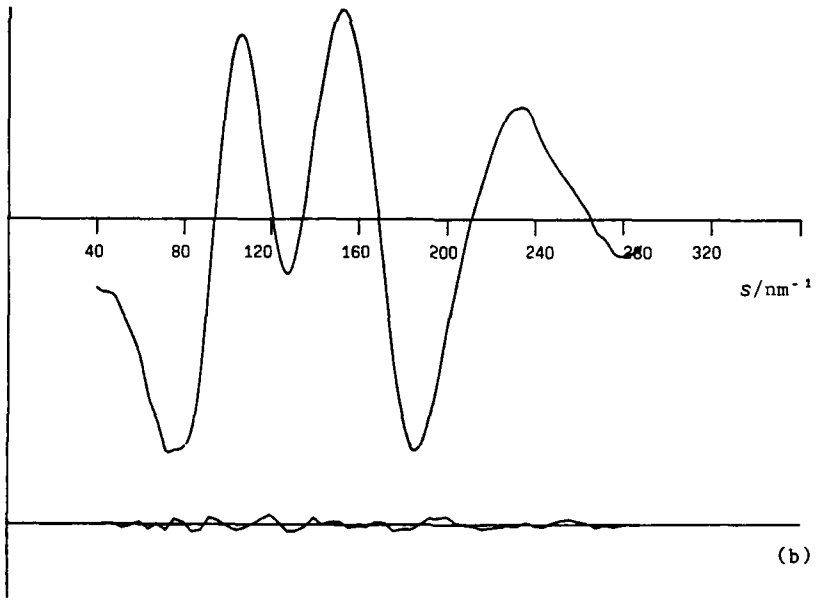
40
80
120
160
200
240
280
320
s/nm⁻¹
(b)

Figure 2

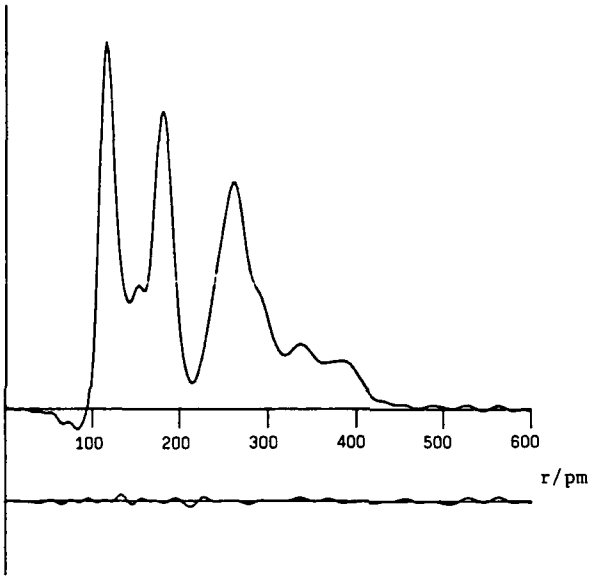

Figure 3

Polyhedron Vol. 6, No. 10, pp. 1849–1858, 1987
Printed in Great Britain

0277-5387/87 $3.00 + .00
© 1987 Pergamon Journals Ltd

THE MOLECULAR STRUCTURES OF PENTABORANE(9) AND PENTABORANE(11) IN THE GAS PHASE AS DETERMINED BY ELECTRON DIFFRACTION

ROBERT GREATREX and NORMAN N. GREENWOOD*

School of Chemistry, University of Leeds, Leeds LS2 9JT, U.K.

and

DAVID W. H. RANKIN and HEATHER E. ROBERTSON

Department of Chemistry, University of Edinburgh, West Mains Road, Edinburgh EH9 3JJ, U.K.

(*Received* 25 *March* 1987; *accepted* 23 *April* 1987)

Abstract—Tne structure of gaseous *arachno*-B_5H_{11} has been redetermined by electron diffraction and shown to be similar to that found in the solid state at low temperature (93 K) except that the inner basal interatomic distance B(3)—B(4) appears to be somewhat shorter in the gas phase. The data are consistent with the presence of asymmetric B(2)—H(2,3)—B(3) and B(5)—H(4,5)—B(4) bridges with the two halves of each bridge differing in length by *ca.* 12 pm. The unique *endo*-face-capping H atom attached to the apical B(1) atom has not been located with high precision, but the best fit to the data is obtained for an asymmetric structure with the distances B(2)...$H(1)_{endo}$ and B(5)...$H(1)_{endo}$ differing by 31 pm. For comparison, the structure of *nido*-B_5H_9 has also been redetermined by electron diffraction. The interatomic distances are in excellent agreement with those previously obtained from microwave data. The directly-bonded B–H(bridge) distances reveal an unusually large amplitude of vibration of the bridging H atoms but it was not possible to establish whether this was a real effect or whether the structure has a lower symmetry than that expected.

There is an unresolved problem in the structure of *arachno*-B_5H_{11}. The boron framework has long been established as that of an open-sided tetragonal pyramid (structure **I**) but there is some uncertainty about the precise location of the unique *endo* face-capping H atom attached to the apical B(1) atom. Early X-ray diffraction work[1] suggested that the H atom was asymmetrically disposed above the open triangular face (structure **II**), but subsequent refinement of the data favoured C_s symmetry (structure **III**) rather than C_1 (structure **II**).[2]

Later, a more precise low-temperature study clearly established that the molecule has C_1 point symmetry in the crystalline state.[3] The most recent theoretical study, involving complete optimization at the 3-21G level, whilst favouring C_1 symmetry, points to a very low barrier (7 kJ mol^{-1}) for the C_1–C_s–C_1 fluxional process.[4] It is therefore not surprising that the proton and boron NMR spectra on

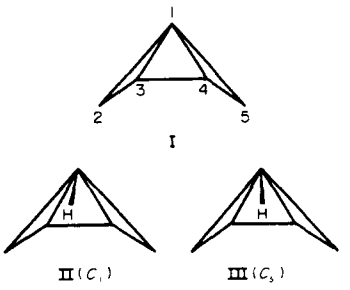

I

II (C_1) III (C_s)

Structures I–III.

* Author to whom correspondence should be addressed.

the neat liquid revealed no evidence for the asymmetry.[5] The question therefore remains as to whether the asymmetry observed in the X-ray diffraction study is the result of crystal-packing forces, or whether it arises from some more deep-seated electronic-bonding effect. There has been no accurate determination of the structure of the gaseous molecule, the interpretation of early electron diffraction data being either palpably incorrect[6] or yielding no direct information about the hydrogen atom positions.[7]

In order to define as accurately as possible the positions of the atoms, including the so-called "anomalous" *endo* face-capping hydrogen atom, we have now re-investigated the structure of the gaseous *arachno*-B_5H_{11} molecule by electron diffraction. Because it was readily available in the laboratory, we have also taken the opportunity of redetermining the molecular parameters of *nido*-B_5H_9 by the same technique for comparison with the results obtained by previous electron diffraction[8] and X-ray diffraction[8,9] studies and in particular with the more recent microwave data.[10]

EXPERIMENTAL

Preparation and purification of materials

The boranes were handled in a conventional high-vacuum system equipped with greaseless O-ring taps and spherical joints [J. Young (Scientific Glassware) Ltd]. *Nido*-B_5H_9 was supplied by Dr R. E. Williams (Chemical Systems, Inc. California). *Arachno*-B_5H_{11} was prepared from B_4H_{10} by the general method of Shore and coworkers.[11] Specifically, deprotonation was achieved using KH in dimethyl ether, and BCl_3 was used as the hydride-abstracting agent. The B_4H_{10} intermediate was prepared by the action of BF_3 on $[NMe_4][B_5H_8]$.[11] The B_5H_{11} was purified by repeated fractionation on a low-temperature fractional distillation column,[12] the effluent from which was sampled continuously by mass spectrometry. Traces of B_5H_9 are difficult to remove from B_5H_{11} and are also difficult to detect by mass spectrometry because of the similarity of the spectra of the two compounds. The sample of B_5H_{11} used in the electron diffraction study was shown by ^{11}B NMR to contain $< 0.5\%$ B_5H_9 as the only detectable impurity; its vapour pressure at 0 °C was 52.5 mmHg, in excellent agreement with the published value.[13]

Electron diffraction

Electron diffraction scattering intensities were recorded on Kodak electron image plates, using the Edinburgh apparatus,[14] with nozzle-to-plate distances of 128 and 285 mm, and an accelerating voltage of *ca.* 44 kV. The nozzle was maintained at room temperature, 285 K, during the experiments and the samples were kept at room temperature (B_5H_9) or 250 K (B_5H_{11}). We have noticed that plates for boranes and related compounds have often shown dark patches, suggesting that there is some reaction between sample and emulsion, and this problem was particularly severe with B_5H_{11}. To minimize these effects, the plates were pumped for 24 h before being removed from the diffraction apparatus, and they were then washed thoroughly with water before development.

Data were obtained in digital form using a computer-controlled Joyce-Loebl MDM6 microdensitometer at the S.E.R.C. Laboratory, Daresbury, using the scanning program described previously.[15] Electron wavelengths were determined from the scattering patterns of gaseous benzene, recorded on the same occasions as the sample data. Calculations were carried out using standard data-reduction[16] and least-squares refinement programs. Weighting points used in setting up the off-diagonal weight matrices are given in Table 1, with other pertinent data. In all calculations the complex scattering factors of Schäfer *et al.*[17] were used.

RESULTS AND DISCUSSION

Refinement of the structure of B_5H_9

For almost all refinements it was assumed that B_5H_9 had C_{4v} symmetry, with one terminal hydro-

Table 1. Weighting functions, correlation parameters and scale factors

Compound	Camera height (mm)	Wavelength (pm)	Δs	s_{min}	sw_1	sw_2 (nm^{-1})	s_{max}	Correlation parameter	Scale factor
B_5H_9	285.7	5.690	2	20	40	124	144	0.486	0.651(11)
	128.3	5.689	4	60	80	300	340	−0.037	0.580(14)
B_5H_{11}	285.4	5.717	2	20	40	124	144	0.463	0.540(10)
	128.3	5.688	4	60	80	300	352	0.471	0.594(13)

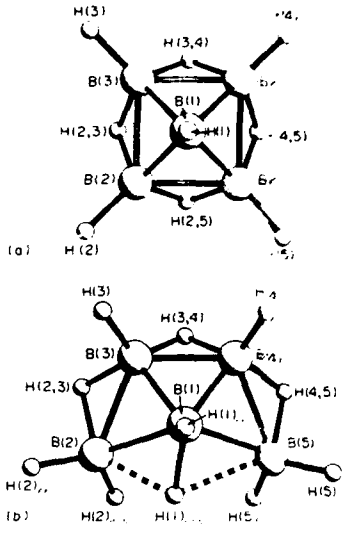

Fig. 1. Structures of (a) B_5H_9 and (b) B_5H_{11}, showing the atom numbering scheme used in this work.

gen atom associated with each boron atom, and with four bridging hydrogen atoms, each one bonding equally to two boron atoms. The atom numbering scheme used in this work is shown in Fig. 1(a). The structure was then defined by the two different B—B interatomic distances (base–base and base–apex), the mean B—H distance, the difference between bridging and mean terminal B—H distances, the difference between the lengths of the basal and apical terminal B—H bonds, and two angles defining the positions of the terminal and bridging hydrogens associated with the base of the pyramid. These angles were chosen to be B(1)B(2)H(2), and the angle between the base plane and the plane BH(bridge)B, which is labelled "H(2,3)dip" in Table 2.

Table 2. Molecular parameters for B_5H_9 (distances in pm, angles in degrees)

p_1	r(B—B) (base–base)	181.1(4)
p_2	r(B—B) (base–apex)	169.4(4)
p_3	r(B—H) (mean)	127.1(8)
p_4	Δr(B—H) (bridge–terminal)	16.7(18)
p_5	$\angle$ B(1)B(2)H(2)	125.4(73)
p_6	H(2,3)dip	68.8(29)
p_7	Δr(B—H) (terminal, base–apex)	0.5(fixed)

All geometrical and vibrational parameters relating to the B$_5$ pyramid refined easily, as did the mean B—H distance and the difference between terminal and bridging B—H bond lengths, and the amplitudes of vibration for both terminal and bridging bonds. The small difference in lengths of the two types of terminal bonds could not be refined, and was fixed at the value found by microwave spectroscopy.[18]

The two remaining parameters, defining the positions of hydrogen atoms, were much more difficult to determine, because there are five different non-bonding B...H distances between 240 and 280 pm, and the non-bonding B...B distance also falls in this region. In the end it was possible to refine three vibrational parameters for the B...H atom pairs, as well as the two angles, but strong correlations between these parameters [Table 3(a)] make their estimated standard deviations relatively large. The refined parameters are listed in Table 2, and interatomic distances and vibrational amplitudes are given in Table 4. In both these tables the quoted errors are estimated standard deviations obtained in the least-squares analysis, increased to allow for systematic errors.

In this refinement the amplitudes of vibration for the atom pairs B(2)...H(5) and B(2)...H(1) were assumed to be equal, and that for B(1)...H(2) was fixed at a value close to that obtained for the other two, as all of these relate to a boron atom and a terminal hydrogen on an adjacent boron atom. However, the values obtained for these atom pairs are *smaller* than that for the directly-bonded B—H(bridge) pairs. This unusually large value suggests that either the bridging hydrogen atoms are involved in a large-amplitude vibration in which they move tangentially to the C_2 axis (an a_2 mode) or they are displaced from the positions equidistant from the neighbouring boron atoms, so that the molecular symmetry is reduced to C_s. Tests using a model with C_2 symmetry showed that substantial displacements of these atoms could be accommodated with little effect on the quality of the fit. For this purpose an additional parameter was introduced, representing the difference between the lengths of the two parts of the B—H—B bridges. The possibility of simultaneous displacement of the other basal hydrogen atoms was not investigated. With the difference between the lengths of the two parts of the bridge set to 20 pm, the R factor (R_1) rose only from 0.0874 to 0.0875, and the amplitude of vibration for the two bridge distances reduced from 13.9 to 11.5 pm. The results are therefore inconclusive on this point.

The results quoted in Tables 2–4 are for the C_2 model. Atomic coordinates are given in Table 5(a),

Table 3. Least-squares correlation matrices showing all elements > 50%

(a) B_3H_7

Geometrical parameter	Vibrational amplitudes						Scale factor	
p_1	u_1	u_2	u_3	u_4	u_5	u_{11}	k_1	
		55						p_1
	57							p_2
				77				p_3
			−78	−74	55			p_4
87					−67	−59		p_5
					−64			p_6
		87						u_1
				54				u_2
						68		u_3
	60	63					53	k_2

(b) B_5H_9

Geometrical parameters				Vibrational amplitudes				Scale factors		
p_2	p_4	p_5	p_7	u_3	u_5	u_6	u_{14}	k_1	k_3	
74	94	−65			60					p_1
	71				51					p_2
56		75		−69						p_3
					56					p_4
					−53					p_5
						8				p_6
			−57			−61				p_7
							76			p_{10}
							61	−71		p_{11}
				52					8	k_1
				57						k_2

Table 4. Interatomic distances (r_a, pm) and amplitudes of vibration (u, pm) for B_5H_9

		Distance	Amplitude
r_1	B(2)—B(3)	181.1(14)	5.8(4)
r_2	B(1)—B(2)	169.4(4)	5.4(4)
r_3	B(2)—H(2)	121.0(12)	8.9(8)
r_4	B(1)—H(1)	120.5(12)	
r_5	B(2)—H(2,3)	137.4(11)	13.9(13)
r_6	B(2)···B(4)	256.1(6)	7.9(8)
r_7	B(2)···H(5)	278.5(21)	11.9(12)
r_8	B(2)···H(1)	264.5(14)	
r_9	B(2)···H(3,4)	255.3(38)	15.9(37)
r_{10}	B(1)···H(2)	259.1(85)	11.3(fixed)
r_{11}	B(1)···H(2,3)	243.5(18)	10.3(25)
r_{12}	B(2)···H(4)	274.8(30)	12.4(19)

Note: H···H distances were also included in the refinement but are not listed here.

so that angles of interest may be calculated. The observed and final weighted difference molecular scattering intensities are shown in Fig. 2, and the radial distribution curve in Fig. 3.

Refinement of the structure of B_5H_9

The numbering of atoms is shown in Fig. 1(b).

The boron framework. This structure was defined by five parameters – the mean nearest neighbour B—B interatomic distance, the difference of the average interatomic distance between neighbouring basal boron atoms from the average of those between base and apex, the difference between distances B(1)—B(2) and B(1)—B(3), the difference between B(3)—B(4) and B(2)—B(5), and the angle at the apex of the open face, ∠B(2)B(1)B(5). In all refinements the mean B—B distance was close to

Table 5. Atomic coordinates (pm)

Atom	x	y	z
(a) B_5H_9			
B(1)	0.0	0.0	110.9
B(2)	128.1	0.0	0.0
H(1)	0.0	0.0	231.5
H(2)	245.7	0.0	28.6
H(2,3)	90.4	−90.4	−96.3

Coordinates of the remaining atoms are given by applying C_s operations about the z axis to B(2), H(2) and H(2,3).

(b) B_5H_{11}			
B(1)	0.0	52.6	95.6
B(2)	−154.5	0.0	0.0
B(3)	−88.0	168.5	0.0
B(4)	88.0	168.5	0.0
B(5)	154.5	0.0	0.0
$H(1)_{t,t}$	0.0	49.8	214.8
$H(1)_{t,a}$	−17.2	−68.2	43.5
$H(2)_{t,t}$	−261.8	−20.4	47.9
$H(2)_{t,a}$	−125.9	−80.3	−83.3
H(3)	−139.6	244.4	76.1
H(4)	139.6	244.4	76.1
$H(5)_{t,t}$	261.8	−20.4	47.9
$H(5)_{t,a}$	125.9	−80.3	−83.3
H(2,3)	−184.2	118.6	−66.9
H(3,4)	0.0	210.2	−91.3
H(4,5)	184.2	118.6	−66.9

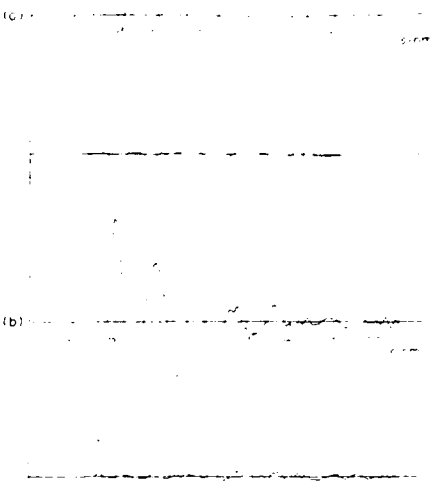

Fig. 2. Observed and final weighted difference molecular scattering intensities for B_5H_9 at nozzle-to-plate distances of (a) 285 and (b) 128 mm.

179 pm, and the angle B(2)B(1)B(5) was around 109°. The interatomic distances B(1)—B(2) were always substantially longer than for B(1)—B(3) so the apical boron atom is displaced away from the open edge of the base. The interatomic distances around the base were consistently shorter than those to the apex, but the difference varied, depending on the refinement conditions. In all the best refinements the difference was around −4 or −5 pm. Similarly, the basal distance B(3)—B(4) was always less than B(2)—B(3), but here the difference varied from −2 to −9 pm, being close to −5 pm in the best refinements.

Hydrogen atoms [*not including the face-capping hydrogen*, $H(1)_{t,a}$]. It was assumed that all terminal B—H distances were equal. The B(3)H(3,4)B(4) bridge was assumed to be symmetrical, with bonds equal in length to the mean of all the bridge bond lengths. The other bridges, B(2)H(2,3)B(3) and B(5)H(4,5)B(4) were asymmetric, with the bonds B(2)—H(2,3) and B(5)—H(4,5) longer than the mean, and the other bonds shorter than the mean by an equal amount. The positions of hydrogen atoms were then defined by the following angle parameters:

$H(1)_{t,t}$ "tilt"-angle between B(1)—$H(1)_{t,a}$ bond and z axis (defined as perpendicular to plane of basal boron atoms). A positive tilt is towards the open face of the cluster.

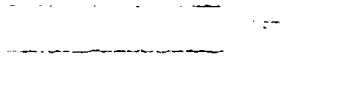

Fig. 3. Observed and final radial distribution curves, $P(r)/r$, for B_5H_9 [after inversion the data were multiplied by $\exp[-0.00002(r/z_1 - r/z_2)^2]$ $(z_1 = 1, z_2 = 2)$].

H(2)$_{t,t}$ "dip"-angle of B(2)—H(2)$_{t,t}$ bond below base plane.

H(2) "wag"-angle between projection of B(2)—H(2)$_{t,t}$ bond in base plane and x axis [defined as parallel to B(2)...B(5)].

H(2)$_{nd,t}$ "dip" and "wag"—defined as for H(2)$_{t,t}$.

H(3) "dip"-angle defined as for H(2)$_{t,t}$. The projection of the bond B(3)—H(3) was assumed to bisect the angle B(2)B(3)B(4).

H(2,3) "dip"-angle of B(2)H(2,3)B(3) below base plane.

H(3,4) "dip"—defined as for H(2,3).

The two B—H interatomic distances both refined consistently, and their values did not change significantly during the whole series of refinements. All the other angles were refined at some time, but only four of the eight could be included in the final refinement. Quoted errors are therefore probably under-estimates. The difference between the lengths of the bridging B—H bonds and the mean was not refined, but was fixed at various values between 0 and 6 pm. The best fit to the data was found with it set at 6 pm, which corresponds to the value reported for the solid phase structure.[2a,3]

The face-capping hydrogen H(1)$_{endo}$. Tests on the position of the anomalous hydrogen atom H(1)$_{endo}$ bound to B(1) were carried out with all positional parameters for terminal hydrogens H(1)$_{t,t}$, H(2,5)$_{t,t}$, H(2,5)$_{nd,t}$, and H(3,4) fixed, except for the mean B—H(terminal) bond length. The position of H(1)$_{nd,t}$ was defined by three parameters, B(1)—H(1)$_{nd,t}$, the angle between this bond and the z axis, which is perpendicular to the plane of the basal boron atoms, and a wag angle, which represented displacement of this bond from the mirror plane. With B(1)—H(1)$_{nd,t}$ fixed at 126 pm and the wag set at 5°, the remaining angle [called H(1)$_{nd,t}$ tilt] was refined to 116.7(26)° indicating that the hydrogen atom did indeed lie over the open face of the boron cluster. The distances B(2)...H(1)$_{endo}$ and B(5)...H(1)$_{endo}$ were 161 and 179 pm. Refinements with the wag angle fixed at various values between 0 and 20° showed a minimum R factor at about 8°, and this angle was then allowed to refine to 8.7(31)°. The tilt angle decreased systematically as the wag increased, and when both angles were refined the tilt went to 111.3(44)°. With this structure the distances B(2)...H(1)$_{endo}$ and B(5)...H(1)$_{endo}$ were 159 and 190 pm. Finally, the B(1)—H(1)$_{endo}$ distance was also allowed to refine, to 132(10) pm, and under these conditions the tilt and wag angles were 113.0(67)° and 8.1(36)° respectively, and the B(2)...H(1)$_{endo}$ and B(5)...H(1)$_{endo}$ distances were 159(4) and 190(10) pm.

The parameters, interatomic distances and amplitudes of vibration obtained in the final refinement, for which R_G was 0.063, are given in Tables 6 and 7, and the least-squares correlation matrix is listed in Table 3(b). This last table shows substantial correlations between refining parameters, and it must be realized that correlations with fixed parameters

Table 6. Molecular parameters for B_5H_{11} (distances in pm, angles in degrees)

p_1	r(B—B) (mean)	179.4(4)
p_2	Δr(B—B)$_1$ [(base–base) minus (base–apex)]	−4.0(7)
p_3	Δr(B—B)$_2$ [B(1)—B(2) minus B(1)—B(3)]	15.0(8)
p_4	Δr(B—B)$_3$ [B(3)—B(4) minus B(2)—B(3)]	−5.3(13)
p_5	∠B(2)B(1)B(5)	109.5(7)
p_6	r(B—H) terminal	119.2(4)
p_7	r(B—H) bridge (mean)	133.4(7)
p_8	Δr(B—H) bridge[a]	6.0(fixed)
p_9	H(1)$_{t,t}$ tilt[a]	−1.3(fixed)[b]
p_{10}	H(3,4) dip[a]	65.5(60)
p_{11}	H(3) dip[a]	−39.7(33)
p_{12}	H(2)$_{t,t}$ dip[a]	−23.7(fixed)[b]
p_{13}	H(2)$_{t,t}$ wag[a]	169.2(fixed)[b]
p_{14}	H(2)$_{nd,t}$ dip[a]	44.3(fixed)[b]
p_{15}	H(2)$_{nd,t}$ wag[a]	70.4(26)
p_{16}	H(2,3) dip[a]	43.2(30)
p_{17}	r[B(1)—H(1)$_{nd,t}$]	132.7(fixed)[b]
p_{18}	H(1)$_{nd,t}$ tilt	113.1(fixed)[b]
p_{19}	H(1)$_{nd,t}$ wag	8.1(fixed)[b]

[a] For definition of parameters see text.
[b] Not included in final refinement, but refined earlier—see text.

Table 7. Interatomic distances (r_a, pm) and amplitudes of vibration (u pm) for B_5H_{11}[a]

		Distance	Amplitude
r_1	B(1)—B(2)	189.2(6)	6.3(7)
r_2	B(1)—B(3)	174.2(8)	5.9
r_3	B(2)—B(3)	181.2(7)	6.1 (tied to u_2)
r_4	B(3)—B(4)	176.0(12)	5.9
r_5	B(2)...B(5)	309.1(10)	7.2(8)
r_6	B(2)...B(4)	295.3(6)	
r_7	B(1)—H(1)$_{br}$	119.2(4)	6.8(8)
r_8	B(2)—H(2,3)	139.4(7)	
r_9	B(3)—H(2,3)	127.4(7)	7.3 (tied to u_7)
r_{10}	B(3)—H(3,4)	133.4(7)	
r_{11}	B(1)—H(1)$_{endo}$	132.7[b]	8.5
r_{12}	B(2)—H(1)$_{endo}$	159.4(9)	10.0
r_{13}	B(5)—H(1)$_{endo}$	189.9(9)	10.0
r_{14}	B(1)...H(3)	238.1(35)	
r_{15}	B(1)...H(2)$_{exo}$	275.9(7)	
r_{16}	B(1)...H(2)$_{endo}$	256.0(19)	
r_{17}	B(1)...H(2,3)	254.4(13)	
r_{18}	B(1)...H(3,4)	244.5(20)	
r_{19}	B(2)...H(3)	256.5(16)	
r_{20}	B(2)...H(1)$_{br}$	269.3(8)	
r_{21}	B(2)...H(3,4)	276.4(41)	10.5(10)
r_{22}	B(3)...H(1)$_{br}$	260.8(8)	
r_{23}	B(3)...H(2)$_{exo}$	261.2(9)	
r_{24}	B(3)...H(2)$_{endo}$	265.2(16)	
r_{25}	B(3)...H(4)	251.7(16)	
r_{26}	B(3)...H(4,5)	284.7(16)	
r_{27}	B(3)...H(1)$_{endo}$	250.9(13)	
r_{28}	B(4)...H(1)$_{endo}$	262.7(12)	
r_{29}	B(2)...H(4)	390.0(24)	
r_{30}	B(2)...H(4,5)	365.1(21)	
r_{31}	B(2)...H(5)$_{exo}$	419.6(11)	15.0(fixed)
r_{32}	B(2)...H(5)$_{endo}$	303.4(29)	
r_{33}	B(3)...H(5)$_{exo}$	400.4(8)	
r_{34}	B(3)...H(5)$_{endo}$	338.6(25)	

[a] 31 H...H distances were also included in the refinements, but are not listed here.

[b] Fixed in final refinement: see text.

would increase these values further. Atomic coordinates listed in Table 5(b) enable bond angles to be calculated. Molecular scattering intensities are shown in Fig. 4 and the radial distribution curve in Fig. 5.

GENERAL CONCLUSIONS

The main results of the present structural determinations of gaseous pentaborane(9) and pentaborane(11), based on electron-diffraction data, are compared in Tables 8 and 9 with those derived from various other methods. The interatomic distances for B_5H_{11} are seen to correspond well with the earlier electron diffraction results, but are now defined with considerably improved precision and agree to within 1% with the microwave data. The unusually large value observed for the amplitude of vibration of the directly-bonded B—H(bridge) pairs is worthy of comment, but unfortunately we are unable to say whether this is a real effect or whether the structure is of lower symmetry than expected. The rotational spectrum [8] indicated that the molecule must have some low-frequency mode, but the rotation constants themselves are insensitive to a distortion of a_2 symmetry.

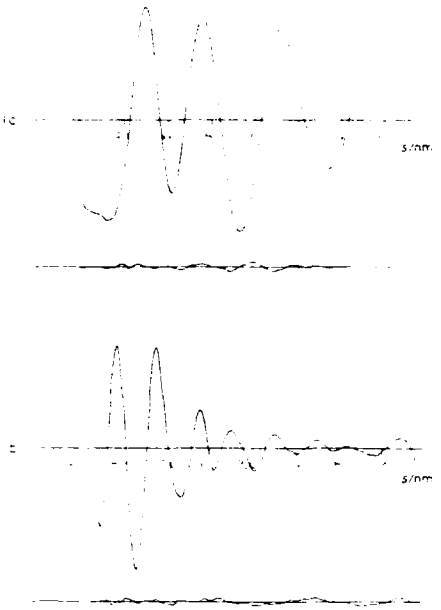

Fig. 4. Observed and final weighted difference molecular scattering intensity curves for B_5H_{11} at nozzle-to-plate distances of (a) 286 and (b) 128 mm.

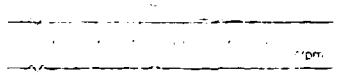

Fig. 5. Observed and final difference radial distribution curves, $P(r)/r$, for B_5H_{11}. Before Fourier transformation the data were multiplied by $\exp[-0.00002s^2/(Z_B-f_B)(Z_H-f_H)]$.

In the case of B_5H_{11}, the structure of the boron framework is marked by the length of the interatomic distances to the boron atoms at the open edge. For all reasonable positions of hydrogen atoms the parameters relating to the cluster vary little, and its structure is well determined. The interatomic distances are close to those reported for the compound in the crystalline phase,[2,3] except that B(3)—B(4) is apparently shorter in the gas phase. Admittedly the interatomic distances B(2)—B(3) and B(4)—B(5) have been held equal in the present

Table 8. A comparison of the molecular parameters of pentaborane(9) as determined by various methods[a]

Parameter	Electron diffraction[b]	X-ray	Microwave[c]	Electron diffraction[d]
(a) Distances pm				
B(1)—B(2)	170.0(17)	165.3(10)	169.3(2)	169.4(4)
B(2)—B(3)	180.5(14)	175.1(6)	180.3(2)	181.1(4)
B(1)—H(1)	123.4(66)[e]	114(8)	118.1(2)	120.5(12)[e]
B(2)—H(2)	123.4(66)[e]	107(3)	118.6(2)	121.0(12)[e]
B(2)—H(2,3)	135.9(77)	127(2)	135.2(4)	137.4(11)
(b) Angles				
B(1)—B(2)—H(2)	120(20)	130.05(215)	128.72	125.4(73)
B(2)—B(1)—B(3)		63.97(37)		
B(2)—H(2,3)—B(3)		87.28(102)		
B(3)—B(2)—H(2,3)		46.38(102)		
B(2)—B(1)—H(1)		131.49(34)		
B(1)—B(2)—B(3)		58.01(19)		
B(3)—B(2)—H(2)		106.61(28)		
H(2,3) dip				68.8(29)

[a] Estimated standard deviations are given in parentheses where values are available. [b] Ref. 8. [c] Ref. 5. [d] Ref. 10(c). This work. [e] The B(1)—H(1) and B(2)—H(2) distances were assumed to be equal. [f] See text. The small difference in length of the two types of terminal bonds was fixed at the value found by microwave spectroscopy.

Table 9. A comparison of interatomic distances in pentaborane(11) as determined by various methods

Interatomic distance	X-ray[a]	Theoretical[b]	Theoretical[c]	Electron diffraction
B(1)—B(2)	187.4(3)	191.45	187.35	189.2(6)
B(1)—B(5)	187.4(3)	193.26	187.47	
B(1)—B(3)	172.3(3)	175.69	172.26	174.2(8)
B(1)—B(4)	171.6(3)	175.74	171.53	
B(2)—B(3)	179.6(3)	184.63	179.62	181.2(7)
B(4)—B(5)	175.1(3)	175.34	175.12	
B(3)—B(4)	179.1(3)	184.55	179.10	176.0(12)
B(2)...B(5)	—	310.93	304.87	309.1(10)
B(2)...B(4)	—	—	—	295.3(6)
B(1)—H(1)$_{term}$	107(1)	117.99	118.00	119.2(4)
B(1)—H(1)$_{endo}$	106(2)	122.76	122.59	132.7[f]
B(2)—H(2)$_{term}$	106(2)	118.16	118.17	119.2(4)[g]
B(2)—H(2)$_{endo}$	111(2)	118.69	118.70	
B(3)—H(3)	106(2)	117.59	117.58	
B(4)—H(4)	110(2)	117.53	117.52	
B(5)—H(5)$_{term}$	111(2)	118.38	118.36	
B(5)—H(5)$_{endo}$	112(2)	118.31	118.40	
B(2)—H(2,3)	134(2)	146.76	143.03	139.4(7)[h]
B(5)—H(4,5)	130(2)	139.70	143.31	
B(3)—H(2,3)	119(2)	124.00	124.15	127.4(7)[h]
B(4)—H(4,5)	119(2)	125.17	125.21	
B(3)—H(3,4)	125(2)	134.44	133.23	133.4(7)[i]
B(4)—H(3,4)	128(1)	132.14	130.84	
B(2)...H(1)$_{endo}$	155(2)	157.73	155.36	159.4(9)
B(5)...H(1)$_{endo}$	183(2)	—	—	189.9(9)

[a] Distances in pm. Estimated standard deviations are given in parentheses where values are available. [b] Ref. 3. [c] Ref. 4. Complete optimization at 3-21G level assuming C_s symmetry. [d] Boron framework fixed to experimental dimensions in Ref. 3. [e] This work; the interatomic distances were constrained to be equal as indicated. [f] Refined to 132(10) pm, but fixed in final refinement, see text. [g] B(3)—H(3,4)—B(4) bridge assumed to be symmetrical.

study, but it is unlikely that this alone is responsible for the observed effect on B(3)—B(4).

The asymmetrical nature of the B(2)—H(2,3)—B(3) and B(5)—H(4,5)—B(4) bridges in gaseous B_5H_{11} has been confirmed. In the present study the best fit to the data was found when the difference between the two halves of the bridge was set at the value reported for the solid phase structure,[3] i.e. 12 pm, leading to values of 139.4(7) and 127.4(7) pm. The average B—H bridge distance is of course substantially longer than is found by X-ray diffraction, as we are looking at nuclear positions and not at centres of electron density. Unsymmetrical B—H—B bridges are a common feature of many polyhedral boranes, including for example $B_5H_9{\cdot}CO$,[7] B_5H_{11},[3] $B_5H_{10}^-$,[8] $B_5H_8(PPh_3)_3$[9] and B_6H_{12}.[10]

As regards the position of the face-capping hydrogen atom $H(1)_{endo}$, the results are to some extent inconclusive. There is no doubt that the best fit to the data has been obtained with an asymmetric structure, but the improvements observed on relaxing the symmetry requirement were not so great that the symmetric structure can be entirely ruled out. The evidence that $H(1)_{endo}$ lies over the open face B(2)B(1)B(5) is fairly strong; the angle of tilt has at no time had an uncertainty of more than 9°. The effect of fixing the parameters relating to other hydrogen atoms and many amplitudes of vibration on the quoted errors can not be determined but must be substantial. All we can say therefore is that the hydrogen atom may well be asymmetrically located above the B(2)B(1)B(5) face, the best fit being obtained when the distances B(2)...H(1)$_{endo}$ and

B(5)···H(1)$_{ax}$ are 159(4) and 190(10) respectively, the difference of 31 pm being 2.2 times the sum of the estimated errors.

Acknowledgement—We thank the SERC for financial support.

REFERENCES

1. (a) L. R. Lavine and W. N. Lipscomb, *J. Chem. Phys.* 1953, **21**, 2087; (b) *ibid.* 1954, **22**, 614; (c) W. N. Lipscomb, *ibid.* 1954, **22**, 985.
2. (a) E. B. Moore, R. E. Dickerson and W. N. Lipscomb, *J. Chem. Phys.* 1957, **27**, 209; (b) G. S. Pawley, *Acta Cryst.* 1966, **20**, 631.
3. J. C. Huffman, Ph.D. Thesis, Indiana University, 1974.
4. M. L. McKee and W. N. Lipscomb, *Inorg. Chem.* 1981, **20**, 4442.
5. (a) R. Schaeffer, J. N. Schoolery and R. Jones, *J. Am. Chem. Soc.* 1957, **79**, 4606; (b) R. E. Williams, S. G. Gibbins and I. Shapiro, *J. Chem. Phys.* 1959, **30**, 320; (c) R. E. Williams, F. J. Gerhart and E. Piers, *Inorg. Chem.* 1965, **4**, 1239; (d) T. Onak and J. B. Leach, *J. Am. Chem. Soc.* 1970, **92**, 3513; (e) R. R. Rietz, R. Schaeffer and L. G. Sneddon, *ibid.* p. 3514; (f) J. B. Leach, T. Onak, J. Spielman, R. R. Rietz, R. Schaeffer and L. G. Sneddon, *Inorg. Chem.* 1970, **9**, 2170; (g) A. O. Clouse, D. C. Moody, R. R. Rietz, T. Roseberry and R. Schaeffer, *J. Am. Chem. Soc.* 1973, **95**, 2496.
6. S. H. Bauer, *J. Am. Chem. Soc.* 1938, **60**, 805.
7. M. E. Jones, K. Hedberg and V. Schomaker, private communication referred to by W. N. Lipscomb, *J. Chem. Phys.* 1954, **22**, 985, ref. 29.
8. K. Hedberg, M. E. Jones and V. Schomaker, *J. Am. Chem. Soc.* 1951, **73**, 3538; *Proc. Natl. Acad. Sci. U.S.* 1952, **38**, 679.
9. W. J. Dulmage and W. N. Lipscomb, *J. Am. Chem. Soc.* 1951, **73**, 3539; *Acta Cryst.* 1952, **5**, 260.
10. H. J. Hrostowski, R. J. Myers and G. C. Pimentel, *J. Chem. Phys.* 1952, **20**, 518; (b) H. J. Hrostowski and R. J. Myers, *ibid.* 1954, **22**, 262; (c) D. Schwoch, A. B. Burg and R. A. Beaudet, *Inorg. Chem.* 1977, **16**, 3219.
11. M. A. Toft, J. B. Leach, F. L. Himpsl and S. G. Shore, *Inorg. Chem.* 1982, **21**, 1952.
12. D. F. Shriver, *The Manipulation of Air-sensitive Compounds*, p. 90. McGraw-Hill, New York (1969).
13. A. B. Burg and H. I. Schlesinger, *J. Am. Chem. Soc.* 1933, **55**, 4009.
14. C. M. Huntley, G. S. Laurenson and D. W. H. Rankin, *J. Chem. Soc.* 1980, 954.
15. S. Cradock, J. Koprowski and D. W. H. Rankin, *J. Mol. Struct.* 1981, **77**, 113.
16. A. S. F. Boyd, G. S. Laurenson and D. W. H. Rankin, *J. Mol. Struct.* 1981, **71**, 217.
17. L. Schäfer, A. C. Yates and R. A. Bonham, *J. Chem. Phys.* 1971, **55**, 3055.
18. J. D. Glore, J. W. Rathke and R. Schaeffer, *Inorg. Chem.* 1973, **12**, 2175.
19. C. J. Dain, A. J. Downs, G. S. Laurenson and D. W. H. Rankin, *J. Chem. Soc. Dalton Trans.* 1981, 472.
20. M. M. Mangion, J. R. Long, W. R. Clayton and S. G. Shore, *Cryst. Struct. Commun.* 1975, **4**, 501.
21. (a) A. Tippe and W. C. Hamilton, *Inorg. Chem.* 1969, **8**, 464; (b) V. S. Mastryukov, O. V. Dorofeeva and L. V. Vilkov, *J. Struct. Chem.* 1975, **16**, 110.

The Molecular Structure of Hexaborane(12) in the Gas Phase as determined by Electron Diffraction

Robert Greatrex, Norman N. Greenwood, and Mary B. Millikan
School of Chemistry, University of Leeds, Leeds LS2 9JT
David W. H. Rankin and Heather E. Robertson
Department of Chemistry, University of Edinburgh, West Mains Road, Edinburgh EH9 3JJ

The structure of gaseous *arachno*-B_6H_{12}, the only simple binary borane for which crystallographic data are not available, has been determined by electron diffraction. The analysis showed unequivocally that the molecule has C_2 symmetry, with two BH_2 terminal groups, four other terminal hydrogen atoms, and four bridging hydrogen atoms, two of which are asymmetric. Models with C_s or C_s symmetries gave unsatisfactory *R* factors, and were rejected. The boron framework is a chiral six-atom fragment of a closed triangular dodecahedron from which two adjacent five-connected vertices have been removed. The results establish a clear structural relationship between the three *arachno* boranes B_4H_{10}, B_5H_{11}, and B_6H_{12}.

Hexaborane(12) is the only simple binary borane for which crystallographic data are not available, previous attempts to solve the structure by *X*-ray crystallography being thwarted because the compound forms a glass at low temperature.[1] N.m.r. evidence[2] and considerations based on geometrical and *topological principles*[3] *are consistent with a (4212) structure of* C_2 symmetry, (**I**), though alternative arrangements of C_s and C_s symmetry, (**II**) and (**III**) respectively, could not be entirely eliminated. An early electron diffraction study of the gaseous molecule failed to distinguish between the various formulations.[4] Geometrical parameters such as interatomic distances and angles are therefore entirely lacking, and for this reason we have undertaken a study of the molecular structure of the gaseous *arachno*-B_6H_{12} molecule by electron diffraction. The results establish that the molecule does indeed have C_2 symmetry and indicate a structural relationship between the three *arachno*-boranes B_4H_{10},[5] B_5H_{11},[6] and B_6H_{12}, all of which have now been studied by electron diffraction.

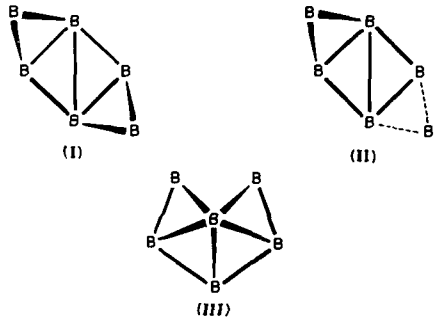

Experimental

Hexaborane(12) was prepared by the method of Shore and co-workers.[7] Pentaborane(9) was obtained from Dr. R. E. Williams (Chemical Systems Inc., California) and was used without further purification. Deprotonation was achieved with KH in a minimum amount of Me_2O at −78 °C. After addition of B_2H_6 to generate the $[B_6H_{11}]^-$ anion, care was taken to remove all traces of the solvent before the addition of HCl. Failure to do this resulted in loss of product by reaction with Me_2O to give B_5H_9. The B_6H_{12} was purified on a low-temperature fractional distillation column, with continuous monitoring of the distillate by mass spectrometry. Useful quantities of B_6H_{10} were also sometimes generated in the preparation, but with care it was possible to achieve an excellent separation of the two boranes. The final product was shown by i.r. and ^{11}B n.m.r. spectroscopy to be essentially free from impurities; its vapour pressure at 0 °C was 17.0 mmHg (*ca.* 2.26 kPa), in excellent agreement with the published value.[2b] The boranes were handled in conventional high-vacuum systems equipped with greaseless O-ring taps and spherical joints [J. Young (Scientific Glassware) Ltd.].

Electron diffraction scattering patterns were recorded photographically on Kodak Electron Image plates using the Edinburgh gas diffraction apparatus,[8] with nozzle-to-plate distances of 285.7 and 128.3 mm (three plates at each distance) and an accelerating voltage of *ca.* 44 kV. The sample was held at 0 °C and the nozzle was held at room temperature (17 °C) during the experiments. The plates were pumped for 24 h after completion of the experiment, before being developed, to minimise the effects of reaction between the sample and photographic emulsion. Calibration plates for benzene were also run at each camera distance, and we believe that by following this procedure systematic errors in the camera distance and electron wavelength are negligible (less than 1 part in 5 000).

Optical densities were obtained from the plates using a computer-controlled Joyce-Loebl MDM6 microdensitometer at the S.E.R.C. Laboratory, Daresbury, using a scanning procedure described previously.[9] Calculations were carried out using our standard data-reduction[9] and least-squares refinement[10] programs, and the scattering factors of Schäfer *et al.*[11] Weighting points, used in setting up the off-diagonal weight matrices, are given in Table 1, together with other experimental details.

Structure Refinement.—As discussed earlier, there are good reasons for supposing, both on theoretical grounds[3] and by analysis of n.m.r. spectra,[2] that B_6H_{12} should have C_2 symmetry. However, as it is possible in principle that the molecules could have C_s or C_s symmetry (the latter would involve fortuitous coincidence of two chemical shifts), we thought it prudent to test models with each of these symmetries. These

Table 1. Camera heights, weighting functions, *etc.*

Camera height mm	Electron wavelength pm	Δs	s_{min}	sw_1	sw_2	s_{max}	Correlation parameter	Scale factor
		nm^{-1}						
285.7	5.685	2	20	40	122	144	0.488	0.647(12)
128.3	5.685	4	60	80	290	340	0.360	0.583(14)

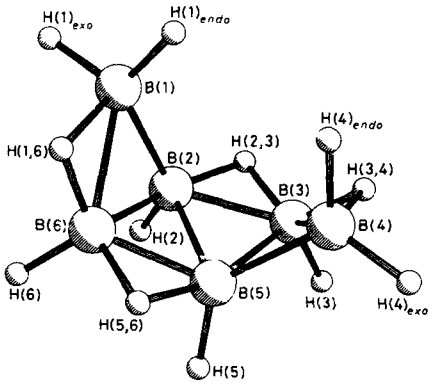

Figure 1. Perspective view of a molecule of B_6H_{12}

tests showed quite unequivocally that C_2 symmetry is correct. With the other models, *R* factors were significantly worse (0.12 for C_s, 0.10 for C_i, compared with 0.08 for C_2), and even these values could only be obtained with highly unlikely distorted structures. Most refinements were therefore performed using the C_2 model, with two BH_2 terminal groups, four other terminal hydrogen atoms, and four bridging hydrogen atoms, as shown in Figure 1.

Even with C_2 symmetry, a lot of parameters are required to define the molecular structure. For example, there are eight different B–H bonded distances, four terminal and four bridging, and ten angular parameters are also required to define the hydrogen atom positions. It was necessary to make a number of assumptions about the hydrogen positions, but no restrictions at all were placed on the boron atoms. The structure of the boron skeleton was thus defined by seven parameters, as listed in Table 2. Five of these describe the five different B–B 'bond' lengths, and these parameters were chosen to be the mean, and various differences. The remaining variables were angles between BBB planes. All seven of the cluster parameters were allowed to refine, even though the five B–B distances came within 15 pm of each other, but a single amplitude of vibration was refined for this group of distances.

The B–H bond lengths for the four distinct types of terminal hydrogen atom were refined as a single parameter, and the amplitude of vibration for this group was also refined, but tied to that for the bridging B–H bonds. For the terminal BH_2 groups the HBH angle was fixed at 112°, and it was initially assumed that the bisector of this angle coincided with the bisector of the angle B(2)B(1)B(6). At a later stage this restriction was relaxed, and the group was allowed to wag (*i.e.* to move in its own plane), or to rock (*i.e.* move perpendicular to its plane). The refined values for these parameters were 3.1(16)° (the displacement being *towards* the rest of the cluster) and −1.3(87)° [rocking *away* from B(2), *towards* B(6)]. Neither of these distortions was significant, so the parameters were subsequently fixed at zero again. The terminal hydrogen atom H(6) was assumed to lie in the plane bisecting the planes B(2)B(6)B(5) and B(1)B(6)B(2), and the remaining terminal atom H(2) was constrained to lie in the central plane of the molecule [bisecting B(3)B(2)B(5) and B(6)B(2)B(5)]. These two atoms were thus each located by the B–H bond length and one angle, but these angles could not be refined.

Table 2. Molecular parameters[a] (r_a, distances pm, angles °)

p_1	r(B–B) mean	179.5(1)
p_2	Δr(B–B) 1 · 6 2 · 6 5—6 minus 1 · 2 2—5	0.4(18)
p_3	Δr(B–B) 1 · 2 minus 2 · 5	−4.3(24)
p_4	Δr(B–B) 1 · 6 5 · 6 minus 2 · 6	2.8(17)
p_5	Δr(B–B) 1 · 6 minus 5 · 6	21.4(20)
p_6	Angle between planes 625 and 325	167.4(22)
p_7	Angle between planes 162 and 562	128.1(12)
p_8	r(B–H) (bridge) mean	130.8(14)
p_9	r(B–H) (terminal)	122.2(13)
p_{10}	H_tBH_t	112.0(fixed)
p_{11}	B(2)B(6)H(6)	110.0(fixed)
p_{12}	B(5)B(2)H(2)	110.0(fixed)
p_{13}	Δr B(1)–H(1,6) minus B(6)–H(1,6)	21.6(58)
p_{14}	B(1)H(1,6)B(6) dip[b]	0.0(fixed)[c]
p_{15}	Δr B(6)–H(5,6) minus B(5)–H(5,6)	0.0(fixed)[c]
p_{16}	B(5)H(5,6)B(6) dip[b]	0.0(fixed)[c]
p_{17}	B(1)H_2 wag[b]	0.0(fixed)[c]
p_{18}	B(1)H_2 rock[b]	0.0(fixed)[c]

[a] In the case of p_2, Δr(B–B) 1 · 6 2 · 6 5 · 6 minus 1 · 2 2 · 5 means the average of the first group of B–B distances minus the average of the second group, and likewise for p_3, p_4, p_5, p_{13}, and p_{15}. Errors, quoted in parentheses, are estimated standard deviations obtained in the least-squares refinements, increased to allow for systematic errors. [b] For definition see text. [c] See text.

The bridging atoms, H(1,6) and H(5,6), were originally located by a single bridging B–H distance, and it was assumed that the bridge bonds lay in the local BBB planes [B(1)B(2)B(6) and B(5)B(2)B(6) respectively]. These restrictions were then relaxed by allowing asymmetry in each of the bridges, while continuing to refine a single mean bridge B–H distance, and by allowing displacement of the bridge atoms from the local BBB planes. For three of these four relaxations the refined parameters were not significantly different from zero, but for the B(1)H(1,6)B(6) bridge the bond to B(1) was found to be longer than that to B(6) by 21.6(58) pm.

The final refined geometrical parameters are listed in Table 2, and interatomic distances and amplitudes of vibration are given in Table 3. Errors quoted in these tables are estimated standard deviations obtained in the least-squares refinements. Table 4 gives the most significant elements of the least-squares correlation matrix, and Table 5 gives atom co-ordinates, from which interatomic distances, bond angles, and dihedral angles of interest may be computed. Figures 2 and 3 show the molecular scattering intensity curves and the radial distribution curve.

Discussion

A perspective view of the chiral *arachno*-B_6H_{12} molecule is shown in Figure 1. The boron framework can be thought of as being derived from a *closo*-dodecahedral B_8 cluster by removal of two adjacent five-connected boron atoms, consistent with the well known Williams Wade cluster geometry and electron-counting rules.[12] In fact, the dihedral angles between adjacent triangular faces in B_6H_{12} are close to, but slightly greater than, the two internal dihedral angles characteristic of a regular triangular dodecahedron (157 and 120°): the observed angles are 167.4 ± 22° between the faces joined by B(2)–B(5), and

Table 3. Interatomic distances and amplitudes of vibration (pm)*

		Distance	Amplitude
r_1	B(1)–B(2)	177.8(18)	
r_2	B(2)–B(5)	182.1(13)	
r_3	B(2)–B(6)	177.7(16)	5.0(10)
r_4	B(1)–B(6)	191.3(7)	
r_5	B(5)–B(6)	169.9(14)	
r_6	B–H(terminal)	122.2(13)	7.9(5)
r_7	B–H(5,6)	130.8(14)	
r_8	B(1)–H(1,6)	141.6(25)	8.5(tied to u_6)
r_9	B(6)–H(1,6)	120.0(38)	
r_{10}	B(1)···B(5)	282.5(22)	16.4(53)
r_{11}	B(1)···B(3)	305.1(16)	9.4(11)
r_{12}	B(3)···B(6)	294.4(29)	
r_{13}	B(1)···B(4)	335.3(39)	31.0(122)
r_{14}	B(1)···H(2)	273.9(20)	
r_{15}	B(1)···H(5,6)	296.8(20)	
r_{16}	B(1)···H(6)	276.3(13)	
r_{17}	B(2)···H(5,6)	258.1(22)	12.0(18)
r_{18}	B(2)···H(3,4)	264.1(33)	
r_{19}	B(6)···H(1)	271.2(12)	
r_{20}	B(6)···H(2,3)	305.0(21)	
r_{21}	B(1)···H(2,3)	257.7(21)	
r_{22}	B(2)···H(1)	261.9(17)	
r_{23}	B(2)···H(1,6)	239.0(20)	
r_{24}	B(2)···H(6)	247.8(19)	8.9(15)
r_{25}	B(2)···H(3)	255.8(17)	
r_{26}	B(2)···H(5)	251.6(14)	
r_{27}	B(6)···H(2)	241.9(17)	
r_{28}	B(6)···H(5)	233.5(20)	
r_{29}	B(1)···H(5)	381.2(23)	
r_{30}	B(1)···H(3,4)	348.8(23)	
r_{31}	B(1)···H(3)	416.0(21)	
r_{32}	B(2)···H(4)$_{endo}$	324.7(30)	
r_{33}	B(2)···H(4)$_{exo}$	392.1(21)	13.6(31)
r_{34}	B(6)···H(3,4)	363.8(24)	
r_{35}	B(6)···H(3)	380.0(26)	
r_{36}	B(6)···H(4)$_{endo}$	333.7(28)	
r_{37}	B(6)···H(4)$_{exo}$	408.8(21)	
r_{38}	B(1)···H(4)$_{endo}$	311.5(54)	20.0(fixed)
r_{39}	B(1)···H(4)$_{exo}$	457.3(46)	

* Non-bonded H···H atom pairs were also included in the refinement but are not listed here.

Table 4. Least-squares correlation matrix (×100)*

p_3	p_4	p_5	p_6	u_1	u_{10}	u_{11}	u_{14}	k_2	
−63	−76				−70		60		p_2
	51								p_3
							−57		p_4
				−90					p_5
	−52	−68			−66	−53	76		p_6
			−82						p_8
			83						p_{13}
						56	−62		u_{10}
						58			u_{21}
						75			u_{29}
								54	k_1

* u_n Represents the amplitude of vibration for distance r_n in Table 3, and k_2 represents a scale factor; only elements with absolute values > 50 are included.

Table 5. Atomic co-ordinates pm

Atom	x	y	z
B(1)	−102.87	132.35	139.02
B(2)	0.00	91.03	0.00
B(3)	147.03	7.49	16.23
B(4)	102.87	−132.35	139.02
B(5)	0.00	−91.03	0.00
B(6)	−147.03	−7.49	16.23
H(1)$_{endo}$	−69.41	101.10	252.35
H(1)$_{exo}$	−171.00	233.82	137.73
H(1,6)	−202.33	34.67	114.06
H(6)	−220.64	11.16	−79.55
H(5,6)	122.15	−135.90	13.49
H(2)	0.00	132.84	−114.86
H(4)$_{endo}$	69.41	−101.10	252.35
H(4)$_{exo}$	171.00	−233.82	137.73
H(3,4)	202.33	−34.67	114.06
H(3)	220.64	−11.16	−79.55
H(2,3)	122.15	135.96	13.49
H(5)	0.00	−132.84	−114.86

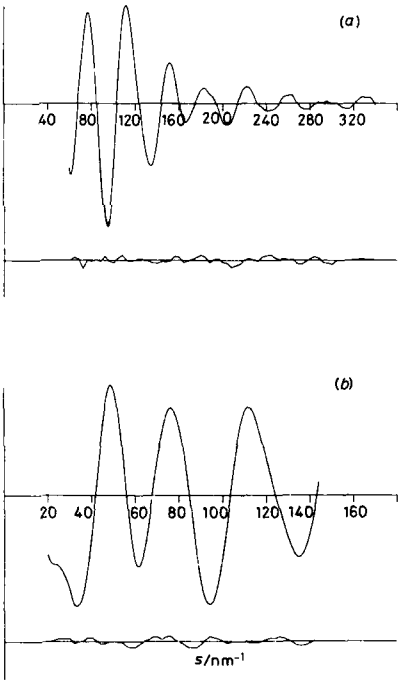

Figure 2. Observed and final weighted difference molecular electron scattering intensity curves at nozzle-to-plate distances of (*a*) 128 and (*b*) 286 mm

128.1 ± 12° between the faces joined by B(2)–B(6) and by B(3)–B(5), respectively. The only other comparable compound for which structural data are available is the *hypho* adduct $B_6H_{10}(PMe_3)_2$, which has been described as a fragment of the equatorial belt of an icosahedron.[13] The dihedral angles calculated from data for this *hypho* adduct are 140° at the central 'hinge' and 154° at the two outer hinges; the former is indeed very close to the regular icosahedral angle of 138.2° (*i.e.*

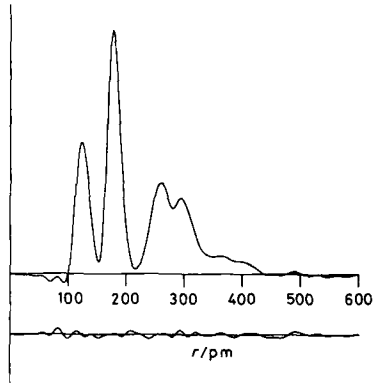

Figure 3. Observed and final difference radial distribution curves. $P(r)/r$. Before Fourier inversion the data were multiplied by $\exp[-0.000\,02s^2/(Z_P - f_P)(Z_S - f_S)]$

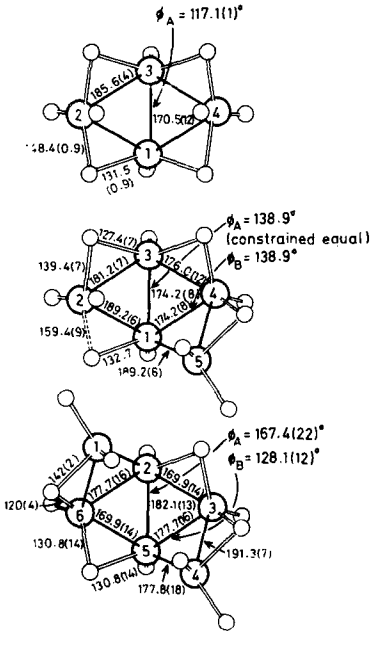

Figure 4. Structural relationship between the *arachno* boranes B_4H_{10}, B_5H_{11}, and B_6H_{12} (see text for discussion); distances in pm

$\pi - \sin^{-1}\frac{2}{3}$), whereas the latter two are somewhat more open. In further comparing the detailed structures of *arachno*-B_6H_{12} and *hypho*-$B_6H_{10}(PMe_3)_2$, it is apparent that the notional replacement of two terminal hydrogen atoms in *arachno*-B_6H_{12} by the phosphine ligands induces substantial re-arrangement of the remaining hydrogen atoms. In particular, in B_6H_{12} all the peripheral B–B contacts apart from B(1)–B(2) and B(4)–B(5) are bridged by hydrogen atoms, whereas in $B_6H_{10}(PMe_3)_2$ these are the only pairs which *do* carry hydrogen bridges. Despite these differences, many of the interatomic B–B distances are remarkably similar in the two molecules.

Of greater interest, because of its possible relevance to the mechanisms of borane interconversion reactions,[14] is the clear relationship which is established as a result of this work, between the structures of the three *arachno* binary boranes B_4H_{10}, B_5H_{11}, and B_6H_{12}.[2c] This is emphasized in Figure 4, which indicates that B_5H_{11} is related to B_4H_{10} by replacement of a hydrogen bridge by a BH_2 group, with the simultaneous conversion of a terminal hydrogen on B(4) into a bridging position between atoms B(4) and B(5). Hexaborane(12) is then derived from B_5H_{11} by a similar modification to the opposite side of the molecule. It should be pointed out that the hydrogen atom bridging B(1) and B(2) of B_5H_{11} is sometimes viewed as a terminal hydrogen atom attached to B(1). However, both low-temperature *X*-ray diffraction data[15] and our own recent gas-phase electron diffraction measurements[6] indicate that the hydrogen is asymmetrically disposed above the B(1)B(2)B(5) face and can therefore be regarded as having at least partial bridging character between atoms B(1) and B(2). When the structure of B_5H_{11} is viewed in relation to that of B_4H_{10} it becomes easier to understand why this should be. Further confirmation that this is a useful way of viewing the relationship between these molecules comes from a comparison of their actual dimensions. There is, for example, a regular increase in the 'hinge' B–B internuclear distance from 170.5(12) pm in B_4H_{10}, through 174.2(8) pm in B_5H_{11}, to 182.1(13) pm in B_6H_{12}, and this is accompanied by a progressive decrease in the 'unsubstituted' B–B interatomic distance from B(3)–B(2) 185.6(4) pm in B_4H_{10}, through B(3)–B(4) 176.0(12) pm in B_5H_{11}, to B(2)–B(3) 169.9(14) pm in B_6H_{12}. There is also a systematic opening of the dihedral angle of the 'butterfly' structure from 117.1(7), through 138.9, to 167.4(22)°. For comparison, values ranging from 115 to 119° have been found in a series of six metallaborane derivatives with the MB_3 framework,[16] and a value of 127° in $[(OC)_4MnB_3H_7\text{-}Br\text{-}4(exo)]$;[17] interestingly the value found in B_5H_{11} (138.9°) is close to that (138.2°) calculated for a regular icosahedron.

A final point worthy of mention is that the B(1)HB(6) bridge has been found to be distinctly asymmetric, the two halves differing by some 21.6 pm. The nature of this asymmetry in B_6H_{12} is consistent with that found in other binary boranes[6] where the distance from a bridging H atom to the boron atom of a BH_2 group is generally longer than that to a BH group.

Acknowledgements

We thank the U.S. Government through its European Research Office of the U.S. Army for a maintenance grant (to M. B. M.), the S.E.R.C. for financial support, and Dr. M. Thornton-Pett for calculation of some of the dihedral angles.

References

1 W. N. Lipscomb, personal communication, cited in ref. 2*c*.
2 (*a*) D. F. Gaines and R. Schaeffer, *Proc. Chem. Soc.*, 1963, 267; (*b*) D. F. Gaines and R. Schaeffer, *Inorg. Chem.*, 1964, **3**, 438; (*c*) C. A. Lutz, D. A. Philips, and D. M. Ritter, *ibid.*, p. 1191; (*d*) A. L. Collins and R. Schaeffer, *ibid.*, 1970, **9**, 2153; (*e*) J. B. Leach, T. Onak, J. Spielman, R. R. Rietz, R. Schaeffer, and L. G. Sneddon, *ibid.*, p. 2170; (*f*) A. O. Clouse, D. C. Moody, R. R. Rietz, T. Roseberry, and R. Schaeffer, *J. Am. Chem. Soc.*, 1973, **95**, 2496.
3 W. N. Lipscomb, *J. Phys. Chem.*, 1961, **65**, 1064 and refs. therein, *Inorg. Chem.*, 1964, **3**, 1683.
4 R. Foster, unpublished work referred to in ref. 2*f*.
5 C. J. Dain, A. J. Downs, G. S. Laurenson, and D. W. H. Rankin, *J. Chem. Soc., Dalton Trans.*, 1981, 472.

6 R. Greatrex, N. N. Greenwood, D. W. H. Rankin, and H. E. Robertson, *Polyhedron*, 1987, **6**, 1849 and refs. therein.
7 R. J. Remmel, H. D. Johnson, I. S. Jaworiwsky, and S. G. Shore, *J. Am. Chem. Soc.*, 1975, **97**, 5395.
8 C. M. Huntley, G. S. Laurenson, and D. W. H. Rankin, *J. Chem. Soc., Dalton Trans.*, 1980, 954.
9 S. Cradock, J. Koprowski, and D. W. H. Rankin, *J. Mol. Struct.*, 1981, **77**, 113.
10 A. S. F. Boyd, G. S. Laurenson, and D. W. H. Rankin, *J. Mol. Struct.*, 1981, **71**, 217.
11 L. Schäfer, A. C. Yates, and R. A. Bonham, *J. Chem. Phys.*, 1971, **55**, 3055.
12 R. E. Williams, *Adv. Inorg. Chem. Radiochem.*, 1976, **18**, 67; K. Wade, *ibid.*, p. 1.
13 M. Mangion, J. R. Long, W. R. Clayton, and S. G. Shore, *Cryst. Struct. Commun.*, 1975, **4**, 501; M. Mangion, R. K. Hertz, M. L. Denniston, J. R. Long, W. R. Clayton, and S. G. Shore, *J. Am. Chem. Soc.*, 1976, **98**, 449.
14 N. N. Greenwood and R. Greatrex, *Pure Appl. Chem.*, 1987, **59**, 857.
15 J. C. Huffman, Ph.D. Thesis, Indiana University, 1974.
16 I. Macpherson, Ph.D. Thesis, Leeds University, 1987 and refs. therein.
17 M. W. Chen, J. C. Calabrese, D. F. Gaines, and D. F. Hillenbrand, *J. Am. Chem. Soc.*, 1980, **102**, 4928.

Received 27*th November* 1987; *Paper* 7/2104

END